Structural characteristics of Wood Warbler habitats in Switzerland:
an analysis with remote sensing methods

Master Thesis

Department of Environmental Sciences, ETH Zürich
Forest and Landscape Management

Nica Huber

April 14, 2013

Supervised by:

PD Dr. Gilberto Pasinelli, Christian Ginzler,
Prof. Dr. Felix Kienast

ETH Eidgenössische Technische Hochschule Zürich Swiss Federal Institute of Technology Zurich
DUSYS Department of Environmental Systems Science
vogelwarte.ch
WSL Eidg. Forschungsanstalt für Wald, Schnee und Landschaft WSL

Acknowledgments

First of all, I wish to thank PD Dr. Gilberto Pasinelli from the Swiss Ornithological Institute for being such a dedicated supervisor. He was always open for questions, took time for discussions and gave a lot of good advice and constructive criticism. Second, I would like to thank Christian Ginzler from the Swiss Federal Institute for Forest, Snow and Landscape Research WSL for his quick and uncomplicated support during the processing of the lidar data and the programming work with Python. Furthermore, I would like to thank Prof. Dr. Felix Kienast from the Swiss Federal Institute for Forest, Snow and Landscape Research WSL for his many inputs and good advice during the project.

Concerning the statistical analyses, I am very grateful to Rafael Wüest for all his advice, answers and inputs. Then, I wish to thank Dr. Peter Rotach from the Group Forest Management - Silviculture ETH for an interesting and informative discussion of my results. I thank Alex Grendelmeier for giving me insight into the research project *Settlement behavior, population fluctuations and population structure of Wood Warbler* of the Swiss Ornithological Institute and for showing me some of the study areas. Furthermore, I wish to thank Lorena Segura for her competent help while doing the first programming steps with Python. Last but not least, I wish to thank Julian Helfenstein for proofreading the abstract, introduction and conclusion.

Abstract

Information on the distribution and abundance of endangered species is integral for wildlife conservation and land use planning. The Wood Warbler (*Phylloscopus sibilatrix*) is a ground-nesting, long-distance migratory passerine with a distinctly European range. In Western Europe, Wood Warbler populations have declined in the last three decades. In Switzerland, the Wood Warbler has been classified as vulnerable in the red list of the breeding birds. Furthermore, the species is one of the 50 priority species of the Swiss species recovery program.

Remote Sensing (RS) methods were used to achieve an increased understanding of the factors that may influence the territory choice of Wood Warblers in Switzerland and to identify potentially suitable habitats in the Swiss Jura Mountains and the Swiss Plateau. The structural habitat needs were analyzed at the scale of the nesting area and at the scale of the territory. First, lidar metrics were correlated with structural habitat variables collected in the course of the research project *Settlement behavior, population fluctuations and population structure of Wood Warbler* of the Swiss Ornithological Institute, Sempach. Second, the following question was addressed: Is it possible to distinguish Wood Warbler territories from control areas without Wood Warblers using lidar data or other RS information? In a third step, predictive models were generated to model the current potential range of the Wood Warbler in the Swiss Jura Mountains and the Swiss Plateau.

The analyses at the two spatial scales, 'nesting area' and 'territory', suggest that Wood Warblers prefer rather uniform forests stands of intermediate age. Stands of these stages of development are characterized by a closed canopy, low canopy height diversity, an open stem space and a sparse herb and shrub layer, features promoting the occurrence of the Wood Warbler. The analyses further showed that Wood Warbler occurrence is positively related to inclination and solar radiation during March. Since the Wood Warbler is a ground-nesting bird, the species may benefit from small-scale variation of snow melting and vegetation development. Alternatively, reduced disturbance due to recreational activity or low forest management intensity in steep areas may explain the observed effect. Solar radiation may positively influence food availability, and higher food availability on south-facing slopes than on north-facing slopes could attract Wood Warblers.

According to the predictive models, the current potential range of the Wood Warbler is predominantly located in the Swiss Jura Mountains. This finding corresponds to the abundance map of the Swiss Breeding Bird Atlas 1993-1996.

Locally, forest management may contribute to the deterioration of suitable areas, for example when relatively closed forests are opened up due to harvesting. Therefore, the focus of forest management at a regional scale should be on sustainable regeneration so that suitable stands are always present and new suitable stands are steadily developing. In consideration of the Wood Warbler's habitat needs, the femel harvesting system (*Femelschlag*), leading to a relatively homogeneous age structure, appears to be most promising to maintain structurally suitable stands for Wood Warblers. Selection forestry (*Plenterwald*/*Dauerwald*),

leading to a heterogeneous age structure and many gaps at a local scale, is rather unsuitable for the Wood Warbler.

Overall, this study suggests that RS variables derived from lidar data or other sources are suitable for distinguishing structural characteristics of Wood Warbler habitat from non-habitat. Additionally, lidar metrics and other RS variables convey additional information not captured by variables gathered in the field, and therefore have the potential to contribute to understanding the ecological niche of species.

Content

List of figures and tables

List of abbreviations

95% CI	95% confidence interval
AIC	Akaike Information Criterion
AICc	Akaike Information Criterion corrected for small sample sizes
ALS	airborne laser scanning
a.s.l.	above sea level
AUC	area under the ROC curve
CH	canopy height
dbh_{100}	dominant diameter at breast height (diameter 1.3 m above ground of the 100 thickest trees per hectare)
depth	soil depth
dist_f	distance to forest edge
DSM	digital surface model
DTM	digital terrain model
e.g.	exempli gratia / for example
ES	model-averaged estimate
Fig.	figure
forest_tpe	forest type (e.g. broad-leaved forest)
fneg	false negative rate
fpos	false positive rate
GLMMs	generalized linear mixed-effect models
GLMs	generalized linear models
H	hypothesis
i.e.	id est
K	number of variables included in a particular model
kappa	Cohen's kappa
lidar	light detection and ranging
LL	log-likelihood
maxVH	maximum vegetation height
meanCC	mean canopy cover above 3 m
meanCC_10m	mean canopy cover above 10 m
meanCC_15m	mean canopy cover above 15 m
meanCC_20m	mean canopy cover above 20 m
meanCH	mean canopy height
meanCH>3m	mean canopy height above 3 m
meanVH	mean vegetation height
meanVH<3m	mean vegetation height less than 3 m
meanVH>3m	mean vegetation height above 3 m
mkna	"minimum known number alive", minimum number of caught rodents
nDSM	normalized digital surface model
NFI2	Swiss National Forest Inventory 2 (1993-1995)
NFI3	Swiss National Forest Inventory 3 (2004-2006)
nutrients	soil nutrients
pen5_1	penetration rate 5-1 m above ground

pen10_2	penetration rate 10-2 m above ground
pen50_2	penetration rate 50-2 m above ground
permeability	water permeability
pers. comm.	personal communication
r_march	mean direct solar radiation during March
RS	remote sensing
r_s	Spearman's rank correlation coefficient
ROC curve	receiver operating characteristic curve
SD	standard deviation
sdCH	standard deviation of canopy height
sdCH>3m	standard deviation of canopy height above 3 m
sdVH	standard deviation of vegetation height
SE	standard error
sens	sensitivity
skeleton	soil skeleton
spec	specificity
Swisstopo	Swiss Federal Office of Topography
TSS	true skill statistic
UK	United Kingdom
VH	vegetation height
VH95	95% percentile of vegetation height
W	Akaike weight
WHC	water holding capacity

1 Introduction

1.1 General introduction

Information on the distribution and abundance of **endangered species** is integral for wildlife conservation and land use planning. For a species of interest, detailed knowledge of habitat needs is crucial for habitat protection (e.g. Johnson et al., 2004; Whittingham et al., 2005; Sellars & Jolls, 2007; Salek & Lövy, 2012), the restoration of the species to previously occupied habitat (Merrill et al., 1999), the identification of dispersal corridors (Reunanen et al., 2002; Gibson et al., 2004; Chetkiewicz & Boyce, 2009) or for predicting species distribution and locating suitable habitat (Sperduto & Congalton, 1996; Dettmers & Bart, 1999; Reunanen et al., 2002; Luoto et al., 2002; Nelson et al., 2005). While the potential range consists of the area exhibiting favorable ecological conditions for the species' existence independently of its actual presence, the realized range describes the area currently occupied by the species (Campell & Reece, 2003). The absence of a species in a particular area within the potential range may be caused by at least one or more of the following four ecological processes: lack of dispersal, unsuitable habitat, predation or competition, and unfavorable physical or chemical factors (Ricklefs, 1990).

The relationship between an organism and its environment is often **dependent on the spatial scale investigated** (e.g. Wiens et al., 1986). With regard to **habitat selection**, this implies that an area has to fulfill the physical, chemical and biotic needs of a species at a landscape scale. Within this area, a smaller area is selected as territory or home range. On an even smaller scale, the choice of the reproduction site takes place, for which again specific habitat needs exist (Piper, 2011). Thus, the specific regional and local habitat needs of a species may vary from those at the landscape scale. As an example, Fig. 1 illustrates how the occurrence of four vertebrate species can be explained by different habitat characteristics depending on the spatial scale investigated.

Remote sensing (RS) has become an important basis for mapping, understanding and modeling ecosystems, including the modeling of species' distributions and potential habitats (e.g. Sperduto & Congalton, 1996; Dettmers & Bart, 1999; Reunanen et al., 2002; Luoto et al., 2002). Typically, the RS data used in such models does not characterize the vertical habitat structure (Vierling et al., 2008), because the images acquired from conventional sensors are not capable of completely representing the three-dimensional structure of the surface (Müller et al., 2009). However, many species, especially forest bird species, are associated with specific three-dimensional habitat structures (Dunlavy, 1935; Shaw et al., 2002).

Lidar (light detection and ranging) or airborne laser scanning (ALS) is an active remote sensing technology. A lidar sensor emits laser pulses to the earth's surface and then measures the time elapsed from the emission of the pulses to the detection of their reflections. The exact position of the reflection can be derived with the help of this time span multiplied by the speed of light, the information about the sensor's position and certain alignments (Baltsavias, 1999; Wagner et al., 2003). When a laser pulse hits an object, it will

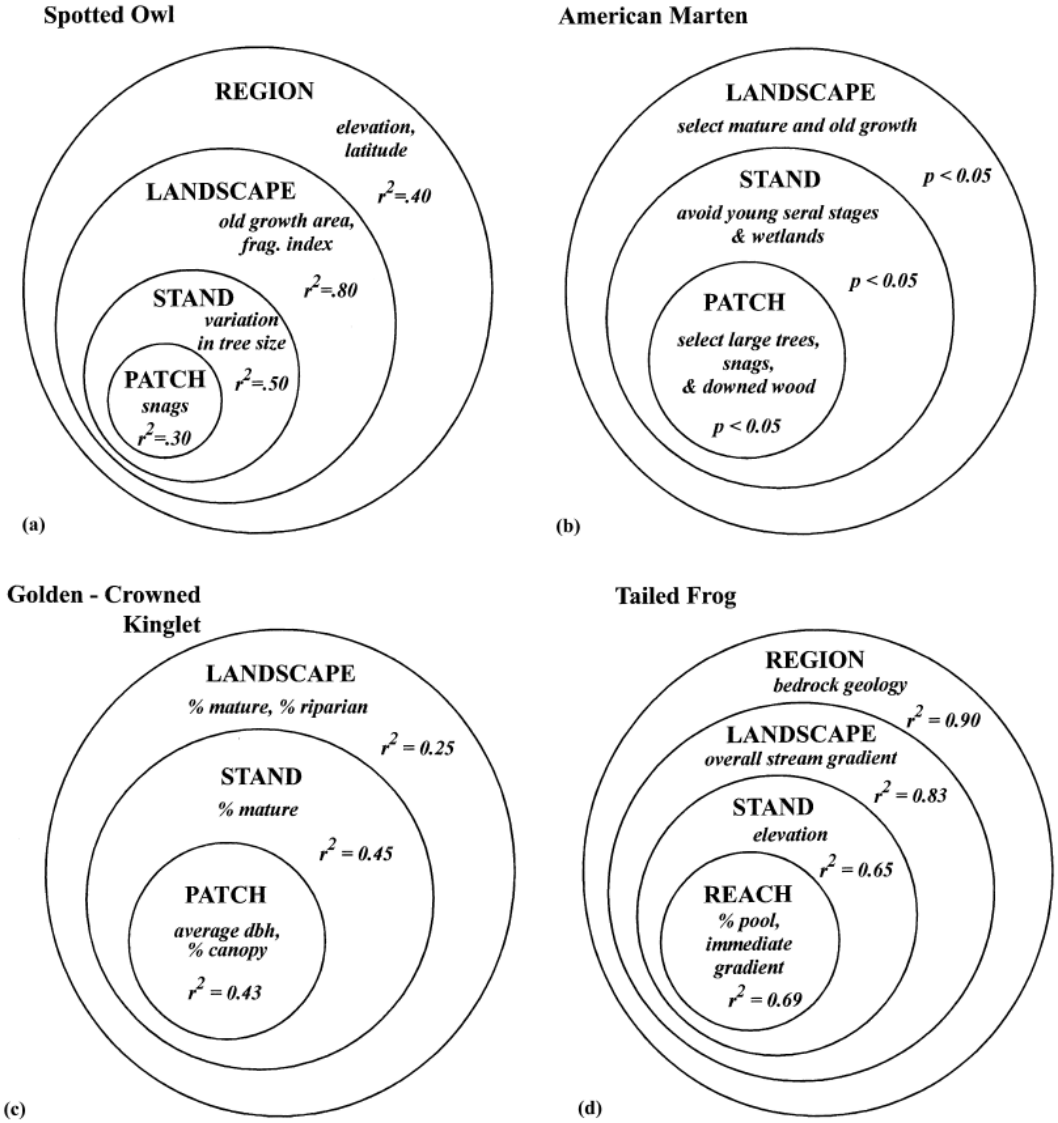

Fig. 1: Habitat needs at different spatial scales of the four species: (a) spotted owl, (b) American marten, (c) golden-crowned kinglet and (d) tailed-frog (Bunnell & Huggard, 1999).

be partly reflected and partly absorbed, but it will not be transmitted through the structure. Therefore, the laser signals returned from a structurally complex surface, such as vegetation canopy, contain information from objects located at varying depths within the canopy, such as leafs or branches, and from the ground (Fig. 2) (Lefsky et al., 2002). In contrast to conventional sensors, lidar sensors are able to measure the height of plant canopies and the subcanopy structure with high resolution over large spatial extents. Thus, they provide three-dimensional information about the micro-topography and the structure of the vegetation, such as vegetation height, vegetation cover and canopy structure (Müller et al., 2009).

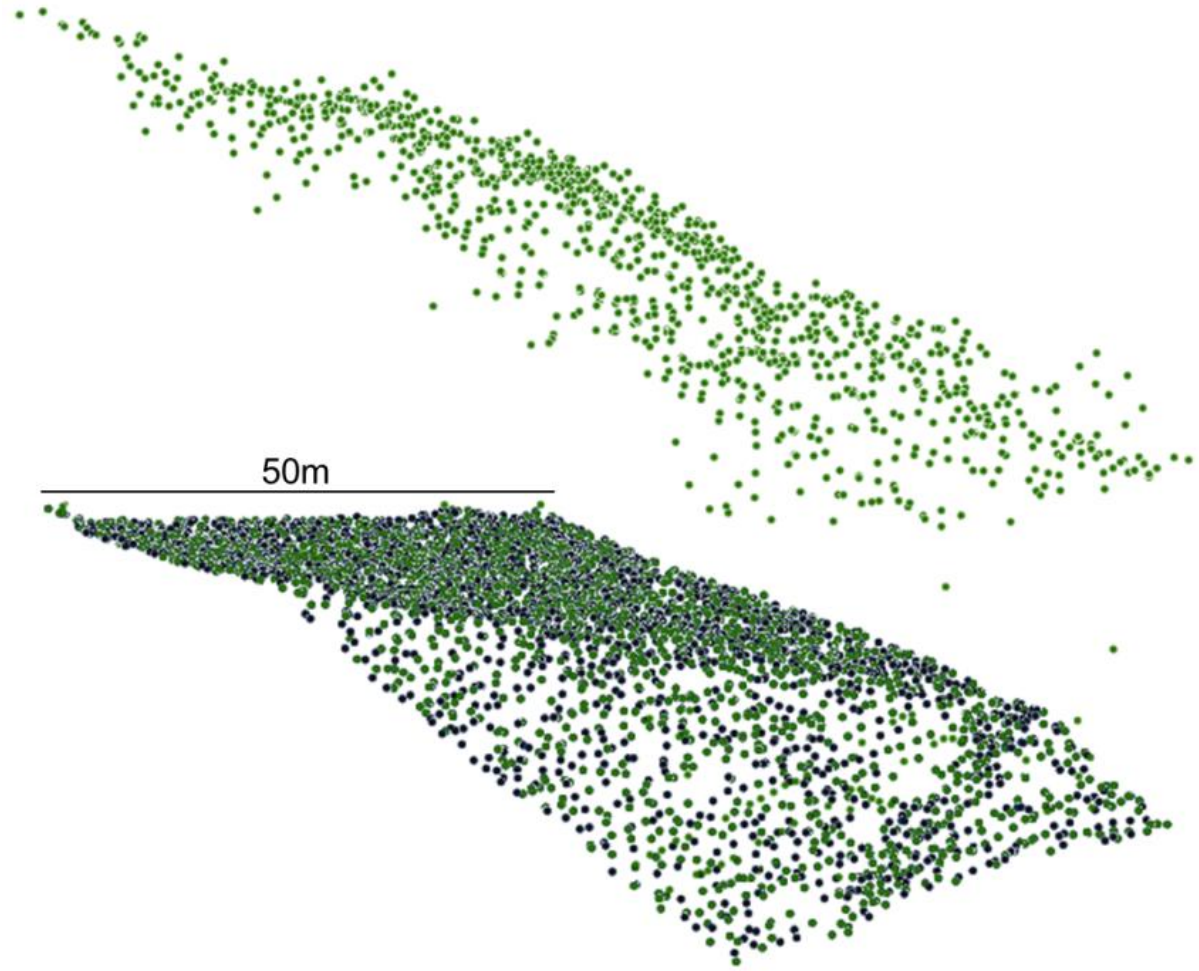

Fig. 2: **Exemplary visualization of lidar data.** Black points represent laser signals classified as terrain. Green points represent laser signals classified as vegetation or terrain.

The **Wood Warbler** (*Phylloscopus sibilatrix*) is a ground-nesting, long-distance migratory passerine with a distinctly European range (Glutz von Blotzheim & Bauer, 1991). In Switzerland, the species occupies deciduous and mixed forests at low to medium altitudes (Glutz von Blotzheim & Bauer, 1991). Within these forests, stands are preferred that feature an open stem space, a closed canopy (60%-90% closure), a small herb and shrub layer, and trees with low branches for song-flight behavior (Quelle & Tiedemann, 1972; Schifferli et al., 1980; Bibby, 1989; Glutz von Blotzheim & Bauer, 1991). Furthermore, territories are preferentially located on slopes with eastern or southerly aspects, while slopes with western and northern aspects are avoided (Quelle & Tiedemann, 1972; Hölzinger, 1999; Glutz von Blotzheim & Bauer, 1991). The species is not specialized to a specific tree species. In Switzerland, Wood Warblers most often breed in stands of sessile oak (*Quercus petraea*), common oak (*Quercus robur*), common beech (*Fagus sylvatica*), common hornbeam (*Carpinus betulus*) and Scots pine (*Pinus sylvestris*). But the species also settles in stands of weeping birch (*Betula pendula*), downy birch (*Betula pubescens*), trembling poplar (*Populus tremula*), European larch (*Larix decidua*), common spruce (*Picea abies*), Spanish chestnut (*Castanea sativa*), maple (*Acer sp*.) and lime tree (*Tilia sp*.) (Glutz von Blotzheim & Bauer,

1991). Gerber (2011) showed that occupied territories in Switzerland had denser herb layer, higher number of trees, lower rodent density and were located on steeper slopes than random control areas and abandoned territories. Reinhardt (2003) found that territories abandoned by Wood Warblers in forests along Lake Constance, Germany, tended to have older, higher and fewer trees than occupied territories. Additionally, territories of mated males more often featured a coherent herb layer and a higher number of grass or sedge tussocks compared to territories of unpaired males (Reinhardt, 2003). Pavlovic (2009) used lidar signals to show that Wood Warblers in the *Nationalpark Bayerischer Wald* in Germany preferred homogeneously structured forests with a sparse shrub layer.

Wood Warbler populations in Eastern Europe are subject to strong annual fluctuations but seem to persist (Glutz von Blotzheim & Bauer, 1991; Burfeld et al., 2004). Low natal and breeding philopatry and the avoidance of areas with high rodent density are considered responsible for these strong annual fluctuations (Glutz von Blotzheim & Bauer, 1991; Wesolowski et al., 2009). In Western Europe, Wood Warbler populations have declined in the last three decades (Glutz von Blotzheim & Bauer, 1991; Burfeld et al., 2004; Flade & Schwarz, 2004; Wesolowski & Maziarz, 2009). In Switzerland, the Wood Warbler has been classified as vulnerable in the red list of breeding birds (Keller et al., 2010a). Furthermore, the species is one of the 50 priority species of the Swiss species recovery program (Keller et al., 2010b; Spaar et al., 2012).

The reasons for the population decline of Wood Warblers in Western Europe are still unknown. The following hypotheses are controversially discussed in the research community: (1) structural habitat changes due to changing forestry practices (Bibby, 1989; Marchant, 1990; Glutz von Blotzheim & Bauer, 1991; Gatter, 2000; Marti, 2007; Reinhardt & Bauer, 2009; Mallord et al., 2012); (2) increased nest predation due to changes in the predator communities (Gatter, 2000; Wesolowski et al., 2009); (3) changes in the food supply as a consequence of climate change (Gatter, 2000; Both et al., 2010); (4) increase in disturbances due to augmented recreational activities (Miller et al., 1998; Miller & Hobbs, 2000; Kangas et al., 2010; Spaar et al., 2012); and (5) habitat changes in migration stopover sites and/or in wintering sites (Weber et al., 1999; Flade & Schwarz, 2004; Reinhardt & Bauer, 2009).

This master thesis addressed the first of the above hypotheses. The purpose of this study was (1) to achieve an increased understanding of the factors that may influence the territory choice of Wood Warblers in Switzerland and (2) to identify potentially suitable habitats in Switzerland. Both goals were addressed with the help of RS methods, particularly lidar. Furthermore, the habitat needs of Wood Warblers were analyzed at two spatial scales, namely at the scale of the nesting area and at the scale of the territory.

Firstly, lidar metrics were correlated with structural habitat variables collected in the course of the research project *Settlement behavior, population fluctuations and population structure of Wood Warbler* of the Swiss Ornithological Institute (Swiss Ornithological Institute, 2013). Secondly, the following question was addressed: Is it possible to distinguish Wood Warbler territories from control areas without Wood Warblers using lidar data or other RS information? Based on the results obtained, thirdly, predictive models were generated to

model the current potential range of the Wood Warbler in parts of Switzerland, namely in the Swiss Jura Mountains and the Swiss Plateau.

1.2 Hypotheses and predictions

To address the second question, RS variables were compiled that possibly influence territory choice of Wood Warblers. These independent RS variables were divided into the following **five thematic groups**: Height, vertical diversity, penetration rate, canopy cover and geography. Based on the current knowledge of the Wood Warbler's habitat preferences, one or more hypotheses were derived and tested for every group (Fig. 3):

Height group

H1: *The probability of Wood Warbler occurrence shows a concave (inverse U-shaped) relationship with vegetation height.*

Trees with a height of at least 8-10 m are required (Glutz von Blotzheim & Bauer, 1991). Furthermore, a certain stand age and therefore a certain vegetation height is necessary to allow for an open stem space (Schifferli et al., 1980; Glutz von Blotzheim & Bauer, 1991). Thus, suitability of a forest stand is expected to first increase with tree height. After an optimum, a negative trend is expected because Reinhardt (2003) and Gerber (2011) found that occupied Wood Warbler territories have higher number of trees than abandoned territories and control areas, and tree number is known to decrease with increasing stand height (Spurr & Barnes, 1980).

Vertical diversity group

H2: *The probability of Wood Warbler occurrence is negatively related to the standard deviation of vegetation height.*

Stands are preferred that feature a high canopy cover (60%-90%) and an open stem space with few bushes (Glutz von Blotzheim & Bauer, 1991). Such stands tend to have a homogeneous stand height and therefore a small standard deviation of vegetation height. In contrast, a high standard deviation of vegetation height results from stands with a mixture of large and small trees, and therefore from stands with a scattered crown closure (Müller et al., 2009).

Penetration rate group

H3: *The probability of Wood Warbler occurrence shows a concave relationship with the tree layer's penetration rate.*

Wood Warblers prefer stands with a well-developed canopy. On the other hand, stands are avoided that are either really dense or rather scattered (Glutz von Blotzheim & Bauer, 1991). Stands with a dense tree layer reflect a large proportion of lidar signals at the top of the canopy, with the result that a relatively small number of lidar signals reaches the ground. Therefore, the penetration rate of the tree layer is low in such stands. In open stands, however, many lidar signals are reflected on the ground. Therefore, the penetration rate of the tree layer is high in open stands (Müller et al., 2009). The optimum for Wood Warbler occurrence is expected to lie between high and low penetration rates.

H4: *The probability of Wood Warbler occurrence is positively related to the penetration rate of the mid-story layer and the penetration rate of the shrub and regeneration layer.*

Wood Warblers prefer stands with an open stem space and therefore a sparse mid-story layer (Quelle & Tiedemann, 1972; Bibby, 1989; Glutz von Blotzheim & Bauer, 1991). A sparse mid-story layer does not reflect many lidar signals, and therefore the penetration rate of the mid-story layer is high. Furthermore, the occurrence of Wood Warblers is positively related to the number of grass or sedge tussocks (Gerber, 2011), into which the nests are often placed. Therefore, it is expected that the probability of Wood Warbler occurrence decreases with increasing development of the shrub and regeneration layer because the shrub and regeneration layer inhibits the development of the underlying herb and grass layer (Irrgang, 1990).

Canopy cover group

H5: *The probability of Wood Warbler occurrence shows a concave relationship with canopy cover.*

Wood Warblers prefer stands with a canopy cover of 60%-80% for settlement (Quelle & Tiedemann, 1972; Bibby, 1989; Glutz von Blotzheim & Bauer, 1991).

Geography group

H6: *The probability of Wood Warbler occurrence increases with inclination.*

Some studies showed a positive correlation of Wood Warbler occurrence and inclination (Hölzinger, 1999; Reinhardt & Bauer, 2009; Gerber, 2011; Mallord et al., 2012).

H7: *The probability of Wood Warbler occurrence is positively related to solar radiation during March.*

Solar radiation is strongly dependent on topography and altitude (Zimmermann & Kienast, 1999). The period of March is important for spatial differentiation of snow melting in early spring and therefore for spatial differentiation of vegetation phenology (Fischer, 1990). Wood Warblers, returning from the wintering areas to their breeding grounds in April (Glutz von

Blotzheim & Bauer, 1991), may be affected by such small-scale differences in vegetation phenology. Furthermore, solar radiation is affected by aspect. Solar radiation is higher on south-facing slopes than on north-facing slopes. On west and east facing slopes, solar radiation is similar to that on horizontal surfaces (Tian et al., 2001). Apart from solar radiation, aspect is of significance for prevailing wind direction and precipitation. Wood Warbler territories with a northern or western aspect are rare (Quelle & Tiedemann, 1972; Hölzinger, 1999; Glutz von Blotzheim & Bauer, 1991; Reinhardt & Bauer, 2009), suggesting an avoidance of areas with relatively low solar radiation and/or an avoidance of the weather side. Another hypothesis is that Wood Warblers are attracted by higher food availability on south-facing slopes than on north-facing slopes (Jedrzejewsk & Jedrzejewski, 1998).

H8: *The probability of Wood Warbler occurrence is positively related to the proportion of broadleaf and conifer-broadleaf mixed forests*.

Forest type was considered because Wood Warblers in Switzerland predominantly settle in broadleaf and conifer-broadleaf mixed forests. Some studies observed a preference for mixed forests, consisting of either broadleaf forests with few conifers or coniferous forests with few broadleaves (Quelle & Tiedemann, 1972; Glutz von Blotzheim & Bauer, 1991).

H9: *The probability of Wood Warbler occurrence increases with distance to forest edge.*

Wood Warblers prefer stands with an open stem space and a sparse mid-story layer (Glutz von Blotzheim & Bauer, 1991). Close to forest edge, the lateral influx of light is increased, allowing for the development of lush undergrowth of bushes, regeneration or herb layer (Wales, 1972; Chen et al., 1992). According to Glutz von Blotzheim & Bauer (1991), Wood Warblers only settle close to forest edge if it is well developed. In this case, the light conditions near the forest edge are similar to those within the forest. Another hypothesis is that Wood Warblers avoid forest edge because of increased predator activity along habitat edges (Batary & Baldi, 2004).

H10: *The probability of Wood Warbler occurrence is dependent on soil conditions*. *In particular, it is expected that Wood Warbler occurrence decreases with soil deepness and both nutrient and water availability.*

The distribution of plant communities is determined by environmental factors. Important primary factors, directly affecting plant communities, are availability of light, water and nutrients (Schulze et al., 2005). Soil conditions directly influence the water and nutrient conditions and therefore the formation and distribution of ground vegetation (Willmanns, 1989). Very simplified and without considering light conditions within a forest stand, it can be assumed that deep, nutrient-rich and/or moist soils favor the development of a dense and tall herb layer possibly including bramble (*Rubus* sp.), while shallow, nutrient-poor and/or dry soils favor the occurrence of grasses and sedges (Ellenberg & Klötzli, 1972).

Wood Warblers generally avoid stands with a well-developed and tall herb layer (Schifferli et al., 1980; Glutz von Blotzheim & Bauer, 1991). But the nesting territories are often characterized by a dense grass layer (Reinhardt, 2003; Gerber, 2011). The availability of

grass and sedges may be important for enhanced cover, while a dense herb layer may interferes with the nesting activities.

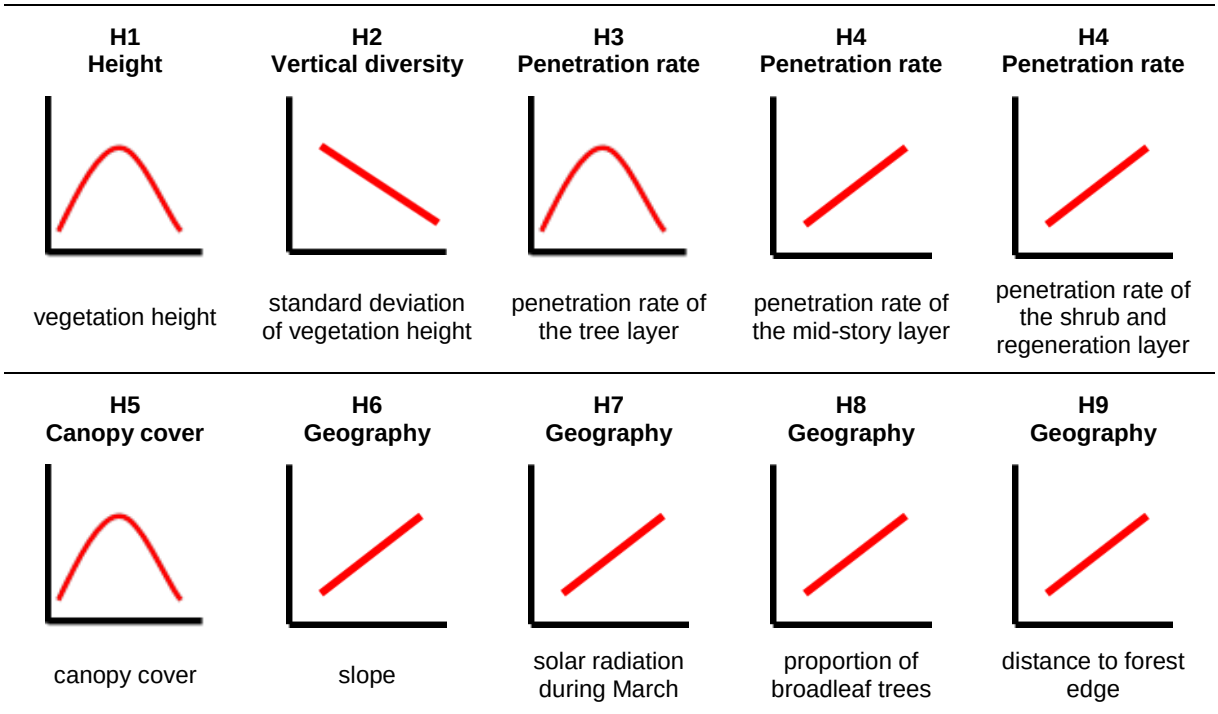

Fig. 3: Expected relationships between independent variables (x-axis) and the probability of Wood Warbler occurrence (y-axis).

2 Material and methods

2.1 Study areas

The study areas were located in northern Switzerland, particularly in the eastern Jura Mountains but also in the Swiss Plateau and the Pre-Alps (Fig. 4). They were all situated in woodland, predominantly in beech-dominated forests.

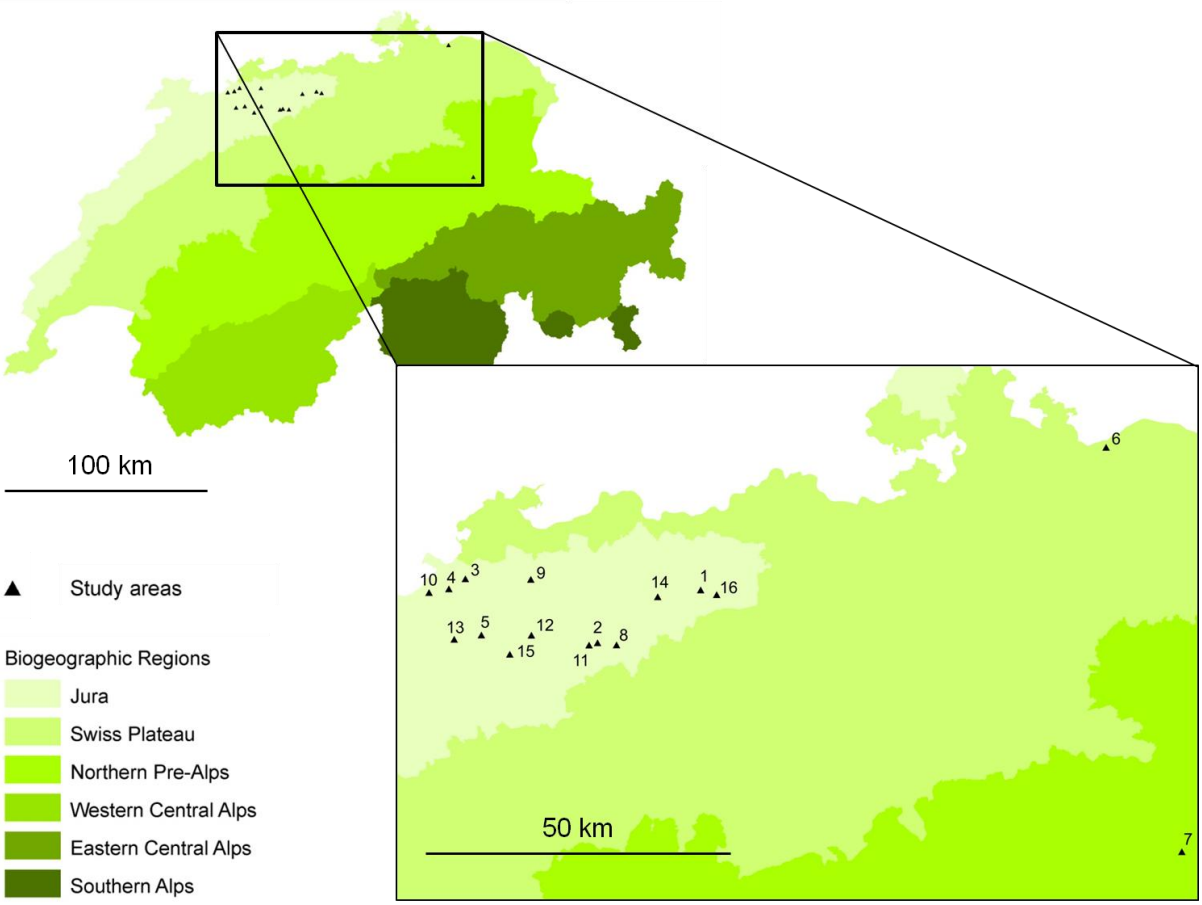

Fig. 4: **Study areas.** 1 *Bänkerjoch* AG (645'144 / 254'539), 2 *Belchen* SO (627'988 / 245'763), 3 *Blauen* BL (605'989 / 256'391), 4 *Dittingen* BL (603'249 / 254'717), 5 *Erschwil* SO (608'659 / 247'056), 6 *Gündelhart* TG (712'618 / 278'229), 7 *Ennenda* GL (725'218 / 211'059), 8 *Homberg* SO (631'140 / 245'407), 9 *Hochwald* SO (616'881 / 256'293), 10 *Kleinlützel* SO (599'946 / 254'110), 11 *Langenbruck* BL (626'575 / 245'376), 12 *Lauwil* BL (616'981 / 247'025), 13 *Montsevelier* JU (604'131 / 246'345), 14 *Oltingen* BL (638'000 / 253'403), 15 *Scheltenpass* SO (613'382 / 243'854) and 16 *Staffelegg* AG (647'810 / 253'757) (Biogeographic regions according to Gonseth et al. (2001) © BFS GEOSTAT / BUWAL).

Within each study area, sample areas were defined (Fig. 5). A sample area can have one of the following two occupation statuses: 1) occupied by a pair of Wood Warblers having a nest or 2) non-occupied. As sample areas served occupied areas and control areas mapped between 2010 and 2012 in the course of the research project *Settlement behavior, population fluctuations and population structure of the Wood Warbler* of the Swiss Ornithological Institute (Swiss Ornithological Institute, 2013). The nest position was considered the center of the occupied area. Control areas were assigned to the majority of

the occupied areas with their centers located 200-300 m away from the occupied ones. In the following, control areas associated with occupied areas are referred to as primary control areas. Further details of the nest mapping procedure and the choice of control areas can be found in Gerber (2011) and Grendelmeier (2011).

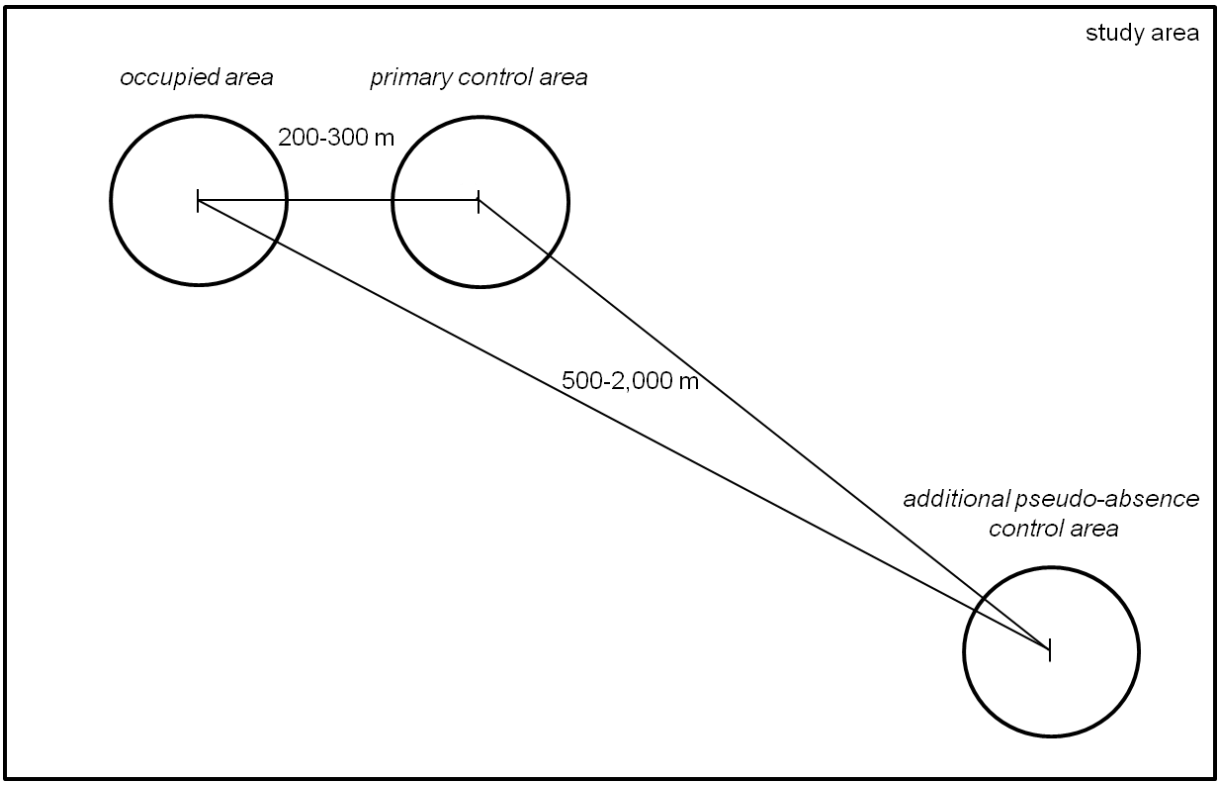

Fig. 5: Schematic illustration of the arrangement of the sample areas (occupied area, primary control area and additional pseudo-absence control area) within a study area.

Out of 136 occupied areas and 99 primary control areas, only sample areas were selected that did not overlap more than 10% with one another. Furthermore, occupied areas and primary control areas located in areas with an insufficient quality of the lidar data were excluded (see 2.3). Finally, 115 occupied areas and 84 primary control areas remained for the analyses.

With regard to the intended model of the potential Wood Warbler range, 113 additional pseudo-absence control areas were sampled. This was done because variables influencing habitat choice at a larger spatial scale may not be identified when only comparing occupied and non-occupied areas located in close proximity to each other. Thus, additional pseudo-absence control areas increased the range of environmental conditions considered. Additional pseudo-absence control areas were selected based on the precondition that they were located (1) in the forest, and (2) between 500 and 2,000 m away from the occupied areas and primary control areas. Given these preconditions, additional pseudo-absence control areas were then randomly selected. The choice of the distance is subject to a trade-

off. With regard to the model of the potential Wood Warbler range, the distance should be as large as possible to allow for increased environmental variation. However, with increasing distance, the probability rises that possibly existing occupied areas are mistakenly classified as pseudo-absence control areas. Within 500 to 2,000 m from the sample areas, the probability that the species was really absent is relatively high because the study areas were intensively examined (Gerber, 2011; Grendelmeier, 2011).

All analyses performed refer to two spatial scales, namely 1) to the scale of the nesting area and 2) to the scale of the territory. By using two spatial scales, the fact could be taken into account that variables influencing habitat choice at one scale will not necessarily influence habitat choice at another scale (e.g. Wiens et al., 1986).

A territory is defined as any defended area (Noble, 1939). If intraspecific competition permits, Wood Warbler males occupy territories of 1 to 3 ha (Glutz von Blotzheim & Bauer, 1991). Within the territory of the male, the female selects the place for the nest. After the choice of the nest site, the territory is reduced to a maximum area of approximately 0.12-0.19 ha (Glutz von Blotzheim & Bauer, 1991). Very small territories of, for example, 0.05 ha are occasionally occupied at high population density or as secondary territories of bigynous males (Glutz von Blotzheim & Bauer, 1991).

For this study, the nesting area was represented by a circular area of 0.01 ha (1,000 m^2) around the nest, corresponding to a circle with a radius of 17.8 m centered on the nest. At the scale of the territory, a circular area was examined that covered 0.6648 ha (6,648 m^2) around the nest. The corresponding radius was 2.5 times the radius of the nesting area, reflecting the spatial relationship between nesting area and territory.

2.2 Habitat variables

Habitat variables (Table 1) were collected for occupied areas and primary control areas between 2010 and 2012 within the framework of the research project accomplished by the Swiss Ornithological Institute. Further details on the methodology of habitat sampling can be found in Gerber (2011) and Grendelmeier (2011). Habitat variables were available for 62 occupied territories and 63 primary control areas.

2.3 RS variables

The RS variables fall into two groups: lidar metrics and non-lidar RS variables. The lidar metrics will be presented first. All RS data was processed in the Geographic Information System ESRI ArcInfo 9.3 and 10.0 (ESRI, Redlands, CA), in PyScripter for Python 3.3 and in the statistical environment R version 2.14.1 (R Development Core Team, 2011). LAStools were used for the operational processing of lidar data (Isenburg, 2012).

Table 1: Habitat variables examined in this study.

Variable	Definition
inclination	inclination of the hillside
canopy cover	proportion of ground surface covered by tree crowns, determined by crown photographs
dead wood	running meter of dead wood
vegetation cover	proportion of ground surface covered by vegetation < 50 cm
number of tussocks	number of grass and sedge tussocks
number of bushes	number of bushes and young trees with a height > 50 cm and a trunk circumference < 25.1 cm (dbh < 8 cm)
number of trees	number of trees with a trunk circumference > 25.1 cm (dbh > 8 cm)
amount of polewood	number of trees with a trunk circumference from 25.1 cm to 62.8 cm (8 cm < dbh < 20 cm)
number of immature trees	number of trees with a trunk circumference from 62.8 cm to 110.0 cm (20 cm < dbh < 35 cm)
number of conifers	number of conifers with a trunk circumference > 25.1 cm (dbh > 8 cm)
tree diversity	Shannon Index of tree diversity
number of dead trees	number of standing dead wood with a trunk circumference > 25.1cm (dbh > 8 cm)
number of trees branched below 4 m	number of trees branched below 4 m
number of trees branched below 10 m	number of trees branched below 10 m
average tree diameter	average of the diameter at breast height (DBH) of all trees
mkna	„minimum known number alive“, minimum number of caught rodents

2.3.1 Lidar metrics

The airborne laser scanning data used for the calculation of the lidar metrics (Table 2) was collected by private companies in the years 2000 to 2007, mainly outside the growing season (Swisstopo, 2009). The data consisted of two digital height models provided by the Swiss Federal Office of Topography (Swisstopo), namely the digital terrain model (DTM) and the digital surface model (DSM). The DTM contains only laser signals classified as terrain. Its interpolation into a regular 2 m grid results in the swissALTI3D (Swisstopo, 2003). The DSM consists of laser signals classified as vegetation, artificial structures or buildings, and terrain (Swisstopo, 2005). The two models, covering the area of Switzerland below 2,000 m a.s.l., have an average density of 0.5 laser signals per m^2 (Swisstopo, 2005). In the sample areas examined the average density was 1.5 laser signals per m^2. The height accuracy ranges from 0.5 m in open terrain to 1.5 m in terrain with vegetation (Swisstopo, 2005).

For all sample areas, lidar metrics were calculated for both the nesting area and the territory scale of 1,000 m^2 and 6,648 m^2, respectively. In addition to the two height models, the normalized digital surface model (nDSM), representing vegetation height, was derived by subtracting the DSM from the swissALTI3D. Values deviating negatively by three or more times the standard deviation from the mean of all negative values of the nDSM were treated as outliers and excluded from further analyses (Grubbs, 1969).

The lidar metrics were assigned to the thematic groups introduced in paragraph 1.2: height, vertical diversity, penetration rate, canopy cover and geography. All metrics were derived from the nDSM except slope, which was directly calculated from the swissALTI3D.

Metrics of the **first and second group** refer to vegetation (VH) or canopy height (CH). VH equates to the nDSM and therefore contains the information about the height above ground of every lidar signal of the DSM. To calculate CH, a 2x2 m grid was laid over every sample area, and the maximum lidar signal for each 2x2 m cell was extracted. Finally, the following metrics were calculated per sample area: mean vegetation and mean canopy height (meanVH and meanCH), maximum vegetation height (maxVH), the 95% percentile of vegetation height (VH95), and the standard deviation of both vegetation and canopy height (sdVH and sdCH). In addition, three metrics were generated referring specifically to the tree layer, namely mean vegetation height above 3 m (meanVH>3m), mean canopy height above 3 m (meanCH>3m) and the standard deviation of canopy height above 3 m (sdCH>3m). The three metrics were calculated including only laser signals reflecting from objects more than 3 m above ground. Thereby, contrary to the other lidar metrics, the calculation of these metrics did not include lidar signals that were reflected from the ground. Mean vegetation height less than 3 m (meanVH<3m) refers to the shrub and regeneration layer and is represented by the arithmetic mean of all lidar signals less than 3 m above ground. Therefore, this metric also includes lidar metrics reflected from the ground.

MeanVH is an index of vegetation height in general and describes the vertical structure of a stand, whereas meanCH refers specifically to the upper canopy layer. The standard deviation provides a measure of the vertical variation of VH and CH. A small standard deviation arises from sample areas with a homogeneous vegetation or tree height. On the other hand, a large standard deviation reflects a mixture of heterogeneous vegetation or tree height (Müller et al., 2009).

Metrics of the **third group** comprise penetration rates for three different vegetation layers. Pen50_2 refers to the tree layer, pen10_2 to the mid-story layer and pen5_1 to the shrub and regeneration layer. To calculate pen50_2, the sum of all lidar signals below 2 m above ground was divided by the sum of all lidar signals below 50 m above ground. Pen10_2 is described by the ratio of the sum of all lidar signals below 2 m and the sum of all lidar signals below 10 m. To describe the shrub and regeneration layer, the ratio of the sum of all lidar signals below 1 m and the sum of all lidar signals below 5 m was calculated (Müller et al., 2009).

A particular layer, i.e. the tree layer, the mid-story layer, or the shrub and regeneration layer, is more developed the lower the corresponding penetration rate is. For example, sample areas with a dense tree layer exhibit a small pen50_2, because many lidar signals are reflected at the top of the canopy and therefore a relatively small number of signals reaches the ground (Müller et al., 2009; Pavlovic, 2009).

The **canopy cover group** contains metrics describing canopy cover at four height levels, namely at 3 m, 10 m, 15 m and 20 m above ground. The calculation of canopy cover was based on the data of CH. The respective canopy cover results from the ratio of the number of 2x2 m cells with values above the particular height level and the total number of 2x2 m cells

per sample area (Fig. 6). Canopy cover is higher the more lidar signals are present above the particular height level.

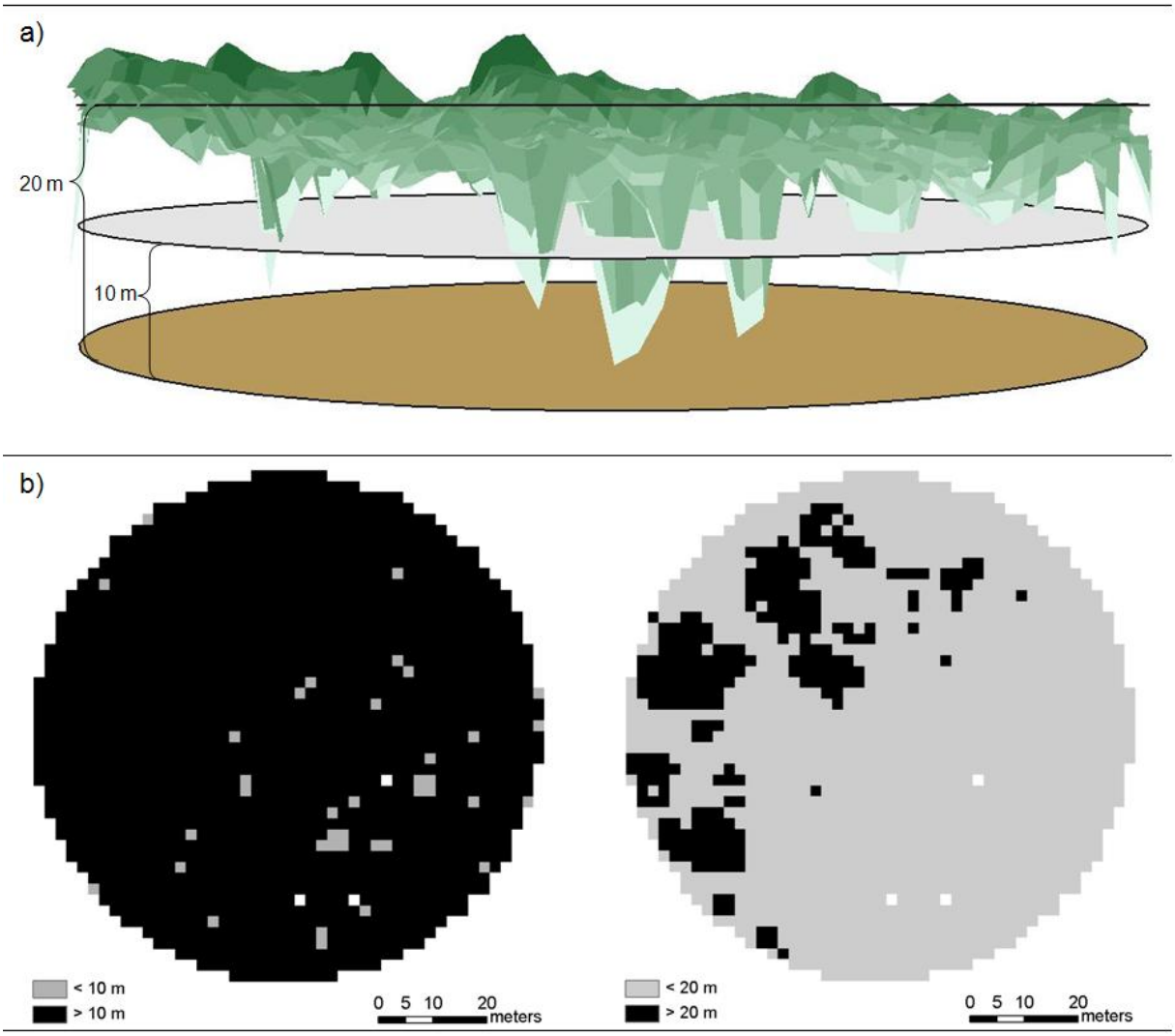

Fig. 6: **Illustration of the relationship between canopy cover (CC) and canopy height (CH).** The figure shows a sample area characterized by almost closed canopy at 10 m above ground and sparse canopy above 20 m. This would represent a closed forest stand with few trees higher than 20 m. a) shows canopy height (CH) and the two height levels 10 m and 20 m for a sample area. The darker the color, the higher is CH. In b), the two metrics meanCC_10m and meanCC_20m are pictured (CC = canopy cover). CC results from the ratio of the number of 2x2 m cells with values above the particular height level (black cells) and the total number of 2x2 m cells per sample area. In white cells, no lidar signal was detected above 3 m (DSM, swissALTI3D © Swisstopo).

The **geography group** only comprises one lidar metric, namely the slope metric. Slope values were extracted from the swissALTI3D grid and averaged per sample area.

Table 2: Lidar metrics. The metrics are grouped according to the five thematic groups and the hypotheses introduced in paragraph 1.2.

Hypo-thesis	Metric	Unit	Definition	Interpretation
Height (H1)	meanVH	[m]	mean vegetation height	MeanVH describes the vertical structure of a stand. A well-developed overstorey leads to a high meanVH, because many lidar signals are reflected by the uppermost layer. In contrast, an intermediate or a low meanVH is expressed by stands with a well-developed medium layer and scattered or young stands.
	meanCH	[m]	mean canopy height	MeanCH is a measure for stand height. It is low when either the tree height is low or the stand structure is scattered so that few high trees are present.
	meanVH<3m	[m]	mean vegetation height less than 3 m	MeanVH<3m specifically refers to the regene-ration and underwood comprised of young trees and shrubs. The metric will be around zero, if no regeneration and underwood is present and higher the more young trees and shrubs are present.
	meanVH>3m	[m]	mean vegetation height above 3 m	MeanVH>3m incorporates laser signals reflected by trees higher than 3 m. It does not consider laser signals reflected by the regeneration, underwood or ground. MeanVH is higher the higher the trees are and the better developed the canopy is.
	meanCH>3m	[m]	mean canopy height above 3 m	MeanCH>3m is a measure for stand height corrected for gaps located within the forest and the non-forested surrounding of forest edge.
	maxVH	[m]	maximum vegetation height	MaxVH represents the maximal tree height within a sample area.
	VH95	[m]	95% percentile of vegetation height	VH95 represents the height above ground below which 95% of all lidar signals were detected. Compared to maxVH, VH95 is less sensitive to outliers.
Vertical diversity (H2)	sdVH	[m]	standard deviation of vegetation height	SdVH is a measure for the stratification of a stand. High values arise from stands with a heterogeneous tree height, while stands with a homogeneous tree height express low sdVH values.
	sdCH	[m]	standard deviation of canopy height	SdCH describes the heterogeneity of canopy height. Similar to sdVH, high values arise from stands with a heterogeneous tree height, while stands with a homogeneous tree height express low sdCH values.
	sdCH>3m	[m]	standard deviation of canopy height above 3 m	Equal to sdCH, sdCH>3m is a measure for the heterogeneity of canopy height. In contrast to sdCH, sdCH>3m does not consider gaps within the forest or non-forested surroundings of forest edge.
Penetration rate (H3,H4)	pen50_2	[%]	penetration rate 50-2 m above ground	Pen50_2 refers to the tree layer and describes its penetration. Low penetration rates originate in stands with a well-developed tree layer, while high penetration rates result from scattered or open stands.
	pen10_2	[%]	penetration rate 10-2 m above ground	Pen10_2 describes the density of the mid-story. Low penetration rates originate in stands with a well-developed mid-story, while high penetration rates result from stands with a sparse mid-story.
	pen5_1	[%]	penetration rate 5-1 m above ground	Pen5_1 refers to the shrub and regeneration layer. High pen5_1 values result from stands with a sparse shrub and regeneration layer, while low values originate in stand with a well-developed shrub and regeneration layer.

Table 2 continued from previous page

Hypo-thesis	Metric	Unit	Definition	Interpretation
Canopy cover (H5)	meanCC	[%]	mean canopy cover above 3 m	MeanCC describes mean cover of all trees higher than 3 m of a sample area. High values represent a high cover, while low values originate in scattered or open stands.
	meanCC_10m	[%]	mean canopy cover above 10 m	MeanCC_10m is a measure for canopy cover at 10 m above ground. High values represent closed stands, while low values originate in scattered or open stands.
	meanCC_15m	[%]	mean canopy cover above 15 m	MeanCC_15m describes canopy cover at 15 m above ground. High values represent closed stands with many trees higher than 15 m, while low values represent scattered or open stands and stands with many tall trees.
	meanCC_20m	[%]	mean canopy cover above 20 m	MeanCC_20m is a measure for canopy cover of trees equal or higher than 20 m. High values originate in stands with many trees higher than 20 m, while open or scattered stands and stands with many tall trees express low values.
Geography (H6)	slope	[°]	slope	Slope describes mean inclination per study area.

In addition, the following three **quality variables** were calculated to ensure that the data quality of the nDSM was broadly similar in all sample areas: number of lidar signals, number of lidar signals less than 1 m, and the ratio of the latter to the former. In doing so, it was detected that the data collected by Toposys was filtered in a different way than the data collected by other companies, so that few vegetation signals remained in the DSM (Christian Ginzler, pers. comm., 29.10.2012). Therefore, the sample areas affected were excluded from further analyses.

2.3.2 Non-lidar RS variables

In addition to the lidar metrics, the following non-lidar RS variables (Table 3) were calculated: potential direct solar radiation during March (r_march), forest type (forest_type), distance of the center of the sample area to forest edge (dist_f), and various soil condition variables, such as soil depth, soil skeleton, water holding capacity (WHC), soil nutrients, water permeability and waterlogging.

The values for the non-lidar RS variables were derived from the data sources listed in Table 3. **R_march** describes the potential direct solar radiation during March (Zimmermann & Kienast, 1999). The r_march values were extracted from the data source and averaged per sample area. **Forest_type** was obtained by extracting the vegetation classification, reaching from one to four representing coniferous to broadleaf forest, respectively (Federal Statistical Office, 2001). The classification values were averaged per sample area. **Dist_f** represents the shortest distance from the center of the sample area to the edge of the forest, extracted from the swissTLM3D. The **soil condition variables** were derived at the center of the sample areas.

Table 3: Non-lidar RS variables. The variables are grouped according to the five thematic groups and the hypotheses introduced in paragraph 1.2.

Hypothesis	Variable	Unit	Definition	1) Data source; 2) Data processing
Geography (H7-H10)	r_march	[100 KJoule/m^2]	direct solar radiation during March	1) Bioclimatic carts of Switzerland on the basis of long-term station data collected by MeteoSwiss; 25x25 m resolution © WSL (Zimmermann & Kienast, 1999) 2) resampled to a resolution of 5x5 m
	forest_type	[1-4]	forest type	1) Waldmischungsgrad der Schweiz; 25x25 m resolution © Federal Statistical Office, GEOSTAT, CH-2010 Neuchâtel (Federal Statistical Office, 2001) 2) resampled to a resolution of 5x5 m
	dist_f	[m]	distance to forest edge	1) swissTLM3D © Federal Office of Topography swisstopo (Swisstopo, 2012) 2) selection: GDB-Code = 12 (*Wald*)
	depth	[1-6]	soil depth	1) Bodeneignungskarte der Schweiz © Federal Statistical Office, GEO-STAT, CH-2010 Neuchâtel
	skeleton	[1-6]	soil skeleton	
	WHC	[1-6]	water holding capacity	
	nutrients	[1-6]	soil nutrients	
	permeability	[1-6]	water permeability	
	waterlogging	[1-6]	waterlogging	

2.4 Statistical analyses

All analyses were performed in the statistical environment R version 2.14.1 (R Development Core Team, 2011). The following packages were used: lme4 (Bates et al., 2012), AICcmodavg (Mazerolle, 2012) and PresenceAbsence (Freeman, 2012).

2.4.1 Correlation analyses

To analyze the intercorrelations of the RS variables based on Spearman's rank correlation coefficients (r_s), the area of the territory (6,648 m^2) was used. In order to avoid spatial dependencies of the independent variables, the number of sample areas was reduced from 312 to 264 so that the sample areas remaining did not overlap more than 10%.

The analysis between the lidar metrics and habitat variables was based on data from 125 sample areas, consisting of 62 occupied areas and 63 primary control areas, all referring to an area of 1,000 m^2. Again, Spearman's rank correlation coefficients (r_s) were calculated.

2.4.2 Data partitioning

Prior to the statistical analysis described below, the dataset was divided into two equal parts, referred to as training data and testing data (Table 4) (Fielding & Bell, 1997). The training data was used for model building and verification, while the testing data was used for

validation. The partitioning of the data was done at random with the following constraints: (1) primary control areas paired with an occupied area belonged to the same data set as the corresponding occupied area; (2) if the sum of the occupied areas and the primary control areas was less than 10 per study area, it was ensured that half of the occupied areas and primary control areas was allocated to the training data and the other half to the testing data; and (3) it was ensured that occupied areas, primary control areas and additional pseudo-absence control areas were assigned equally to the training and testing data. Both the training data and the testing data contained 156 sample areas each.

Table 4: Data partitioning of the sample areas (occupied areas, primary control areas, pseudo-absence control areas) into training data and testing data.

Study area	Occupied areas		Primary control areas		Additional pseudo-absence control areas	
	training data	testing data	training data	testing data	training data	testing data
Bänkerjoch AG	1	1	0	1	5	3
Belchen SO	2	2	2	1	0	0
Blauen BL	4	4	2	1	3	2
Dittingen BL	1	2	1	0	0	2
Erschwil SO	1	1	1	1	5	3
Gündelhart TG	1	0	1	0	2	4
Ennenda GL	3	4	3	2	2	1
Homberg SO	3	3	2	3	3	3
Hochwald SO	2	2	2	1	2	3
Kleinlützel SO	9	8	6	9	6	5
Langenbruck BL	3	4	3	2	5	5
Lauwil BL	8	10	6	6	3	2
Montsevelier JU	9	5	6	4	3	7
Oltingen BL	0	1	0	1	2	2
Scheltenpass SO	9	9	7	8	9	9
Staffelegg AG	1	2	0	2	7	5
Total	**57**	**58**	**42**	**42**	**57**	**56**

2.4.3 Model structure and model selection

Generalized linear models (GLMs) and generalized linear mixed-effect models (GLMMs) were used to determine the importance of the independent RS variables for Wood Warbler's territory choice. All RS variables were standardized (mean = 0, standard deviation = 1).

The statistical analysis was performed as follows: First, occupied areas and corresponding primary control areas were analyzed at the scale of the nesting area (1,000 m^2) to answer the question whether the RS variables calculated were suitable to distinguish occupied areas from control areas. This analysis was performed using GLMMs with two random effects, namely study area and occupied-control pairs nested within study area. A subset of the training data was used (Table 5), because only paired occupied areas and primary control

areas and no additional pseudo-absence control areas could be included in the analysis. The binomial response variable was specified as occupation status of the sample areas, with 1 denoting occupied areas and 0 primary control areas.

Second, GLMs were applied to the whole training data (Table 4), containing occupied areas, primary control areas and additional pseudo-absence control areas. This analysis was performed at both nesting area (1,000 m^2) and territory (6,648 m^2) scale. The binomial response variable was specified as occupation status of the sample areas, with 1 denoting occupied areas and 0 primary control areas and additional pseudo-absence control areas.

Table 5: Subset of training and testing data of paired occupied areas and primary control areas used for GLMMs.

Study area	Occupied areas		Primary control areas	
	training data	testing data	training data	testing data
Bänkerjoch AG	0	1	0	1
Belchen SO	2	1	2	1
Blauen BL	2	1	2	1
Dittingen BL	1	0	1	0
Erschwil SO	1	1	1	1
Gündelhart TG	1	0	1	0
Ennenda GL	1	1	1	1
Homberg SO	2	3	2	3
Hochwald SO	2	1	2	1
Kleinlützel SO	6	8	6	8
Langenbruck BL	3	2	3	2
Lauwil BL	5	6	5	6
Montsevelier JU	6	3	6	3
Oltingen BL	0	1	0	1
Scheltenpass SO	7	8	7	8
Staffelegg AG	0	2	0	2
Total	**39**	**39**	**39**	**39**

Model selection and model averaging were based on AIC (Akaike Information Criterion), following an approach described by Burnham & Anderson (2002). This approach accounts for model selection uncertainty and leads to more robust inferences, because they are not based on a single best model (Burnham & Anderson, 2002). AIC is an estimate of the mean log-likelihood and a measure of model fit (Akaike, 1974). It takes into account both the statistical goodness of model fit (log-likelihood) and the number of independent variables estimated to achieve this particular degree of fit. A penalty is imposed for increasing the number of independent variables (Everitt, 2002). In this study, AICc (corrected Akaike Information Criterion), a derivative of AIC, was used to account for small sample size (second-order bias correction), because the ratio of the number of observations to the

number of variables was below 40 (Hurvich & Tsai, 1989). The candidate models calculated were ranked from best to worst according to their AICc values, with the best supported model having the smallest AICc. AICc differences (ΔAICc) were calculated. Models with ΔAICc values < 2 compared to the best supported one are considered to have similar support. Models with ΔAICc values > 2 compared to the best model are considered to be less supported by the data (Burnham & Anderson, 2002).

The independent variables (Table 2 and Table 3) were assigned to the five **thematic groups** introduced in paragraph 1.2. According to the hypotheses formulated, quadratic effects were included for the variables meanVH, meanCH, meanVH>3m, meanCH>3m, maxVH, VH95, pen50_2, meanCC, meanCC_10m, meanCC_15m and meanCC_20m. The variables describing soil conditions were excluded *a priori* because they hardly varied between occupied areas and control areas (Fig. 16/Appendix A1).

For each thematic group, a set of candidate models was first constructed. These five sets included models with all combinations of the variables of the particular group, except that variables correlating more than |0.5| were never included together in the same model. Also, no interactions were considered. For GLMMs, the null model included the intercept and the two random effects study area and occupied-control pairs nested within study area, while, for GLMs, the null model consisted of the intercept only. A variable was considered relevant if (1) it was included in the best supported model or in a model with a ΔAICc value < 2 compared to the best supported one and (2) had a model-averaged estimate across all models per group greater than the model-averaged standard error (SE). These conditions are referred to as selection criteria for the variables.

Secondly, an **across-group analysis** was performed including only the relevant variables of each thematic group. In the across-group analysis, variables appearing in the best supported model or a model with a ΔAICc value < 2 compared to the best supported one were **categorized** according to their performance. Variables considered to have a **strong effect** were those with a model-averaged estimate greater than the model-averaged SE and a 95% confidence interval (CI) excluding zero. Variables with a model-averaged estimate greater than the model-averaged SE and a 95% CI including zero were denoted as variables with **moderate effect**. Variables considered to have a **weak effect** only fulfilled the criterion of occurring in the best supported model or a model with a ΔAICc value < 2 compared to the best supported one.

2.4.4 Model fit

Model performance and robustness were evaluated based on verification, validation and a 10-fold cross validation for both the nesting area scale and the territory scale. Among the best supported models (ΔAICc value < 2) of the across-group analysis, model performance and robustness was evaluated for all models that included variables with strong and moderate effects. Model-averaged estimates of the across-group analysis were used as coefficients.

For **verification**, the models were applied to the training data, while, **for validation**, the testing data was used. The following accuracy measures were calculated for verification and validation: false positive rate (fpos), false negative rate (fneg), sensitivity (sens), specificity (spec), true skill statistic (TSS) and area under the ROC (receiver operating characteristic) curve (AUC).

Fpos, fneg, sensitivity and specificity were used to evaluate the success of the models to correctly predict presence and absence of Wood Warblers. All of these accuracy measures were derived from the classification matrix (Table 6) (Everitt, 2002), also denoted as error matrix or confusion matrix (Allouche et al., 2006).

Table 6: Classification matrix used to evaluate predictive accuracy of presence-absence models. *a*, observed presences correctly predicted by the model; *b*, observed absences for which the model predicted presence; *c*, observed presences for which the model predicted absence; *d*, observed absences correctly predicted by the model (Allouche et al., 2006).

		Observation	
		Presence	Absence
Prediction	Presence	*a*	*b*
	Absence	*c*	*d*

Fpos equates to the proportion of sample areas predicted occupied but actually unoccupied to all observed absences ($b/(b+d)$). **Fneg** is the proportion of sample areas predicted unoccupied but actually occupied to all observed presences ($c/(a+c)$) (Morrison et al., 1992). **Sensitivity** is the proportion of observed presences that are predicted as such to all observed presences ($a/(a+c)$), and **specificity** describes the proportion of observed absences that are predicted as such to all observed absences ($d/(b+d)$) (Allouche et al., 2006).

Further, **TSS** was used to evaluate the overall agreement between predictions and observed data. TSS corrects the overall accuracy of model predictions by the accuracy expected to occur by chance. TSS is a special case of Cohen's kappa, given that the proportions of presences and absences in the validation set are equal. Therefore, TSS is not dependent on prevalence, which is described by the proportion of observed presences ($(a+c)/n$). TSS is defined as sum of sensitivity and specificity less one (Allouche et al., 2006). The values obtained range from -1 to +1, where +1 indicates perfect agreement, zero a performance no better than random and -1 a systematically incorrect prediction (Cohen, 1960; Allouche et al., 2006). To describe the relative strength of agreement associated with Cohen's kappa, Landis & Koch (1977) assigned the following labels to the corresponding ranges of Cohen's kappa: <0.00 = poor, 0.00-0.20 = slight, 0.21-0.40 = fair, 0.41-0.60 = moderate, 0.61-0.80 = substantial, 0.81-1.00 = almost perfect. Because TSS is a special case of Cohen's kappa, the same benchmark can be applied to assess the relative strength of agreement.

To calculate the accuracy measures introduced above, a **cut-off threshold** is necessary to classify the non-dichotomous scores derived by the model into presence and absence values

(Allouche et al., 2006). For verification, the threshold was used that maximized TSS. Validation was performed using the same threshold.

AUC is another measure to evaluate overall accuracy. Contrary to the accuracy measures just described, AUC is a threshold-independent measure for model performance and represents the area under the ROC curve. Each point on the ROC curve represents a sensitivity/(1 – specificity) pair corresponding to a particular cut-off threshold. The closer the ROC curve is to the upper left corner, the more the AUC value approaches to its maximum value of 1, representing a perfect discrimination of occupied and non-occupied areas (Zweig & Campell, 1993).

In addition to the verification and validation, a **10-fold cross validation** was performed with the testing data to evaluate model robustness. For this purpose, the testing data was randomly split into 10 subsets of equal size. Afterwards, the model was fitted based on the data of nine subsets. Then, the fitted coefficients were used to predict the values of the subset not used before. Based on this prediction, the same accuracy measures were calculated as for verification and validation. This procedure was repeated until every subset once served as validation data (Hastie et al., 2009). For every model, the 10-fold cross validation was performed 10 times. Finally, the mean value and both the 5% and 95% quantiles were calculated for every accuracy measure. The two quantiles calculated include 90% of all values obtained.

2.5 Modeling of the current potential range in parts of Switzerland

Among the models evaluated, two models were selected (see 3.3.1) to model the current potential range of Wood Warblers in the Swiss Jura Mountains and the Swiss Plateau. Model-averaged estimates of the across-group analysis were used as coefficients. To calculate the lidar metrics required, PyScripter for Python 3.3 was applied (Appendix A4). A prediction was calculated for 631,281 cells of 80x80 m located in the forest. The area covered by these forest cells corresponds to the entire forest area (swissTLM3D, GDB-Code = 12 (*Wald*)) within the two biogeographic regions Swiss Jura Mountains and Swiss Plateau. Only, areas with an insufficient quality of the lidar data were excluded (see 2.3.1). The output of the prediction was averaged within a circle with a radius of 1,000 m for each 80x80 m forest cell for increased distinguishability of areas including many suitable forest cells for Wood Warbler occurrence.

3 Results

3.1 Correlation analyses

Many lidar metrics were highly correlated with one another (Table 7). In particular, positive correlations occurred between meanVH, meanCH, meanVH>3m, meanCH>3m, maxVH, VH95, sdVH and meanCC_20m. On the other hand, meanVH<3m, pen5_1 and slope were weakly correlated with other lidar metrics. The lidar metrics were weakly correlated with the non-lidar RS variables (Table 7).

As expected, the *inclination* habitat variable and the slope lidar metric were strongly correlated (r_s = 0.82) (Table 8 and Fig. 7). Apart from that, *average tree diameter* and VH95 showed the strongest correlation (r_s = 0.62) (Fig. 7).

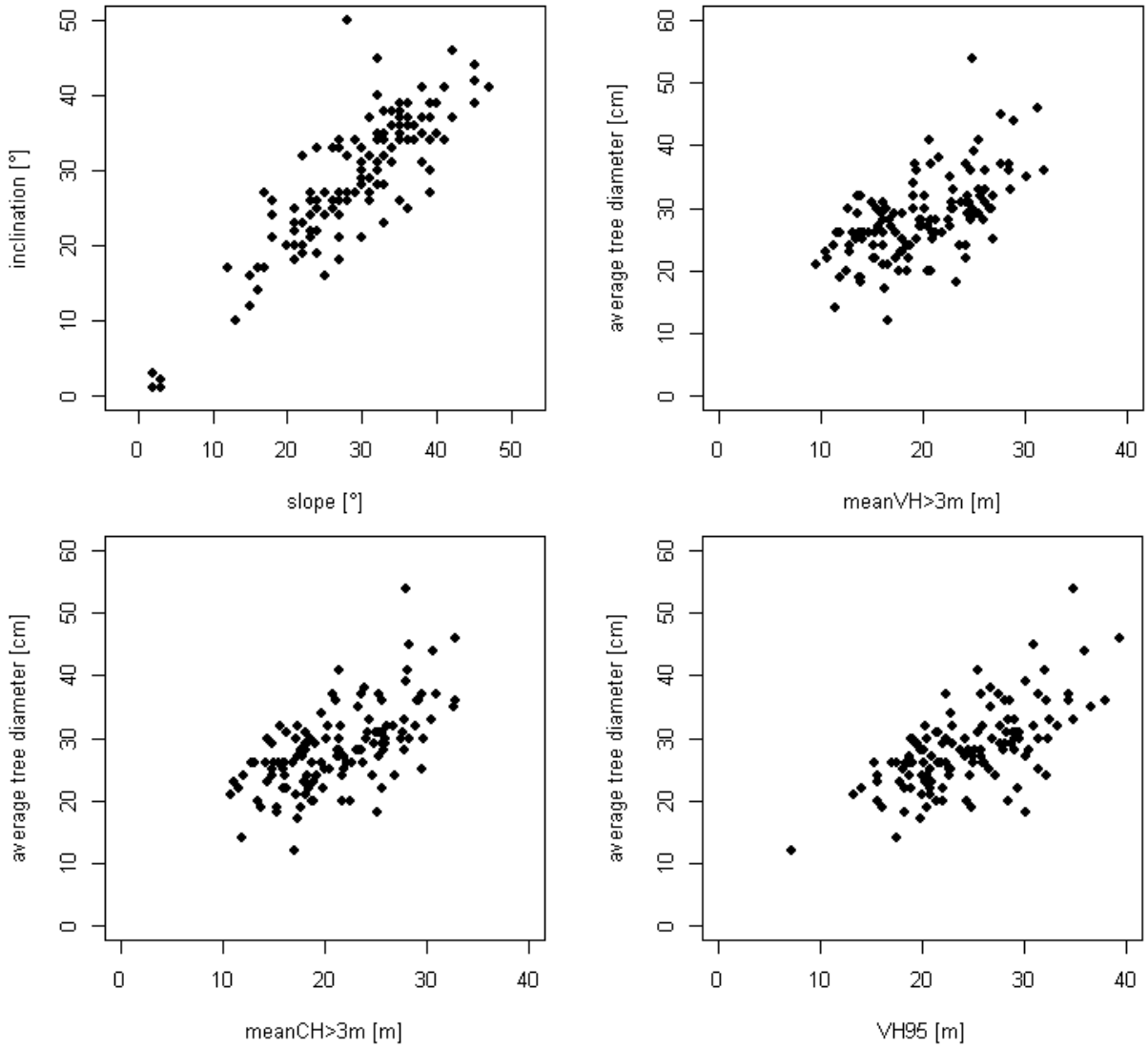

Fig. 7: Scatter plots of habitat variables (y-axis) and lidar metrics (x-axis) with Spearman's rank correlation coefficients (r_s) ≥ 0.6. N = 125.

Furthermore, *average tree diameter* was positively correlated with meanVH, meanCH, meanVH>3m, meanCH>3m, maxVH, sdVH and meanCC_20m. In contrast, *number of tussocks*, *number of trees*, *trees branched below 4 m*, *trees branched below 10 m* and *amount of pole wood* showed moderate to strong negative correlations with the lidar metrics listed before. Furthermore, both *number of immature trees* and *number of dead trees* showed negative correlations with maxVH and VH95. With regard to the metrics of penetration rates, the strongest correlations occurred between *number of conifers* and both pen50_2 and pen10_2. *Canopy cover* was not strongly correlated with the lidar metrics describing canopy cover, such as meanCC, meanCC_10m, meanCC_15m or meanCC_20m (Fig. 8).

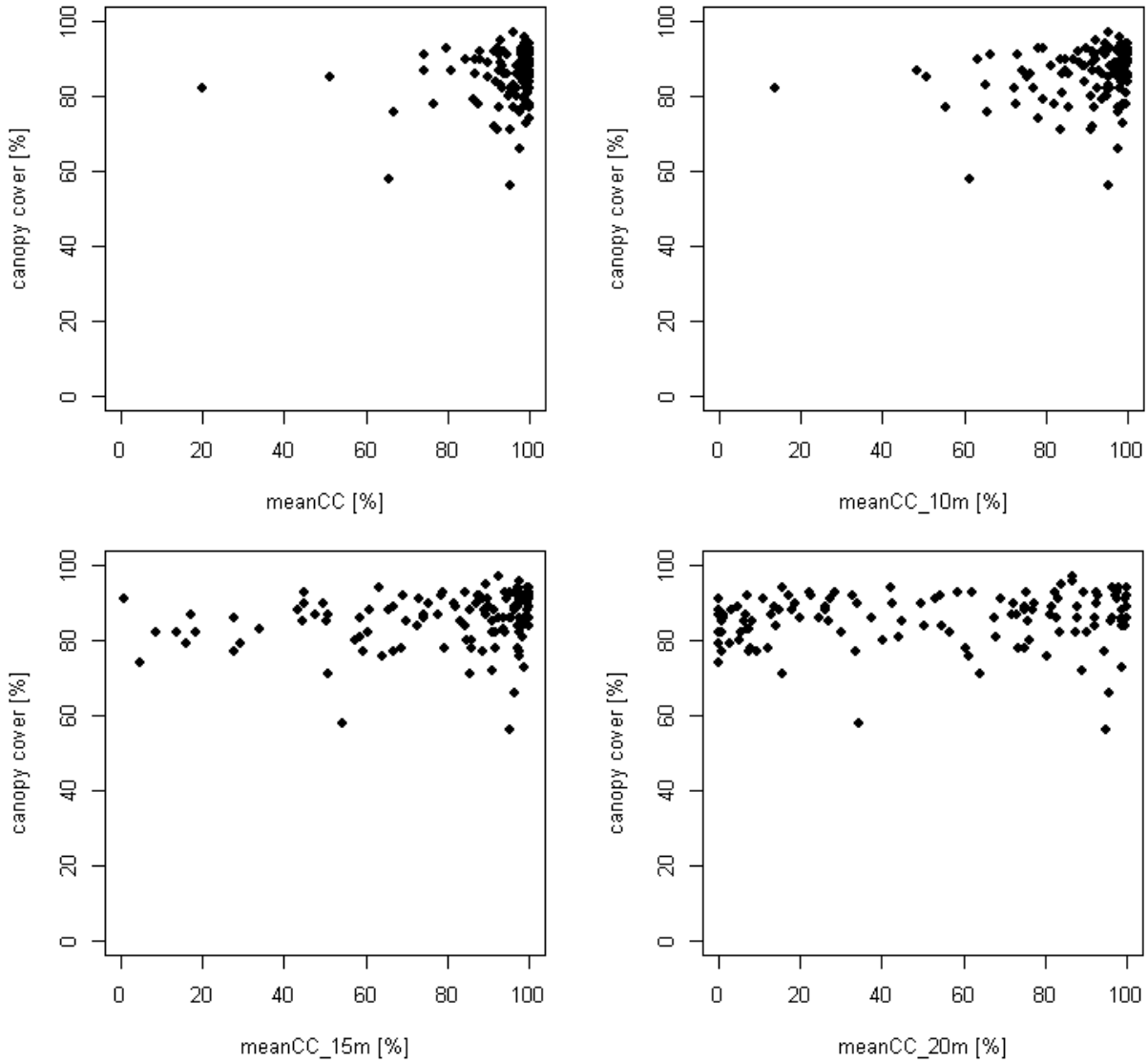

Fig. 8: Scatter plots of the *canopy cover* habitat variable (y-axis) and lidar metrics describing canopy cover (x-axis). N = 125.

Table 7: Spearman's rank correlation coefficients (r_s) of the RS variables based on data from 82 occupied areas, 69 primary control areas and 113 additional pseudo-absence control areas (N=264). Correlations ≥ |0.50| are printed in bold. Variables correlating more than |0.5| were never included together in the same model. A description of the variables can be found in the Tables 2 and 3.

	dist_f	forest_type	r_march	slope	meanCC_20m	meanCC_15m	meanCC_10m	meanCC	pen5_1	pen10_2	pen50_2	sdCH>3m	sdCH	sdVH	VH95	maxVH	meanCH>3m	meanVH>3m	meanVH<3m	meanCH
meanVH	0.1	-0.1	0.0	0.0	**0.7**	**0.7**	**0.6**	0.4	0.0	0.0	**-0.7**	0.0	-0.1	**0.5**	**0.6**	0.4	**0.6**	**0.6**	-0.1	**0.8**
meanCH	0.2	0.1	0.1	-0.1	**0.9**	**0.8**	**0.7**	0.4	0.3	0.4	-0.3	-0.1	-0.1	0.7	0.7	0.4	0.8	0.8	-0.2	**1.0**
meanVH<3m	-0.1	-0.2	-0.1	0.3	-0.2	-0.3	-0.2	0.0	**-0.8**	**-0.6**	-0.2	0.3	0.0	-0.3	-0.1	0.0	-0.3	-0.3	**1.0**	
meanVH>3m	0.1	0.0	-0.2	-0.3	**0.9**	**0.6**	0.2	-0.1	0.4	**0.6**	0.1	0.1	0.4	**0.9**	0.8	0.6	**1.0**	**1.0**		
meanCH>3m	0.1	0.0	-0.2	-0.3	**0.9**	0.1	0.3	0.0	0.3	**0.5**	0.0	0.1	0.4	**0.9**	0.9	0.7	**1.0**			
maxVH	0.0	-0.2	-0.4	-0.1	**0.5**	0.1	-0.2	-0.3	-0.1	0.1	0.0	**0.7**	**0.7**	**0.8**	0.9	**1.0**				
VH95	0.0	-0.1	-0.3	-0.2	**0.7**	0.3	0.0	-0.2	0.1	0.2	0.0	**0.5**	**0.6**	**0.9**	**1.0**					
sdVH	0.0	0.0	-0.2	-0.3	**0.8**	0.4	0.1	-0.2	0.3	0.5	0.2	0.3	0.4	**1.0**						
sdCH	-0.2	-0.2	-0.5	-0.4	0.1	-0.4	**-0.7**	**-0.8**	-0.1	0.1	0.4	**0.8**	**1.0**							
sdCH>3m	-0.2	-0.3	-0.4	-0.1	0.0	-0.4	**-0.6**	**-0.5**	-0.5	-0.4	0.1	**1.0**								
pen50_2	-0.1	0.2	-0.1	-0.2	-0.1	-0.3	**-0.5**	**-0.6**	0.4	**0.5**	**1.0**									
pen10_2	0.1	0.2	0.1	-0.1	0.5	0.4	0.2	-0.1	**0.9**	**1.0**										
pen5_1	0.1	0.3	0.2	-0.2	0.3	0.4	0.3	0.0	**1.0**											
meanCC	0.2	0.2	0.4	0.3	0.2	**0.6**	**0.9**	**1.0**												
meanCC_10m	0.3	0.2	0.4	0.2	0.5	**0.8**	**1.0**													
meanCC_15m	0.3	0.2	0.3	0.1	**0.8**	**1.0**														
meanCC_20m	0.2	0.0	0.0	-0.2	**1.0**															
slope	-0.2	0.2	0.4	**1.0**																
r_march	0.1	0.4	**1.0**																	
forest_type	0.0	**1.0**																		

Table 8: Spearman's rank correlation coefficients (r_s) between habitat variables (column names) and lidar metrics (row names) based on data from 62 occupied areas and 63 primary control areas (N=125). Missing values were present for *dead wood* (99), *average crown contacts* (1) and *mkna* (2). Correlations ≥ 0.60 are printed in bold. A description of the lidar metrics is given in Table 2, while the habitat variables are described in Table 1.

	inclination	canopy cover	dead wood	vegetation cover	number of tussocks	number of bushes	number of trees	amount of pole wood	number of immature trees	number of conifers	tree diversity	number of dead trees	number of trees branched below 10 m	number of trees branched below 4 m	average tree diameter	average crown contacts	mkna
meanVH	-0.33	0.09	0.07	-0.17	-0.36	-0.01	-0.32	-0.34	-0.33	0.14	-0.05	-0.11	-0.43	-0.43	0.49	0.08	0.25
meanCH	-0.26	0.16	0.09	-0.27	-0.46	-0.06	-0.42	-0.49	-0.30	-0.16	-0.27	-0.18	-0.51	-0.49	0.55	0.14	0.18
meanVH<3m	0.10	0.06	-0.14	-0.14	-0.13	0.09	0.03	0.10	-0.03	0.18	0.10	-0.03	0.09	0.05	-0.05	0.15	0.04
meanVH>3m	-0.24	0.10	-0.03	-0.22	-0.44	0.02	-0.46	-0.56	-0.32	-0.18	-0.32	-0.28	-0.57	-0.54	**0.60**	0.12	0.23
meanCH>3m	-0.27	0.11	0.00	-0.23	-0.46	0.01	-0.46	-0.55	-0.35	-0.15	-0.30	-0.27	-0.56	-0.54	**0.61**	0.11	0.21
maxVH	-0.26	0.06	-0.08	-0.26	-0.52	0.10	-0.51	-0.51	-0.48	-0.05	-0.25	-0.36	-0.52	-0.55	0.58	0.14	0.23
VH95	-0.25	0.10	-0.05	-0.25	-0.51	0.08	-0.47	-0.51	-0.42	-0.07	-0.24	-0.32	-0.52	-0.53	**0.62**	0.16	0.21
sdVH	-0.16	0.08	-0.13	-0.25	-0.45	0.08	-0.43	-0.54	-0.30	-0.23	-0.32	-0.32	-0.48	-0.46	0.56	0.11	0.14
sdCH	0.00	-0.12	-0.16	-0.02	-0.18	0.29	-0.22	-0.14	-0.32	0.09	-0.04	-0.30	-0.07	-0.16	0.15	-0.02	0.08
sdCH>3m	0.05	-0.10	0.21	-0.08	-0.24	0.36	-0.22	-0.03	-0.38	0.14	0.10	-0.28	-0.02	-0.13	0.09	0.11	0.04
pen50_2	0.21	-0.01	-0.17	-0.07	-0.01	0.03	-0.06	-0.16	0.11	-0.46	-0.28	-0.11	-0.02	0.01	-0.02	0.04	-0.13
pen10_2	0.05	0.19	-0.07	-0.16	-0.14	-0.16	-0.19	-0.41	0.06	-0.45	-0.39	-0.17	-0.34	-0.25	0.26	0.14	0.09
pen5_1	-0.03	0.06	-0.14	0.00	0.05	-0.17	-0.13	-0.32	0.10	-0.28	-0.22	-0.10	-0.26	-0.18	0.23	0.03	0.01
meanCC	-0.11	0.19	0.09	-0.10	-0.05	-0.21	0.07	0.06	0.12	-0.01	0.00	0.17	-0.04	0.02	0.01	0.08	-0.05
meanCC_10m	-0.13	0.23	0.27	-0.17	-0.11	-0.30	-0.06	-0.14	0.08	-0.17	-0.14	0.13	-0.23	-0.14	0.17	0.13	0.03
meanCC_15m	-0.16	0.26	0.28	-0.29	-0.31	-0.26	-0.26	-0.38	-0.09	-0.27	-0.27	0.01	-0.42	-0.34	0.41	0.19	0.09
meanCC_20m	-0.22	0.19	0.10	-0.31	-0.49	-0.10	-0.40	-0.51	-0.29	-0.18	-0.30	-0.21	-0.51	-0.49	0.57	0.19	0.14
slope	**0.82**	0.10	-0.28	-0.15	0.13	-0.24	0.11	0.07	0.22	-0.28	0.06	0.07	0.15	0.20	-0.14	0.28	-0.32

3.2 Occupied territories versus control areas

3.2.1 Nesting area scale (1,000 m^2)

GLMMs

Wood Warbler occurrence was strongly related to the **height variables**. The ΔAICc value between the null model and the best supported one was 27.77 (Table 10). The model ranked highest included only maxVH. Moreover, the linear effect or the quadratic effect of maxVH appeared in every model with a ΔAICc < 2 compared to the best supported one. Additionally, these models included meanVH and meanCH. According to model averaging, the following variables had a model-averaged estimate greater than the model-averaged SE: meanVH>3m, meanCH>3m, maxVH, VH95 and the quadratic effect of VH95 (Table 9). However, following the selection criteria for the variables, only maxVH was considered relevant (the others were not included in the models with ΔAICc < 2 compared to the best one).

Besides the height variables, Wood Warbler occurrence was strongly related to the **vertical diversity variables** too, because the ΔAICc value between the null model and the best supported model was 29.73 (Table 10). SdVH and sdCH>3m were included in the best supported model, which was the only model with strong support. The ΔAICc value to the second best model was 14.24. Both sdVH and sdCH>3m were considered relevant and were therefore included in the across-group analysis.

In the group of **penetration rates**, the null model performed best, followed by models including pen50_2 and pen10_2, respectively (Table 10). No penetration rates variables were included in the across-group analysis, because no variable fulfilled the selection criteria (Table 9).

Wood Warbler occurrence was related to the variables describing **canopy cover**. The best ranking model comprised meanCC_10m and meanCC_20m (Table 10). Besides, meanCC was included in the model ranked second. All three variables were selected for the across-group analysis.

In the **geography group**, Wood Warbler occurrence was strongly related to slope. It was included in every model considered to have substantial support (Table 10). In addition, these models comprised r_march, forest_type and dist_f. Following the selection criteria, slope, r_march and dist_f were included in the across-group analysis.

In the **across-group analysis**, the best supported model included sdVH, sdCH>3m and slope (Table 10). The second best model comprised meanCC_20m instead of sdVH. Furthermore, only dist_f appeared in the other models considered to have substantial support. According to model-averaging, the variables of sdVH, sdCH>3m and meanCC_20m had the strongest effects, with their 95% confident intervals excluding 0 (Table 9). Wood Warbler occurrence was negatively related to all three variables. Slope and dist_f received weaker support. Wood Warbler occurrence was positively related to slope and negatively related to dist_f.

Table 9: Model averaged estimates (ES), standard errors (SE) and 95% confidence intervals (95% CI) across all models per group or across all models of the across-group analysis of the independent variables for GLMMs applied to the nesting area scale (1,000 m^2). The quadratic effect of a variable is composed of a linear (x) and a quadratic component (x^2). A description of the variables can be found in the Tables 2 and 3. The hypotheses are introduced in paragraph 1.2.

Hypothesis	Independent variable	Within-group analysis			Across-group analysis		
		ES	SE	95% CI	ES	SE	95% CI
Height (H1)	meanVH	-0.37	0.45	[-1.3; 0.5]			
	meanCH	0.31	0.61	[-0.9; 1.5]			
	meanVH<3m	-0.16	0.30	[-0.8; 0.4]			
	meanVH>3m	-1.22	0.33	[-1.9;-0.6]			
	meanCH>3m	-1.32	0.34	[-2.0;-0.7]			
	maxVH	-1.61	0.54	[-2.7;-0.6]	-1.58	0.40	[-2.4;-0.8]
	VH95	-1.38	0.35	[-2.1;-0.7]			
	quadratic effect of meanVH						
	linear component	-0.68	0.63	[-1.9; 0.6]			
	quadratic component	-0.54	0.49	[-1.5; 0.4]			
	quadratic effect of meanCH						
	linear component	0.30	0.66	[-1.0; 1.6]			
	quadratic component	-0.22	0.38	[-1.0; 0.5]			
	quadratic effect of meanVH>3m						
	linear component	-1.22	0.34	[-1.9;-0.6]			
	quadratic component	0.00	0.33	[-0.7; 0.6]			
	quadratic effect of meanCH>3m						
	linear component	-1.30	0.34	[-2.0;-0.6]			
	quadratic component	-0.17	0.35	[-0.9; 0.5]			
	quadratic effect of maxVH						
	linear component	-1.62	0.55	[-2.7;-0.5]			
	quadratic component	-0.21	0.46	[-1.1; 0.7]			
	quadratic effect of VH95						
	linear component	-1.67	0.42	[-2.5;-0.8]			
	quadratic component	-0.73	0.30	[-1.3;-0.2]			
Vertical diversity (H2)	sdVH	-1.21	0.34	[-1.9;-0.6]	-1.07	0.37	[-1.8;-0.4]
	sdCH	-1.02	0.29	[-1.6;-0.5]			
	sdCH>3m	-1.47	0.46	[-2.4;-0.6]	-1.63	0.53	[-2.7;-0.6]
Penetration rate (H3,H4)	pen50_2	0.18	0.23	[-0.3; 0.6]			
	pen10_2	-0.11	0.23	[-0.6; 0.3]			
	pen5_1	-0.03	0.23	[-0.5; 0.4]			
	quadratic effect of pen50_2						
	linear component	0.30	0.26	[-0.2; 0.8]			
	quadratic component	-0.15	0.15	[-0.6; 0.2]			
Canopy closure (H5)	meanCC	0.49	0.34	[-0.2; 1.2]	0.11	0.46	[-0.8; 1.0]
	meanCC_10m	0.56	0.32	[-0.1; 1.2]	0.40	0.41	[-0.4; 1.2]
	meanCC_15m	-1.24	0.62	[-2.7;-0.0]			
	meanCC_20m	-1.14	0.34	[-1.8;-0.5]	-0.93	0.31	[-1.6;-0.3]
	quadratic effect of meanCC						
	linear component	0.39	0.54	[-0.7; 1.5]			
	quadratic component	-0.03	0.13	[-0.3; 0.2]			
	quadratic effect of meanCC_10m						
	linear component	0.71	0.51	[-0.3; 1.7]			
	quadratic component	0.05	0.12	[-0.2; 0.3]			
	quadratic effect of meanCC_15m						
	linear component	-1.13	0.68	[-2.5; 0.2]			
	quadratic component	0.42	0.39	[-0.3; 1.2]			
	quadratic effect of meanCC_20m						
	linear component	-1.15	0.32	[-1.8;-0.5]			
	quadratic component	0.15	0.44	[-0.7; 1.0]			
Geography (H6-H9)	slope	0.71	0.29	[0.2; 1.3]	0.71	0.39	[-0.1; 1.5]
	r_march	0.33	0.29	[-0.2; 0.9]	0.03	0.36	[-0.7; 0.7]
	forest_type	0.12	0.28	[-0.4; 0.7]			
	dist_f	-0.40	0.25	[-0.9; 0.1]	-0.42	0.33	[-1.1; 0.2]
	intercept				-0.24	0.34	[-0.9; 0.4]

Table 10: Results of model selection for GLMMs applied to the nesting area scale (1,000 m^2) based on data from 39 occupied areas and 39 primary control areas (N=78). Shown are models with ΔAICc values < 2 and the null model. K denotes the number of parameters included in the particular model (variables, the two random effects and the intercept). Δ represents ΔAICc values. W denotes Akaike weight defined as chance of the model to be the best one given all candidate models. LL denotes log-likelihood and Δb represents ΔAICc values of the best supported models between the groups. The quadratic effect of a variable, composed of a linear and a quadratic component ($x + x^2$), is denoted as (^2). A description of the variables can be found in the Tables 2 and 3. The hypotheses are introduced in paragraph 1.2.

Hypothesis	Variables included in the model	K	AICc	Δ	W	LL	Δb
Height	maxVH	4	86.69	0	0.21	-39.07	1.97
(H1)	meanVH, maxVH	5	88.38	1.69	0.09	-38.77	
	maxVH (^2)	5	88.57	1.88	0.08	-38.87	
	meanCH, maxVH	5	88.61	1.92	0.08	-38.89	
	…						
	null model	3	114.46	27.77	0.00	-54.07	
Vertical diversity	sdVH, sdCH>3m	5	84.72	0	1.00	-36.94	0
	…						
(H2)	null model	3	114.46	29.73	0.00	-54.07	
Penetration	null model	3	114.46	0	0.38	-54.07	29.74
rate	pen50_2	4	116.05	1.60	0.17	-53.75	
(H3,H4)	pen10_2	4	116.44	1.98	0.14	-53.95	
Canopy	meanCC_10m, meanCC_20m	5	99.42	0	0.25	-44.29	14.7
cover	meanCC, meanCC_20m	5	99.81	0.39	0.21	-44.49	
(H5)	meanCC_20m	4	100.76	1.34	0.13	-46.11	
	…						
	null model	3	114.46	15.04	0.00	-54.07	
Geography	slope, dist_f	5	106.94	0	0.23	-48.05	22.22
(H6-H9)	slope	4	107.20	0.26	0.20	-49.33	
	slope, r_march, dist_f	6	108.17	1.23	0.12	-47.49	
	slope, r_march	5	108.26	1.31	0.12	-48.71	
	slope, forst_type, dist_f	6	108.87	1.93	0.09	-47.84	
	…						
	null model	3	114.46	7.51	0.01	-54.07	
Across	sdVH, sdCH>3m, slope	6	82.85	0	0.14	-34.84	
groups	sdCH>3m, meanCC_20m, slope	6	83.09	0.23	0.13	-34.95	
	sdVH, sdCH>3m, slope, dist_f	7	83.57	0.71	0.10	-33.98	
	sdCH>3m, meanCC_20m, slope, dist_f	7	84.13	1.28	0.08	-34.27	
	sdVH, sdCH>3m, dist_f	6	84.68	1.83	0.06	-35.75	
	sdVH, sdCH>3m	5	84.72	1.87	0.06	-36.94	
	…						
	null model	3	114.46	31.60	0.00	-54.07	

GLMs

As before, maxVH appeared in every **height model** considered to have substantial support (Table 12). Contrary to the GLMMs, the quadratic effect of meanCH was substantial. The GLMs yielded broadly similar results for the groups of **vertical diversity, penetration rate** and **canopy cover** as the GLMMs (Table 10 and Table 12). In the **geography group**, dist_f did no longer receive support.

Table 11: Model averaged estimates (ES), standard errors (SE) and 95% confidence intervals (95% CI) across all models per group or across all models of the across-group analysis of the independent variables for GLMs applied to the nesting area scale (1,000 m^2). The quadratic effect of a variable is composed of a linear (x) and a quadratic component (x^2). A description of the variables can be found in the Tables 2 and 3. The hypotheses are introduced in paragraph 1.2.

Hypothesis	Independent variable	Within-group analysis			Across-group analysis		
		ES	SE	95% CI	ES	SE	95% CI
Height	meanVH	0.14	0.28	[-0.4; 0.7]			
(H1)	meanCH	0.72	0.35	[0.0; 1.4]			
	meanVH<3m	0.08	0.24	[-0.4; 0.6]			
	meanVH>3m	-0.87	0.21	[-1.3;-0.5]			
	meanCH>3m	-0.86	0.20	[-1.3;-0.5]			
	maxVH	-1.62	0.46	[-2.5;-0.7]	-1.22	0.56	[-2.3;-0.1]
	VH95	-0.91	0.21	[-1.3;-0.5]			
	quadratic effect of meanVH						
	linear component	-0.08	0.37	[-0.8; 0.7]	-0.56	0.34	[-1.2; 0.1]
	quadratic component	-0.81	0.33	[-1.5;-0.2]	-0.55	0.30	[-1.1; 0.0]
	quadratic effect of meanCH						
	linear component	0.63	0.40	[-0.2; 1.4]	-0.59	0.36	[-1.3; 0.1]
	quadratic component	-0.65	0.28	[-1.2;-0.1]	-0.58	0.29	[-1.2;-0.0]
	quadratic effect of meanVH>3m						
	linear component	-0.89	0.22	[-1.3;-0.5]			
	quadratic component	-0.12	0.21	[-0.5; 0.3]			
	quadratic effect of meanCH>3m						
	linear component	-0.95	0.23	[-1.4;-0.5]			
	quadratic component	-0.31	0.22	[-0.7; 0.1]			
	quadratic effect of maxVH						
	linear component	-1.75	0.51	[-2.8;-0.8]			
	quadratic component	-0.27	0.32	[-0.9; 0.4]			
	quadratic effect of VH95						
	linear component	-1.49	0.33	[-2.1;-0.8]			
	quadratic component	-0.74	0.25	[-1.2;-0.3]			
Standard	sdVH	-0.78	0.22	[-1.2;-0.4]	-0.60	0.26	[-1.1;-0.1]
deviation	sdCH	-0.86	0.20	[-1.3;-0.5]			
(H2)	sdCH>3m	-1.20	0.32	[-1.8;-0.6]	-1.57	0.42	[-2.4;-0.7]
Penetration	pen50_2	-0.26	0.18	[-0.6; 0.1]	-0.12	0.25	[-0.6; 0.4]
rates	pen10_2	-0.12	0.16	[-0.4; 0.2]			
(H3,H4)	pen5_1	0.20	0.18	[-0.2; 0.6]	-0.07	0.31	[-0.7; 0.5]
	quadratic effect of pen50_2						
	linear component	-0.24	0.19	[-0.6; 0.1]			
	quadratic component	-0.06	0.14	[-0.3; 0.2]			
Canopy	meanCC	1.34	0.37	[0.6; 2.1]	0.97	0.60	[-0.2; 2.1]
closure	meanCC_10m	1.19	0.30	[0.6; 1.8]	0.74	0.35	[0.0;1 .4]
(H5)	meanCC_15m	-0.20	0.20	[-0.6; 0.2]			
	meanCC_20m	-1.09	0.25	[-1.6;-0.6]	-0.59	0.21	[-1.0;-0.2]
	quadratic effect of meanCC						
	linear component	1.31	0.40	[0.5; 2.1]			
	quadratic component	-0.08	0.47	[-1.0; 0.9]			
	quadratic effect of meanCC_10m						
	linear component	1.29	0.37	[0.6; 2.0]			
	quadratic component	0.10	0.17	[-0.2; 0.4]			
	quadratic effect of meanCC_15m						
	linear component	-0.40	0.28	[-0.9; 0.1]			
	quadratic component	-0.22	0.21	[-0.6; 0.2]			
	quadratic effect of meanCC_20m						
	linear component	-1.09	0.25	[-1.6;-0.6]			
	quadratic component	0.07	0.31	[-0.5; 0.7]			
Geography	slope	0.67	0.23	[0.2; 1.1]	0.96	0.31	[0.4; 1.6]
(H6-H9)	r_march	0.81	0.23	[0.4; 1.3]	0.52	0.25	[0.0; 1.0]
	forest_type	-0.04	0.22	[-0.5; 0.4]			
	dist_f	0.05	0.21	[-0.4; 0.5]			
	intercept				-0.90	0.38	[-1.7;-0.2]

The **across-group analysis** was performed with the following variables: maxVH, the quadratic effect of meanVH, the quadratic effect of meanCH, sdVH, sdCH>3m, pen50_2, pen5_1, meanCC, meanCC_10m, meanCC_20m, slope and r_march. The following variables received strong support: the quadratic effect of meanCH, sdCH>3m, meanCC_20m, slope and r_march (Table 11 and Table 12). Wood Warbler occurrence showed a concave relationship with meanCH (Fig. 9). Further, Wood Warbler occurrence was positively related to slope and r_march and negatively related to sdCH>3m and meanCC_20m (Fig. 9 and 10). Contrary to the GLMMs, sdVH did not occur in the best supported models. The quadratic effect of meanVH received moderate support, while pen50_2 and pen5_1 were weakly supported.

Table 12: Results of model selection for GLMs applied to the nesting area scale (1,000 m^2) based on data from 57 occupied areas, 42 primary control areas and 57 additional pseudo-absence control areas (N=156). Shown are models with ΔAICc values < 2 and the null model. K denotes the number of parameters included in the particular model (variables and intercept). Δ represents ΔAICc values. W denotes Akaike weight defined as chance of the model to be the best one given all candidate models. LL denotes log-likelihood and Δb represents ΔAICc values of the best supported models between the groups. The quadratic effect of a variable, composed of a linear and a quadratic component ($x + x^2$), is denoted as (^2). A description of the variables can be found in the Tables 2 and 3. The hypotheses are introduced in paragraph 1.2.

Hypothesis	Variables included in the model	K	AICc	Δ	W	LL	Δb
Height (H1)	meanCH (^2), maxVH	4	165.16	0	0.31	-78.45	0
	meanCH (^2), meanVH<3m, maxVH	5	166.86	1.70	0.13	-78.23	
	meanCH (^2), maxVH (^2)	5	166.94	1.78	0.13	-78.27	
	meanVH (^2), maxVH	4	167.05	1.90	0.12	-79.39	
	…						
	null model	1	206.84	41.68	0	-102.41	
Vertical diversity (H2)	sdVH, sdCH>3m	3	167.60	0	1.00	-80.72	2.44
	…						
	null model	1	206.84	39.24	0	-102.41	
Penetration rate (H3,H4)	null model	1	206.84	0	0.23	-102.41	41.68
	pen50_2	2	206.91	0.07	0.22	-101.41	
	pen50_2, pen5_1	3	207.40	0.56	0.17	-100.62	
	pen5_1	2	208.06	1.22	0.12	-101.99	
	pen10_2	2	208.38	1.54	0.11	-102.15	
	pen50_2 (^2)	3	208.75	1.91	0.09	-101.30	
Canopy cover (H5)	meanCC_10m, meanCC_20m	3	168.58	0	0.29	-81.21	3.42
	meanCC, meanCC_20m	3	169.06	0.48	0.23	-81.45	
	meanCC_20m (^), meanCC_10m	4	170.35	1.77	0.12	-81.04	
	meanCC_10m (^), meanCC_20m	4	170.41	1.83	0.12	-81.07	
	…						
	null model	1	206.84	38.26	0.00	-102.41	
Geography (H6-H9)	slope, r_march	3	172.47	0	0.53	-83.16	7.31
	…						
	null model	1	206.84	34.37	0	-102.41	
Across groups	meanCH (^2), sdCH>3m, slope, r_march	6	142.48	0	0.15	-64.96	
	sdCH>3m, meanCC_20m, slope, r_march	5	142.85	0.36	0.12	-66.22	
	meanVH (^2), sdCH>3m, slope, r_march	6	143.42	0.94	0.09	-65.43	
	meanCH (^2), sdCH>3m, pen50_2, slope, r_march	7	144.14	1.65	0.07	-64.69	
	meanCH (^2), sdCH>3m, pen5_1, slope, r_march	7	144.26	1.78	0.06	-64.75	
	…						
	null model	1	206.84	64.36	0.00	-102.41	

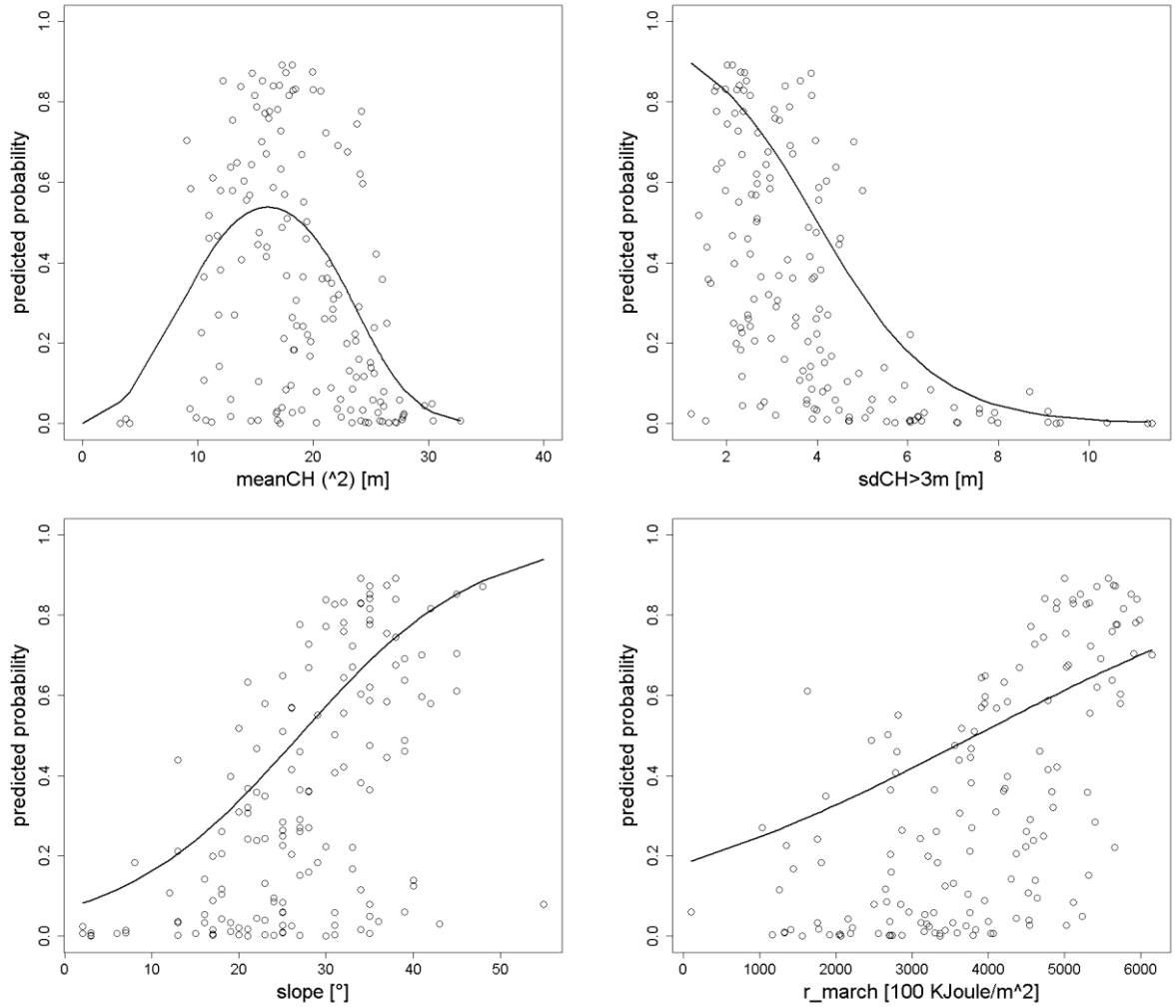

Fig. 9: Wood Warbler occurrence in relation to RS variables at nesting area scale. Variables of the best supported GLM at the nesting area scale are plotted against predicted probability of Wood Warbler occurrence (dots). Model-averaged estimates from the across-group analysis were used as coefficients (N=156). The curves represent the predicted responses for the respective variables (where the other variables are set to their means).

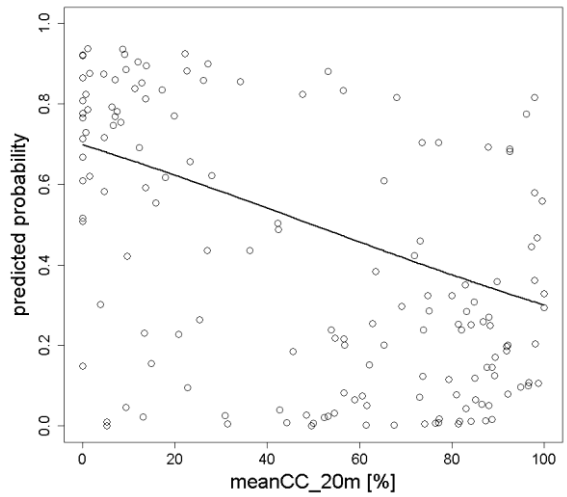

Fig. 10: Wood Warbler occurrence in relation to mean canopy cover at 20 m above ground. This variable was not included in the best GLM at the nesting area scale, but still showed a strong effect (see Table 11). Dots and line calculated as described in the legend of Fig. 9. A description of the variable can be found in the Table 2.

3.2.2 Territory scale (6,648 m²)

GLMs

Wood Warbler occurrence at the territory scale was related to the **height variables** (Table 13). MaxVH and the quadratic effect of meanVH were strongly supported by model-averaging (Table 14). As at the nesting area scale, the model including sdVH and sdCH>3m was ranked highest in the **vertical diversity** group. Contrary to the GLMMs and GLMs of the nesting area scale (Table 10 and 12), the null model was not the best supported model in the **penetration rate** group (Table 13). Two models, including either pen50_2 or pen50_2 and pen5_1, performed slightly better than the null model. Overall, the **canopy cover** group performed best. In the **geography** group, the following variables appeared in the best supported models: slope, r_march and forest_type.

Table 13: Results of model selection for GLMs applied to territory scale (6,648 m²) based on data from 57 occupied areas, 42 primary control areas and 57 additional pseudo-absence control areas (N=156). Shown are models with ΔAICc values < 2 and the null model. K denotes the number of parameters included in the particular model (variables and intercept). Δ represents ΔAICc values. W denotes Akaike weight defined as chance of the model to be the best one given all candidate models. LL denotes log-likelihood and Δb represents ΔAICc values of the best supported models between the groups. The quadratic effect of a variable, composed of a linear and a quadratic component ($x + x^2$), is denoted as (^2). A description of the variables can be found in the Tables 2 and 3. The hypotheses are introduced in paragraph 1.2.

Hypothesis	Variables included in the model	K	AICc	Δ	W	LL	Δb
Height (H1)	meanVH (^2), maxVH	4	165.71	0	0.47	-78.72	5.56
	meanVH (^2), meanVH<3m, maxVH	5	167.65	1.93	0.18	-78.62	
	…						
	null model	1	206.84	41.13	0.00	-102.41	
Vertical diversity (H2)	sdVH, sdCH>3m	3	175.89	0	0.93	-84.86	15.74
	…						
	null model	1	206.84	30.95	0.00	-102.41	
Penetration rates (H3, H4)	pen50_2, pen5_1	3	205.34	0	0.28	-99.59	45.19
	pen50_2	2	205.84	0.50	0.22	-100.88	
	null model	1	206.84	1.50	0.13	-103.41	
	pen50_2 (^2), pen5_1	4	207.01	1.67	0.12	-99.37	
	pen50_2 (^2)	3	207.18	1.84	0.11	-100.51	
Canopy cover (H5)	meanCC_10m, meanCC_20m	3	160.15	0	0.43	-77.00	0
	meanCC_10m (^2), meanCC_20m	4	160.90	0.75	0.29	-76.32	
	…						
	null model	1	206.84	46.69	0.00	-102.41	
Geography (H6-H9)	slope, r_march	3	171.82	0	0.50	-82.83	11.67
	slope, r_march, forest_type	4	173.71	1.89	0.19	-82.72	
	…						
	null model	1	206.84	35.02	0.00	-102.41	
Across groups	meanVH (^2), sdCH>3m, slope, r_march	6	147.52	0	0.20	-67.48	
	maxVH, meanCC_10m (^2), slope	5	149.01	1.49	0.09	-69.30	
	maxVH, meanCC_10m (^2), slope, r_march	6	149.17	1.65	0.09	-68.30	
	meanVH (^2), sdCH>3m, slope	5	149.25	1.74	0.08	-69.43	
	…						
	null model	1	206.84	59.32	0.00	-102.41	

Table 14: Model-averaged estimates (ES), standard errors (SE) and 95% confidence intervals (95% CI) across all models per group or across all models of the across-group analysis of the independent variables for GLMs applied to the territory scale (6,648 m^2). The quadratic effect of a variable is composed of a linear (x) and a quadratic component (x^2). A description of the variables can be found in the Tables 2 and 3. The hypotheses are introduced in paragraph 1.2.

Hypothesis	Independent variable	Within-group analysis			Across-group analysis		
		ES	SE	95% CI	ES	SE	95% CI
Height (H1)	meanVH	0.15	0.22	[-0.3; 0.6]			
	meanCH	0.51	0.25	[0.0; 0.1]			
	meanVH<3m	0.14	0.24	[-0.3; 0.6]			
	meanVH>3m	-0.78	0.21	[-1.2;-0.4]			
	meanCH>3m	-0.73	0.20	[-1.1;-0.3]			
	maxVH	-1.13	0.29	[-1.7;-0.6]	-1.00	0.27	[-1.5;-0.5]
	VH95	-0.97	0.21	[-1.4;-0.6]			
	quadratic effect of meanVH						
	linear component	-0.08	0.32	[-0.7; 0.6]	-0.39	0.35	[-1.1; 0.3]
	quadratic component	-1.00	0.30	[-1.6;-0.4]	-0.83	0.32	[-1.5;-0.2]
	quadratic effect of meanCH						
	linear component	0.59	0.30	[0.0; 1.2]			
	quadratic component	-0.64	0.23	[-1.1;-0.2]			
	quadratic effect of meanVH>3m						
	linear component	-0.78	0.22	[-1.2;-0.4]			
	quadratic component	-0.08	0.19	[-0.5; 0.3]			
	quadratic effect of meanCH>3m						
	linear component	-0.76	0.21	[-1.2;-0.3]			
	quadratic component	-0.20	0.18	[-0.6; 0.2]			
	quadratic effect of maxVH						
	linear component	-1.11	0.29	[-1.7;-0.5]			
	quadratic component	0.07	0.22	[-0.4; 0.5]			
	quadratic effect of VH95						
	linear component	-1.21	0.28	[-1.8;-0.7]			
	quadratic component	-0.44	0.22	[-0.9;-0.0]			
Vertical diversity (H2)	sdVH	-0.57	0.22	[-1.0;-0.2]	-0.82	0.28	[-1.4;-0.3]
	sdCH	-0.83	0.20	[-1.2;-0.4]			
	sdCH>3m	-0.95	0.28	[-1.5;-0.4]	-1.17	0.35	[-1.9;-0.5]
Penetration rate (H3,H4)	pen50_2	-0.35	0.19	[-0.7; 0.0]	-0.04	0.24	[-0.5; 0.4]
	pen10_2	-0.13	0.16	[-0.5; 0.2]			
	pen5_1	0.27	0.19	[-0.1; 0.7]	0.13	0.31	[-0.5; 0.8]
	quadratic effect of pen50_2						
	linear component	-0.31	0.20	[-0.7; 0.1]			
	quadratic component	-0.11	0.15	[-0.4; 0.2]			
Canopy closure (H5)	meanCC	1.50	0.34	[0.8; 2.2]			
	meanCC_10m	1.64	0.34	[1.0; 2.3]	1.06	0.41	[0.3; 1.9]
	meanCC_15m	0.00	0.23	[-0.5; 0.5]			
	meanCC_20m	-1.09	0.23	[-1.6;-0.6]	-0.86	0.26	[-1.4;-0.4]
	quadratic effect of meanCC						
	linear component	1.47	0.37	[0.7; 2.1]			
	quadratic component	-0.13	0.40	[-0.9; 0.7]			
	quadratic effect of meanCC_10m						
	linear component	1.60	0.37	[0.9; 2.3]	0.95	0.44	[0.1; 1.8]
	quadratic component	-0.46	0.45	[-1.3; 0.4]	-0.85	0.53	[-1.9; 0.2]
	quadratic effect of meanCC_15m						
	linear component	-0.14	0.26	[-0.7; 0.4]			
	quadratic component	-0.63	0.28	[-1.2;-0.1]			
	quadratic effect of meanCC_20m						
	linear component	-1.09	0.24	[-1.6;-0.6]			
	quadratic component	-0.01	0.22	[-0.5; 0.4]			
Geography (H6-H9)	slope	0.63	0.23	[0.2; 1.1]	0.81	0.30	[0.2; 1.4]
	r_march	0.84	0.24	[0.4; 1.3]	0.48	0.28	[-0.1; 1.0]
	forest_type	0.11	0.23	[-0.4; 0.6]			
	dist_f	0.04	0.21	[-0.4; 0.4]			
	intercept				-0.56	0.36	[-1.3; 0.2]

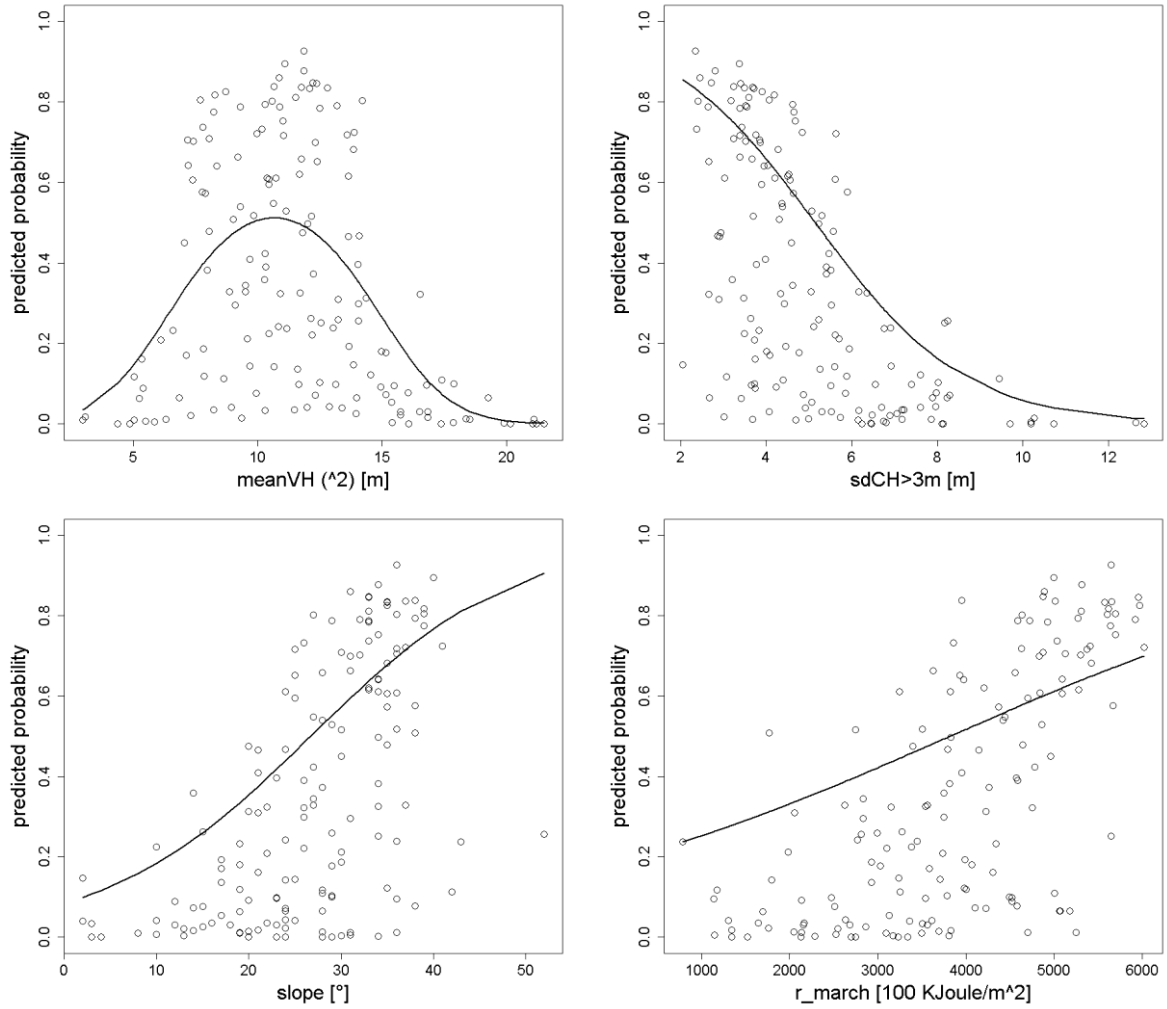

Fig. 11: Wood Warbler occurrence in relation to RS variables at territory scale. Variables of the best supported GLM at the territory scale are plotted against predicted probability of Wood Warbler occurrence (dots). Model-averaged estimates from the across-group analysis were used as coefficients (N=156). The curves represent the predicted responses for the respective variables (where the other variables are set to their means).

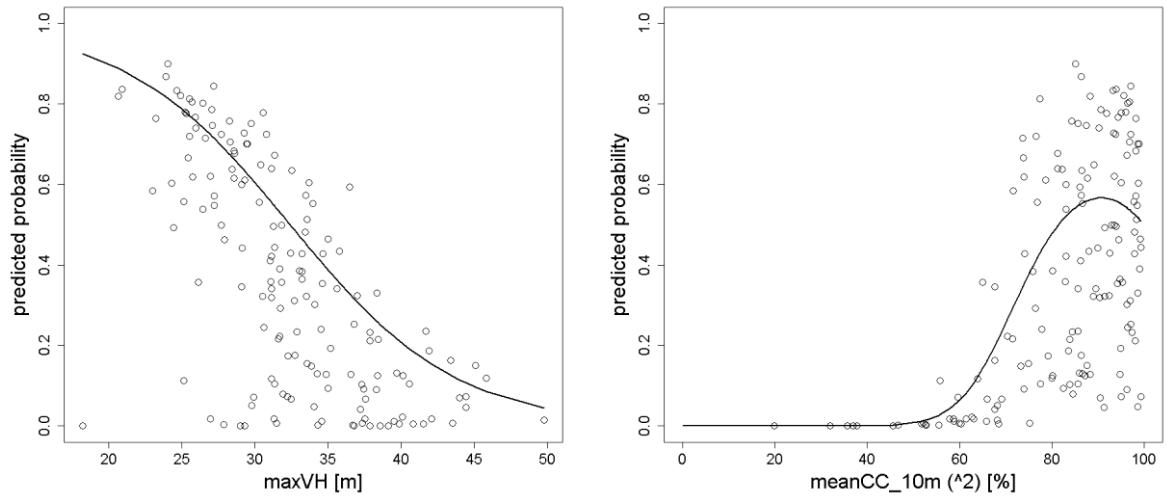

Fig. 12: Wood Warbler occurrence in relation to maximum vegetation height (maxVH) and mean canopy cover at 10 m above ground (meanCC_10m). These variables were not included in the best GLM at the territory scale, but still showed a strong effect (see Table 14). Dots and line calculated as described in the legend of Fig. 11. A description of the variables can be found in the Table 2.

The **across-group analysis** was performed with the following variables: maxVH, sdVH, sdCH>3m, pen50_2, pen5_1, meanCC_20m, slope, r_march and the quadratic effects of both meanVH and meanCC_10m. Variables with strong effect were the quadratic effect of meanVH, maxVH, sdCH>3m and slope (Table 13 and Table 14). Wood Warbler occurrence showed a concave relationship with meanVH (Fig. 11). Furthermore, territory choice was negatively related to maxVH and sdCH>3m, while it showed a positive relationship to slope (Fig. 11). SdVH, the quadratic effect of meanCC_10m and r_march were classed among variables with moderate effect. Wood Warbler occurrence was negatively related to sdVH and positively related to r_march. Furthermore, occurrence showed a concave relationship with meanCC_10m (Fig.12).

3.2.3 Comparison of the results

The comparison of the results between GLMMs and GLMs for both the nesting area scale and the territory scale shows that variables of the vertical diversity group always received strong support (Table 15). Also, variables belonging to the height group, the canopy cover group and the geography group performed well.

Table 15: Classification of the variables included in the best supported model or a model with a ΔAICc value < 2 compared to the best supported one of the across-group analysis. A description of the variables can be found in the Tables 2 and 3.

GLMMs		**GLMs**		**GLMs**	
Nesting area scale		**Nesting area scale**		**Territory scale**	
Variables with strong effect		*Variables with strong effect*		*Variables with strong effect*	
sdVH	-	meanCH (^2)	concave	meanVH (^2)	concave
sdCH>3m	-	sdCH>3m	-	maxVH	-
meanCC_20m	-	meanCC_20m	-	sdCH>3m	-
		slope	+	slope	+
		r_march	+		
Variables with moderate effect		*Variables with moderate effect*		*Variables with moderate effect*	
slope	+	meanVH (^2)	concave	meanCC_10m (^2)	concave
dist_f	-			r_march	+
Variables with weak effect		*Variables with weak effect*		*Variables with weak effect*	
		pen50_2	-		
		pen5_1	-		

The results support the following hypotheses: The probability of Wood Warbler occurrence shows a concave relationship with vegetation height (H1), is negatively related to the standard deviation of vegetation height (H2) and increases with inclination (H6) and solar radiation input during March (H7). The results for H5 are inconclusive: on the one hand, probability of Wood Warbler occurrence was strongly negatively related to meanCC_20m at the nesting area scale, contrary to the expectation for H5 outlined in the introduction.

However, this variable is highly correlated with meanCH, meanVH>3m and meanCH>3m (r_s = 0.92, 0.84 and 0.87, respectively), which all reflect stand height. MeanCC_20m thus also appears to represent stand height rather than canopy cover. On the other hand, there was a moderately strong, concave relationship between occurrence and meanCC_10m at the territory scale, thus supporting H5.

3.2.4 Model fit

For the nesting area scale, model performance and robustness were evaluated for three models (GLMs). These models correspond to the first three models of the across-group analysis (Table 12). All three models contained the variables sdCH>3m, slope and r_march. Additionally, the first model included the quadratic effect of meanCH, the second model meanCC_20m and the third model the quadratic effect of meanVH. Model performance and robustness was not evaluated for the other two models considered to have substantial support, because they additionally included either pen50_2 or pen5_1, both variables with only weak effects.

For the territory scale, four models were evaluated. They correspond to the best supported models of the across-group analysis with a ΔAICc value < 2 (Table 13).

Verification

For most models, fpos was higher than fneg (Table 16). The values of fpos ranged between 16.16% and 26.26%, while the values of fneg varied between 8.77% and 26.32%. A small fneg is preferable to be certain of correctly predicting as many presences as possible. On the other hand, fpos should be as small as possible to be certain of actually finding the species (Fielding & Bell, 1997).

For most models, sensitivity ranging between 77.19% and 91.23% was higher than specificity ranging between 75.76% and 81.82%. This indicates that for most models the probability that an observed presence is correctly predicted is higher than the probability that an observed absence is correctly predicted.

TSS varied between 52.95% and 73.05% indicating a moderate to substantial strength of agreement between prediction and observation. AUC values reaching from 85.65% to 88.18% slightly varied between the models.

In summary, the models for the nesting area scale performed better than the models for the territory scale. The third model of the nesting area scale received strongest support. Compared to the other models, it exhibited the smallest fneg and the highest sensitivity, specificity, TSS and AUC value.

Table 16: Accuracy measures for verification of the models at the nesting area scale and the territory scale. All numbers are shown in %. The quadratic effect of a variable is composed of a linear (x) and a quadratic component (x^2). A description of the variables can be found in the Tables 2 and 3.

Spatial scale	Model	Variables	fpos	fneg	sens	spec	TSS	AUC
Nesting area	1	meanCH (^2), sdCH>3m, slope, r_march	18.18	12.28	87.72	81.82	69.54	88.14
	2	sdCH>3m, meanCC_20m, slope, r_march	22.22	8.77	91.23	77.78	69.01	88.00
	3	meanVH (^2), sdCH>3m, slope, r_march	18.18	8.77	91.23	81.82	73.05	88.18
Territory	1	meanVH (^2), sdCH>3m, slope, r_march	22.22	10.53	77.19	81.82	59.01	86.87
	2	maxVH, meanCC_10m (^2), slope	16.16	26.32	77.19	75.76	52.95	85.65
	3	maxVH, meanCC_10m (^2), slope, r_march	19.19	21.05	78.95	75.76	54.70	86.18
	4	meanVH (^2), sdCH>3m, slope	26.26	12.28	77.19	80.81	58.00	85.72

Validation

In general, the accuracy measures were poorer for validation (Table 17) than for verification (Table 16). For validation, the values of fpos ranged between 19.39% and 33.67%, while fneg took values between 20.69% and 34.48% (Table 17). Sensitivity and specificity varied between 65.52% and 80.61%. The first model for the nesting area scale expressed the lowest TSS value of 43.84%, while the last model of the territory scale reached the highest TSS value of 49.72%. AUC values varied between 79.77% and 81.18%.

Overall, the fourth model of the territory scale was supported best. It expressed the smallest fneg and the highest sensitivity and TSS value. Furthermore, fpos was higher than fneg and sensitivity exceeded specificity.

Table 17: Accuracy measures for validation of the models at the nesting area scale and the territory scale. All numbers are shown in %. The quadratic effect of a variable is composed of a linear (x) and a quadratic component (x^2). A description of the variables can be found in the Tables 2 and 3.

Spatial scale	Model	variables	fpos	fneg	sens	spec	TSS	AUC
Nesting area	1	meanCH (^2), sdCH>3m, slope, r_march	28.57	27.59	72.41	71.43	43.84	81.18
	2	sdCH>3m, meanCC_20m, slope, r_march	33.67	22.41	77.59	66.33	43.91	79.77
	3	meanVH (^2), sdCH>3m, slope, r_march	30.61	24.14	75.86	69.39	45.25	80.67
Territory	1	meanVH (^2), sdCH>3m, slope, r_march	30.61	20.69	79.31	69.39	48.70	81.07
	2	maxVH, meanCC_10m (^2), slope	19.39	34.48	65.52	80.61	46.13	79.94
	3	maxVH, meanCC_10m (^2), slope, r_march	24.49	29.31	70.69	75.51	46.20	80.05
	4	meanVH (^2), sdCH>3m, slope	29.59	20.69	79.31	70.41	49.72	81.16

10-fold cross validation

The 10-fold cross validation showed broadly similar patterns to the verification (Table 18). Often, the accuracy measures of the models for the territory scale varied to a greater extent than the accuracy measures of the models for the nesting area scale, except for the first model of the territory scale. Therefore, the models for the nesting area scale and the first model of the territory scale seemed to be more robust than the other three models.

Table 18: Accuracy measures for the 10-fold cross validation of the models at nesting area scale and territory scale applied to the training data. All numbers are shown in %. The numbers of the models refer to the numbers of the models of the across-group analysis in the Tables 12 and 13.

Spatial scale	Model		fpos	fneg	sens	spec	TSS	AUC
Nesting area	1	average	23	13	87	77	64	87
		5% quantile	8	0	57	56	30	67
		95% quantile	44	43	100	92	91	100
	2	average	22	17	83	78	61	87
		5% quantile	8	0	57	56	30	67
		95% quantile	44	43	100	92	91	100
	3	average	21	13	87	79	67	87
		5% quantile	0	0	57	50	38	72
		95% quantile	50	43	100	100	90	100
Territory	1	average	28	15	85	72	57	85
		5% quantile	8	0	60	50	27	68
		95% quantile	50	40	100	92	89	100
	2	average	18	27	73	82	55	85
		5% quantile	0	0	33	56	12	67
		95% quantile	44	67	100	100	91	98
	3	average	19	29	71	81	52	84
		5% quantile	0	0	25	60	8	66
		95% quantile	40	75	100	100	83	98
	4	average	31	12	88	69	57	84
		5% quantile	8	0	50	44	20	61
		95% quantile	56	50	100	92	90	100

3.3 Modeling of the current potential range in parts of Switzerland

3.3.1 Models used for the prediction of the current potential range

Among the models evaluated, the first and fourth models of the territory scale were selected as predictive models. Despite their good performance in the verification, the models of the nesting area scale were not considered suitable, because they performed somewhat poorer in the validation than the models for the territory scale. Generally, model performance was broadly similar for the four models of the territory scale. The first and fourth model consisted of the same variables except for r_march. Equally, the second and third model included the same variables except for r_march.

TSS and AUC values were higher for the first and fourth model than for the second and third model (Table 17). For the first and fourth models, fpos was higher than fneg and sensitivity was higher than specificity. Furthermore, sdCH>3m always showed a strong effect (Table

15). Because of that, the first and fourth models were preferred to the second and third model. Biologically, the interpretation of the lidar metrics is broadly the same for all models: Stand height, and therefore stand age, and vertical stand diversity seem to critically influence Wood Warbler occurrence.

3.3.2 Current potential range of the Wood Warbler in the Swiss Jura Mountains and the Swiss Plateau

As an example, Fig. 13 shows the predicted occurrence probabilities for Wood Warbler occurrence for the 80x80 m forest cells near Zurich. For further examples see Fig. 14.

According to the predictive models, the current potential range of the Wood Warbler is predominantly located in the Swiss Jura Mountains (Fig. 15). The output of the two models is very similar.

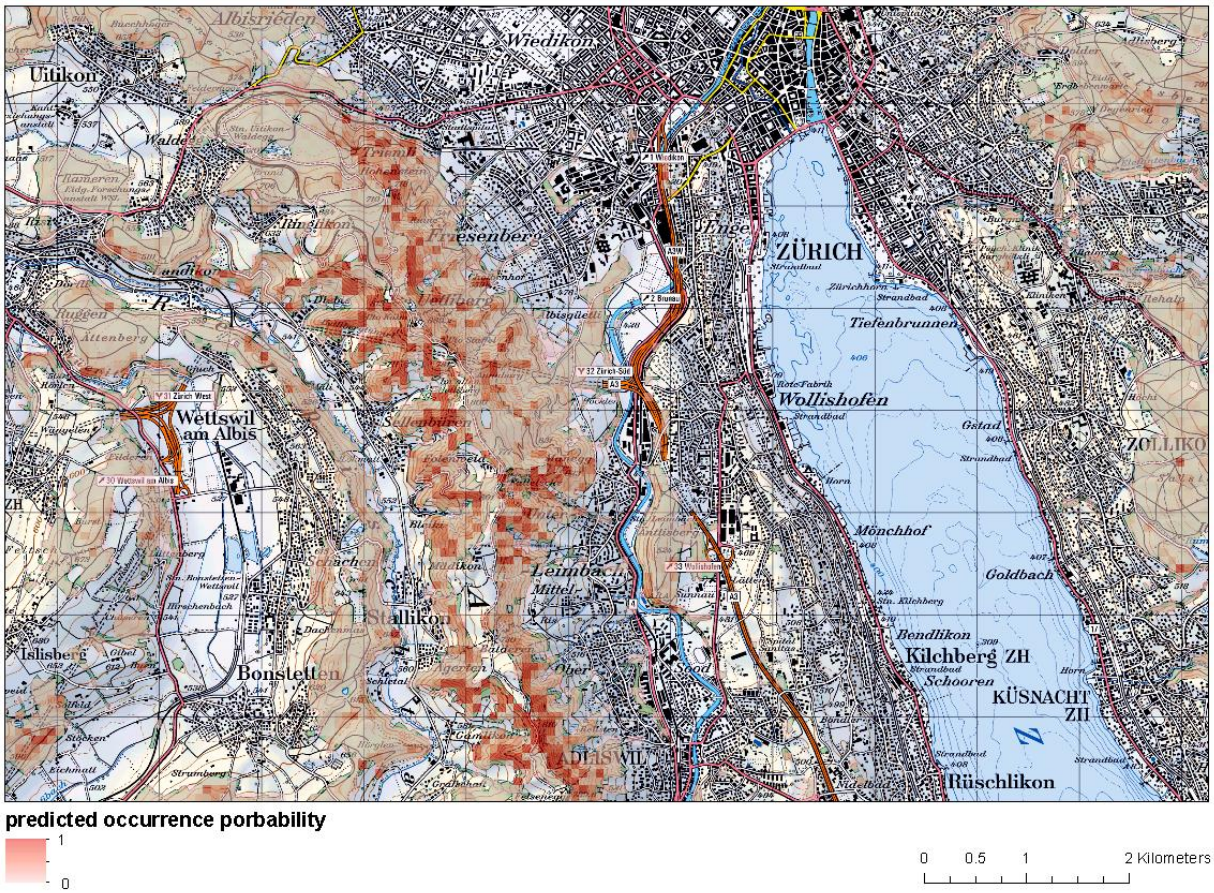

Fig. 13: Predicted Wood Warbler occurrence probabilities near Zurich according to the first model of the territory scale. The following variables were included in the model: meanVH (^2), sdCH>3m, slope and r_march. A description of the variables can be found in the Tables 2 and 3. A prediction was calculated for 80x80 m forest cells corresponding to the forest area of the Swiss Jura Mountains and the Swiss Plateau.

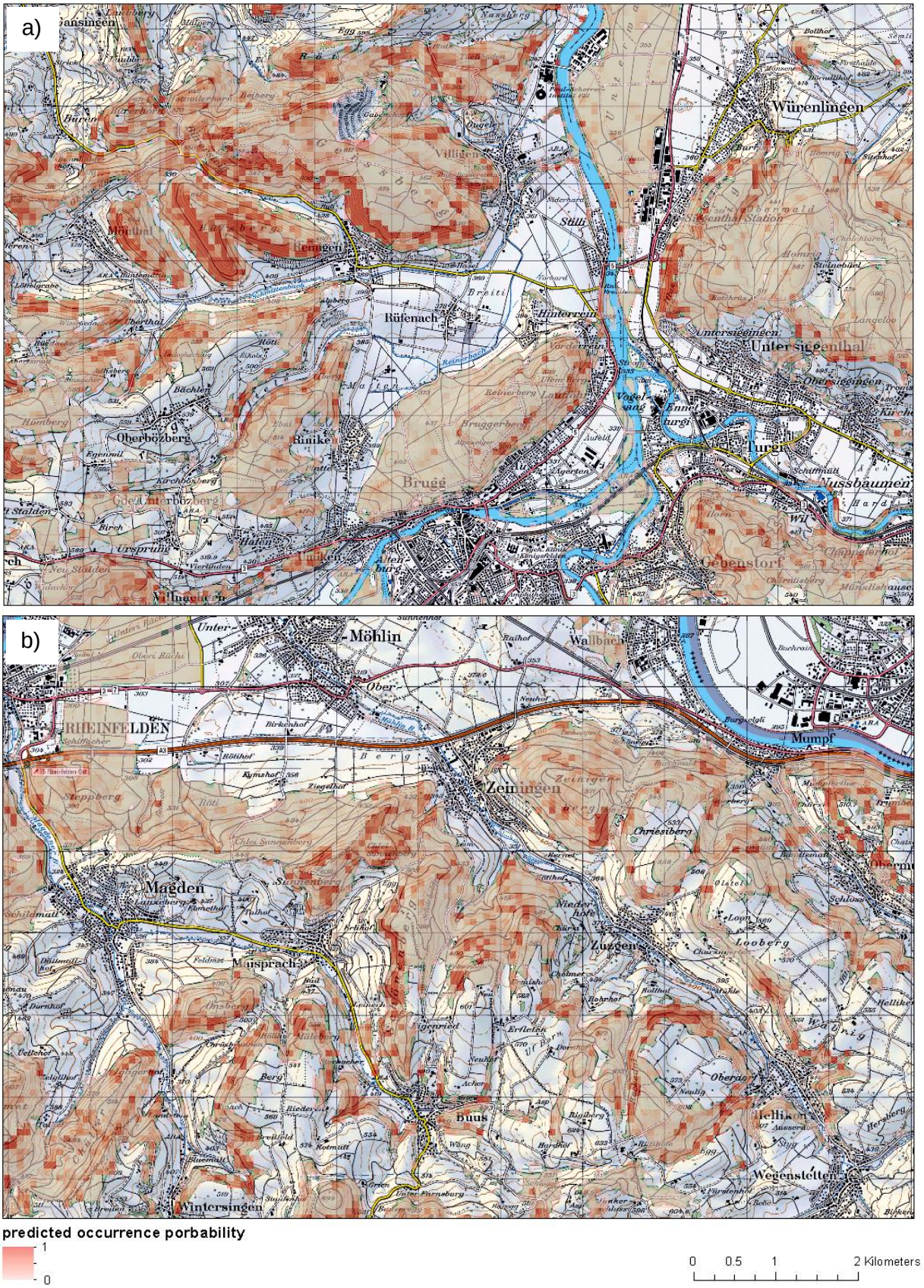

Fig. 14: Predicted Wood Warbler occurrence probabilities according to the first model of the territory scale. a) near Brugg; b) near Rheinfelden. For further details see legend Fig. 13.

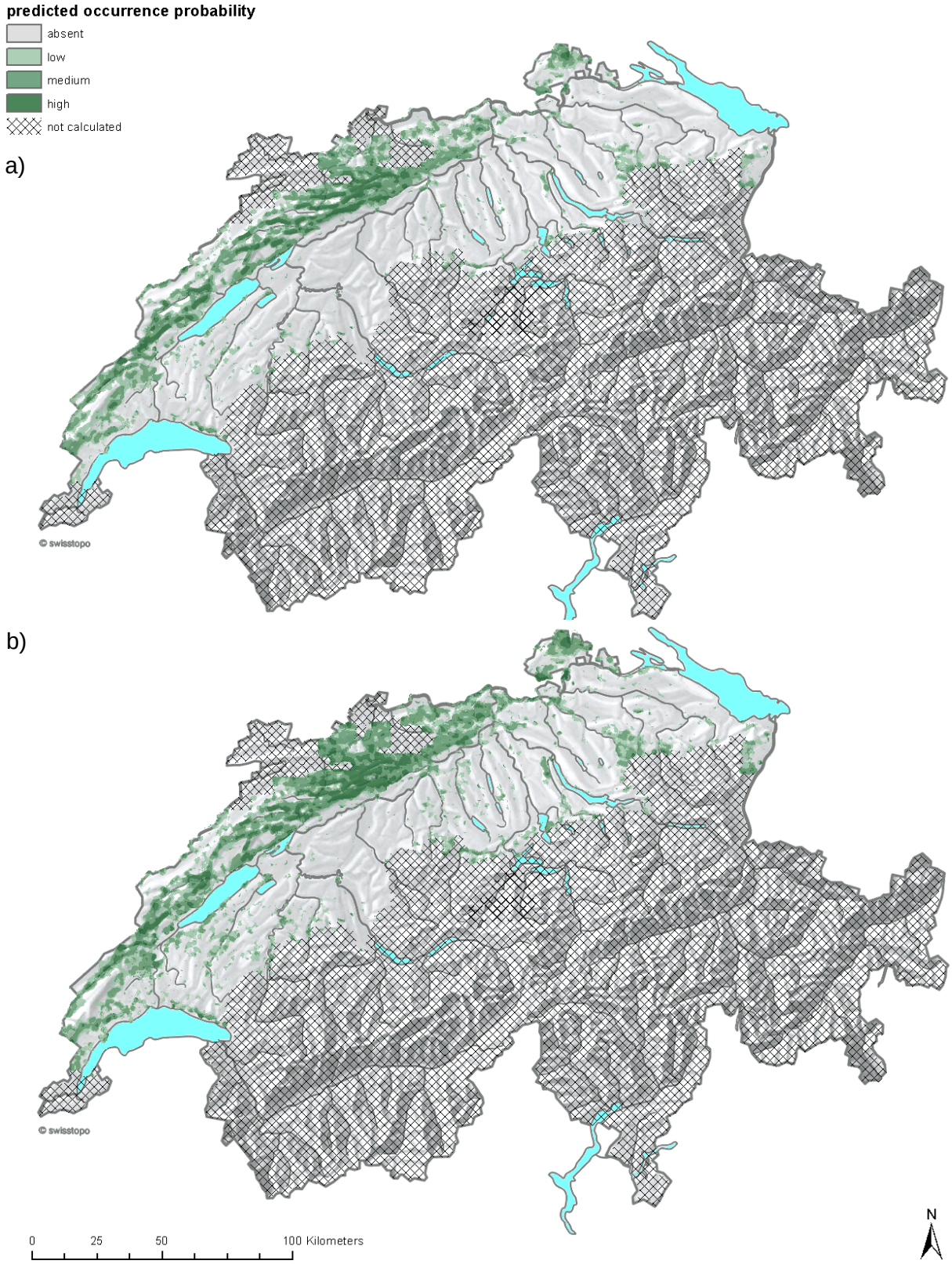

Fig. 15: Predicted occurrence probability. a) according to the first model; b) according to the fourth model of the territory scale. The numbers of the models refer to the numbers of the models of the across-group analysis in Table 13. A prediction was calculated for 80x80 m cells located in forest. The maps show the predicted occurrence probabilities averaged in a circle with a radius of 1,000 m. Absent = predicted occurrence probability < 0.08, low = predicted occurrence probability 0.08-0.12, medium = predicted occurrence probability 0.12-0.23, and high = predicted occurrence probability 0.23-1.

4 Discussion

This study used RS data, particularly lidar, to achieve an increased understanding of the factors influencing territory choice of Wood Warblers in Switzerland and to identify potentially suitable habitats in Switzerland. Habitat needs of Wood Warblers were analyzed at the scale of the nesting area (1,000 m^2) and at the scale of the territory (6,648 m^2). The occurrence of Wood Warblers is negatively related to the vertical diversity of a forest stand and to maximal tree height, described by both maxVH and meanCC_20m. Furthermore, Wood Warbler occurrence shows a concave relationship with stand height and canopy cover at 10 m. In addition, the occurrence of Wood Warblers is positively related to inclination and to solar radiation input during March.

4.1 Lidar metrics versus habitat variables

Overall, few strong correlations occurred between the lidar metrics and the habitat variables (Table 8). This result suggests that metrics derived from lidar data convey additional information not covered with the field variables gathered (and vice versa). Lidar metrics mainly provide information on the vertical and horizontal stand structure, while the habitat variables mainly contain information on the number of specific structural elements, such as sedge and grass tussocks, bushes or trees. Nevertheless, the few strong correlations between lidar metrics and habitat variables suggest that habitat variables varying with the age and the height of a forest stand show plausible correlations with the lidar metrics. For example, *number of trees* is negatively correlated with the lidar metrics of the height group, while *average tree diameter* shows a positive correlation with the metrics of the height and canopy cover group.

Interestingly, the *canopy cover* habitat variable was only weakly correlated with the lidar metrics describing canopy cover (Table 8). *Canopy cover* was always high (average 86% ± SD 7%), while the canopy cover lidar metrics showed more variation than *canopy cover* collected in the field (Figure 8). *Canopy cover* was measured by taking photographs of the canopy above 1.5 m above ground. Conceivably, the high values of *canopy cover* originate from surrounding stems also captured on camera. Contrary to *canopy* cover, the lidar metrics describing canopy cover refer to particular height levels, namely 3 m, 10 m, 15 m and 20 m above ground. Only meanCC represents the proportion of ground covered by all tree crowns.

The lidar metrics were not highly correlated with the number of return signals (maximal r_s: meanCC 0.45) and can therefore be considered robust to the resolution of lidar signals. However, the lidar signal densities of the present study (average density of 1.5 laser signals per m^2 for the sample areas) were relatively low compared to other ecological studies (e.g. Morsdorf et al. (2004): > 10 laser signals per m^2; Popescu & Zhao (2008): 2.6 laser signals per m^2; Pavlovic (2009): 25 laser signals per m^2 or studies using full waveform lidar data providing the entire signale trace (Lefsky et al., 2002): Hinsley et al., 2002; Bradbury et al., 2005; Hyde et al., 2005; Hinsley et al., 2006; Hyde et al., 2006; Goetz et al., 2007; Chust et al., 2008).

4.2 Occupied territories versus control areas

The GLMs obtained for the nesting area scale of 1,000 m^2 indicate that the occurrence of Wood Warblers is negatively related to sdCH>3m and meanCC_20m and positively related to slope and r_march (Table 15). Furthermore, occurrence at the nesting area scale shows a concave relationship with meanCH. The quadratic effect of meanVH showed a moderate effect, while pen50_2 and pen5_1 received weak support.

The variables best explaining occurrence at territory scale (6,648 m^2) slightly vary from those at the nesting area scale (Table 15). In contrast to the nesting area scale, maxVH received strong support instead of meanCC_20m; however, both variables were strongly correlated. Territory occurrence showed a concave relationship with the quadratic effect of meanVH, while the effects of maxVH and sdCH>3m were negative and the effect of slope was positive. Furthermore, sdVH, the quadratic effect of meanCC_10m and r_march received moderate support. The penetration rate variables received no support.

Variables that were never selected for the across-group models, neither in GLMMs nor GLMs, were meanVH<3m, meanVH>3m, meanCH>3m, VH95, sdCH, pen10_2, meanCC_15m and forest_type.

The results imply that Wood Warbler occurrence is sensitive to **stand height** and therefore to stand age, thus supporting **H1**. According to model averaging, stand height favoring the occurrence of Wood Warblers reaches an optimum between 12-22 m (Fig. 9, meanCH (^2), GLM for nesting area scale). Thus, the optimal stages of development include late pole wood (dbh_{100} = 20-30 cm) and young timber (dbh_{100} = 31-40 cm) (Christian Ginzler, pers. comm., 29. 01. 2013; Peter Rotach, pers. comm., 22. 02. 2013). With regard to the mosaic-cycle concept of Korpel (1995), which distinguishes the three main development phases growing-up, optimal and break-up, the stages of development favoring Wood Warbler occurrence belong to late growing-up and early optimal. Stands of these stages of development are usually single-layered and characterized by a dense and closed canopy. This allows for an open stem space and inhibits both the development of the herb and shrub layer and the development of regeneration. Natural mortality of the dominant trees of the upper tree layer is very low. In natural beech-dominated stands, hardly any gaps are present at these stages (Korpel, 1995; Pontailler et al., 1997; Meyer et al., 2003; Rozenbergar et al., 2007).

In contrast, the phases growing-up, late optimal and break-up are less suitable for Wood Warbler occurrence. Young stands, arising from natural regeneration, are too dense for Wood Warbler occurrence because high stand density inhibits the song flight, which is important for territory establishment and mate attraction (Glutz von Blotzheim & Bauer, 1991). Old stands become unsuitable because canopy opens up, mainly due to harvesting (Peter Rotach, pers. comm., 22. 02. 2013). As a consequence, shrubs and bushes develop in the gaps due to the ameliorated light conditions. The forest ground becomes unsuitable for the ground-nesting Wood Warbler, inhibiting its occurrence. This conclusion is also supported by the negative correlation of Wood Warbler occurrence with maxVH and

meanCC_20m. Furthermore, the proportion of low branches for song flight behavior decreases with stand age.

The findings concerning the first hypothesis comply with previous studies describing the preferred habitat of Wood Warblers as forest stands with an open stem space, a closed canopy, a little-developed herb and shrub layer, and trees with low branches for song-flight behavior (Quelle & Tiedemann, 1972; Schifferli et al., 1980; Glutz von Blotzheim & Bauer, 1991). Glutz von Blotzheim & Bauer (1991) and Quelle & Tiedemann (1972) also refer to late pole wood and young timber as most suitable age classes. In accordance with the results of this study, Mallord et al. (2012) also found a concave relationship between territory occurrence of Wood Warblers and canopy height. Both Gerber (2011) and Reinhardt (2003) found that occupied territories have a higher number of trees than abandoned territories or random control areas. Because stem number decreases with forest age, Reinhardt (2003) concluded that forests of medium age are most suitable for Wood Warbler occurrence. Pavlovic (2009) hypothesized that Wood Warbler occurrence increases with vegetation height but could not confirm this hypothesis.

Other bird species with a preference for mid-successional forests are, for example, Least Flycatcher (*Empidonax minimus*), American Redstart (*Setophaga ruticilla*) or Philadelphia Vireo (*Vireo philadelphicus*). Least Flycatchers are abundant in well-stratified forest, with a dense upper canopy and a relatively open subcanopy and therefore strongly associated with mid-successional forests (Breckenridge, 1956; Sherry, 1979, Holmes & Sherry, 2001). Also, American Redstarts and Philadelphia Vireos are species shown to frequently occur in early successional and mid-successional forests (Hunt, 1996; Holmes & Sherry, 2001). In their unmanaged study area, Holmes & Sherry (2001) observed a strong decline of all three species between 1969 and 1998. The authors hypothesize that maturing of the forest in the study area may have reduced habitat quality for these species.

In accordance to previous findings (Pavlovic, 2009), a negative relationship was found between Wood Warbler occurrence and increasing **standard deviation** of canopy height (**H2**). Out of the vertical diversity metrics, sdCH>3m performed best indicating that stands with a high tree height diversity negatively influence Wood Warbler occurrence. This relationship was found for both the nesting area and the territory scale, suggesting that stands with even-aged trees and no gaps are preferred. These findings are closely connected with the findings from the first hypothesis because stands of medium height are characterized by homogeneous stand height and therefore by a small vertical diversity of canopy height (Korpel, 1995; Pontailler et al., 1997; Meyer et al., 2003; Rozenbergar et al., 2007).

Few bird species prefer stands with a homogeneous tree height (Scherzinger, 1996; Müller, 2005; Winter et al., 2005; Mollet et al., 2006). In general, avian diversity in forests appears to be positively related to structural diversity, including vertical diversity. For example, Goetz et al. (2007) found that vertical distribution of the canopy was the strongest positive predictor for species richness. Similarly, Müller et al. (2009) found that the occurrence of many species was positively related to vertical variation of canopy height. The only species showing a

negative relationship with vertical variation of canopy height was the Nuthatch (*Sitta europaea*).

Wood Warbler occurrence is related to **canopy cover** (**H5**). According to previous studies, a canopy cover of 60%-90% is preferred (Bibby, 1989; Glutz von Blotzheim & Bauer, 1991). According to this study, canopy cover favoring Wood Warbler occurrence is high at 10 m above ground, while canopy cover 20 m above ground should be low. Canopy cover is defined as area of forest floor covered by the vertical projection of the tree crowns (Jennings et al., 1999). Accordingly, tree crowns at every height above ground are included in the calculation of canopy cover, whereas the canopy cover metrics used in this study do not consider all tree crowns but represent a horizontal cut at a specific height level (Fig. 6). Therefore, canopy cover favoring Wood Warbler occurrence can be described as high due to the effect found for meanCC_10m. Furthermore, meanCC_20m derived from the study forests refers more to stand height than to canopy cover due to the strong correlations with meanCH, meanVH>3m and meanCH>3m (Table 7).

Stands with closed canopy are characterized by few bushes and little ground vegetation, features promoting the occurrence of the Wood Warbler. Again, these findings are closely connected with the findings from the first hypothesis because pole wood and young timber are characterized by a closed canopy.

Gerber (2011) compared occupied territories with control areas in the same study areas in 2010 and found only weak evidence for the often-stated preference for forests with a closed canopy. The same result was found in analyses covering three years of data from the same study areas (Gilberto Pasinelli, pers. comm. 5. 04. 2013). Probably, the variation of the *canopy cover* habitat variable was too small for distinguishing occupied territories from control areas.

According to this study, the Wood Warbler occurrence is positively related to **inclination** (**H6**). This relationship is rarely mentioned in the common habitat descriptions of Wood Warblers (but see Hölzinger, 1999; Reinhardt & Bauer, 2009; Gerber, 2011; Mallord et al., 2012). According to Glutz von Blotzheim & Bauer (1991), Wood Warbler territories are equally situated on flat terrain, on crests and on slope. Therefore, it is unclear whether inclination is directly related to Wood Warbler occurrence or not. Mallord et al. (2012) found a positive association of Wood Warbler territories and slope in mid Wales. The authors bring forward the argument that nowadays Wood Warblers mainly settle in the upland areas of the UK where grazing has remained the dominant form of land management. They argue that the grazing maintains the open woodland structure preferred by Wood Warblers. Also in Switzerland, Wood Warbler occurrence has strongly declined in the lowlands. But the argumentation of grazing is not applicable to the situation in Switzerland, because here, wood pasture was already discontinued after the first half of the 19th century due to changes in agricultural practice (Pfister & Messerli, 1990; Bürgi, 1999).

An explanation for the observed effect of inclination might be that inclined areas, especially areas with southern aspect, warm-up earlier in spring and therefore become snow-free earlier compared to flat areas. This effect may only become important above a certain altitude because of the delayed beginning of the growing season at increased altitudes. Possibly, the predominant location of the study areas in the eastern Jura led to the detection of this relationship.

Alternative explanations for the positive relationship between Wood Warbler occurrence and inclination could be that disturbances due to recreational activity or forest management intensity decrease with increasing inclination. Outdoor recreational activities can affect wildlife (e.g. Boyle & Samson, 1985; Taylor & Knight, 2003). Recreational activities in forests are mainly taking place on trails (Bernasconi & Schroff, 2003; Bernasconi & Schroff, 2008). Trails can create habitat edges, may cause an increase in nest predation or brood parasitism, and increase habitat fragmentation (Paton, 1994; Miller & Hobbs, 2000; Kangas et al., 2010). Some studies showed that bird species composition alters adjacent to trails (Miller et al., 1998). For nearby recreation, areas close to settlements are preferred (Buchecker, 2008). But the study areas of this study were relatively remote and no peri-urban forest stands were investigated.

The date of last treatment is a good indicator for the intensity of forest management (Brändli, 2010). Many study areas are located in areas where last treatment took place 20 to 50 years ago (Brändli, 2010), incuding also study areas situated in forest nature reserves. In particular, inclined areas are often treated less intensively due to higher costs of timber harvesting (Brändli, 2010). Harvesting usually leads to gaps in the canopy, favoring the development of shrubs and regeneration, which negatively affects Wood Warbler occurrence. However, it has to be considered that unmanaged forest stands become unsuitable for Wood Warbler occurrence at a certain age as well because of the lack of structures for song-flight behavior (Glutz von Blotzheim & Bauer, 1991) or due to mortality of the trees of the upper canopy layer leading to increased vertical diversity and the development of shrubs and regeneration.

Wood Warbler occurrence was positively related to **solar radiation during March** (**H7**). At the nesting area scale, this relationship was stronger than at the territory scale. This indicates that solar radiation during March influences the small-scale location of the nesting area. Since the Wood Warbler is a ground-nesting bird, the species may benefit from small-scale variation of snow melting and vegetation development. Because solar radiation is highest on south-facing slopes and lowest on north-facing slopes, this finding may explain why Wood Warbler territories with southern aspect are more common than territories with northern or western aspect (Glutz von Blotzheim & Bauer, 1991; Hölzinger, 1999; Reinhardt & Bauer, 2009). West-facing slopes may be avoided because of prevailing wind direction and precipitation. Alternatively, solar radiation might positively influence food availability. Higher food availability on south-facing slopes than on north-facing slopes could attract Wood Warblers, as Jedrzejewsk & Jedrzejewski (1998) reported positve correlations between Wood Warbler population size and food abundance.

Metrics referring to **penetration rate**, a measure of vertical diversity, and the associated hypotheses (**H3**, **H4**) received little support. For the distinction of a well-developed canopy from other canopies, a smaller height interval should perhaps be used than the whole range between 2 m and 50 m. Müller et al. (2009), who proposed this metric, worked with full waveform data collected after leaf flush in a mixed montane forest. In contrast, the data used in this study consisted of first and last return lidar data collected predominantly outside the growing season in mainly deciduous forests (Swisstopo, 2009). Full waveform lidar data consist of a larger number of return laser signals than first and last return lidar data. Therefore, full waveform lidar data is able to reflect vegetation structure more precisely than the data used in this study (Lefsky et al., 2002). In addition, trees prior to leaf flush reflect fewer lidar signals than trees after leaf flush. Pavlovic (2009) found a positive correlation between the penetration rate of the mid-story and the occurrence of Wood Warblers. For the penetration rate of the shrub and regeneration layer, he unexpectedly found a positive relationship with Wood Warbler occurrence. Comparing the results from Pavlovic (2009) to the findings presented here is complicated by three reasons. First, Pavlovic (2009) worked with lidar data collected in May after leaf flush. Second, average density of laser signals of 25 signals per m^2 was up to 50 times higher than in this study. Third, the stocking of the *Nationalpark Bayerischer Wald* study area mainly consisted of spruce, while the study areas in this study mainly consisted of beech-dominated forests.

The hypothesis concerning **forest type** could not be confirmed (**H8**). It is likely that the spatial resolution of the data source and the classification into four groups representing coniferous to broadleaf forest were not sufficiently accurate to properly test this hypothesis. However, analyses of habitat variables recorded within the project at the Swiss Ornithological Institute did not either reveal a relationship between Wood Warbler occurrence and tree species composition of occupied territories and control areas (Gilberto Pasinelli, pers. comm., 5. 04. 2013). The hypothesis concerning **distance to forest edge** (**H9**) was not supported either. Finally, **H10** could not be evaluated, because the soil condition values hardly varied between occupied areas and control areas.

4.3 Current potential range

The Wood Warbler was widespread in the 1950s across Switzerland up to 1300 m a.s.l. (Knaus et al., 2011) and still common in the entire Swiss Plateau and Jura, and in parts of the Canton of Tessin, Valais and Grisons in 1970s (Schifferli et al.,1980). Twenty years later, however, Wood Warbler's main range was predominantly located in Western Jura and the region Northern Jura - *Hochrhein*. Declines of the population were mainly observed in forests closed to residential areas (Schmid et al., 1998).

According to the predictive models, the current main range of the Wood Warbler is located predominantly in the Jura mountains. Hence, the prediction based on RS variables mirror the situation in 1996.

While interpreting the predicted current potential range, several issues have to be considered. Firstly, the model used to predict the current potential range of Wood Warblers only includes structural forest characteristics and topographical characteristics. However, as in many other species, habitat selection of the Wood Warbler within the structurally and topographically suitable habitat spectrum is influenced by other processes, such as social behavior, predation, disturbance, interspecific competition or food availability (Fuller, 2012), which all can reduce the area of potential habitat. In addition, rodent density influences territory choice of the Wood Warbler as well (Wesolowski et al., 2009; Gerber, 2011).

Secondly, the models used for the prediction are empiric that is they sacrifice generality to realism and precision (Levins, 1966). Therefore the models are only applicable to the situation in Switzerland as it is today (Levins, 1966). Due to the relatively small environmental envelope as a consequence of the relatively small spatial scales (nesting area and territory) assessed here and the predominant location of the study areas in the Jura Mountains, the models are hardly applicable to other countries.

4.4 Wood Warbler population decline in Western Europe: potential causes

The following hypotheses are most often proposed for explaining the decline of Wood Warbler populations in Western Europe: (1) structural habitat changes due to changing forestry practices (Bibby, 1989; Marchant, 1990; Glutz von Blotzheim & Bauer, 1991; Gatter, 2000; Marti, 2007; Reinhardt & Bauer, 2009; Mallord et al., 2012); (2) increased nest predation due to changes in the predator communities (Gatter, 2000; Wesolowski et al., 2009); (3) changes of the food supply as a consequence of climate change (Gatter, 2000; Both et al., 2010); (4) increase in disturbances due to augmented human recreational activities (Miller et al., 1998; Miller & Hobbs, 2000; Kangas et al., 2010; Spaar et al., 2012); and (5) habitat changes in migration stopover sites and/or in wintering sites (Weber et al., 1999; Flade & Schwarz, 2004).

This study addressed the first hypothesis referring to **structural habitat changes** related to forestry. Changes in forest management and non-timber forest uses strongly influence forest types, growing stock or tree species composition and therefore forest structure (Bürgi, 1999). The average age and growing stock of forests have been increasing since the 20th century (Bürgi, 1999). Hence, some authors argue that these changes result in a decrease of suitable habitat for Wood Warblers (Reinhardt & Bauer, 2009; Mallord et al., 2012). Others assume that conversion of woods to conifers is responsible for the population decline of Wood Warblers (Bibby, 1989; Marchant et al., 1990; Glutz von Blotzheim & Bauer, 1991; Marti, 2007). Furthermore, Marti (2007) supposed that extensive extraction of timber leads to habitat loss due to decreased canopy cover, while Gatter (2000) hypothezised that the increasing amount of natural regeneration combined with increased growth of herbs due to nitrification may adversly affect Wood Warbler populations. Other effects may be the promotion of open forests to increase biodiversity in forest or the enhancement of selection forest leading to structurally heterogeneous forest stands.

Many studies showed that structural habitat characteristics are crucial for the occurrence of Wood Warblers (e.g. Bibby, 1989; Reinhardt & Bauer, 2009; Gerber, 2011). However, a number of findings indicate that structural habitat changes due to changing forestry practices hardly seem to be the main cause for the large-scale decrease of Wood Warbler populations in Western Europe.

Firstly, Wood Warbler decline should not mistakenly be associated with the century-old decline of species of open, dry, and warm locations (Gatter, 2000). These species are strongly associated with the centuries-long exploitation of forests in Switzerland that stopped around 1800 with the beginning of modern forestry and the enactment of the *Forstpolizeigesetz* in 1876 (Bürgi, 1999; Gatter, 2000). Since then, forest area and growing stock have been steadily increasing resulting in a decline of open-canopy sites. The Wood Warbler, however, is not a typical species of open, dry and warm locations and the strong population decline in Switzerland started mainly during the 1990s (Schmid et al., 1998). If structural changes caused by increasing growing stock were the major reason for the population decline of Wood Warblers, an onset of the decline should have been observed much earlier than 1990.

Secondly, the proportion of broadleaf on the growing stock and the proportion of natural regeneration have steadily been increasing since 1983 (Brändli, 2010). Therefore, the population decline of Wood Warbler hardly seems to originate from the increase in coniferous species preferred in artificial regeneration in the second half of the 19th century (Bürgi, 1999).

Furthermore, the proportion of regularly managed forests (managed within the last 20 years) in Switzerland declined from 69% in 1985 to currently 63% (Mahrer, 1988; Brändli, 2010). This development is favorable for the habitat needs of the Wood Warbler because a stand is expected to remain suitable for a longer time period under unmanaged circumstances than under managed ones. But even under unmanaged circumstances, forest stands become unsuitable for Wood Warbler occurrence at a certain age due to natural succession, resulting in a lack of structures for song-flight behavior, such as low branches (Glutz von Blotzheim & Bauer, 1991) or opening of canopy due mortality.

To enhance biodiversity, forests are increasingly opened up. So far, the dimension of areas affected is marginal, e.g. the target value in the canton of Zurich is 2% (Bertiller & Keel, 2006).

Also, selection forest in deciduous forest (*Dauerwald*) is often propagated (e.g. Knok, 2010; Huth & Wagner, 2013). Selection forest (*Plenterwald*) is characterized by mixed stages of stand development and high vertical stand diversity (Brändli, 2010). Selection forest covers 8% of the Swiss forest area and is most common in the Alps, where coniferous trees prevail. In lowlands, the proportion of selection forest, and especially selection forest in deciduous forest, is marginal (Brändli, 2010).

Wood Warblers prefer stands of late pole wood and young timber, that is, forest at an intermediate seral stage. In Switzerland, the stages of stand development are not evenly distributed (Brändli, 2010). According to the Swiss National Forest Inventory (2004-2006)

(NFI3), pole wood and young timber cover 17% and 15% of the forest area stocked with uniform high forest (77% of the forest area), corresponding to approximately 139'000 ha and 122'000 ha, respectively (Brändli, 2010). For the area of the Jura Mountains and the Swiss Plateau, the proportion of pole wood and young timber together is 29% and 12%, respectively (Brändli, 2010). According to the Swiss National Forest Inventory (1993-1995) (NFI2), pole wood and young timber covered 44% and 36% of the forest area stocked with uniform high forest in the Jura Mountains and in the Swiss Plateau, respectively (Brassel & Brändli, 1999). In the area of the Jura Mountains, medium timber (dbh: 41-50 cm) covers 40% of the forest area stocked with uniform high forest and is the most widespread stage of stand development. In contrast, old timber (dbh > 50 cm) represents the most common stage of development in the Swiss Plateau and the Northern Pre-Alps (Brändli, 2010).

Whether the population decline of the Wood Warbler has been caused by the maturing of Swiss forests is difficult to assess. The above-mentioned reduction in the extent of pole wood and young timber, favored habitats of the Wood Warbler, might have contributed to the decline. A balanced age structure of the Swiss forest is all the more important in the long term, so that new stands of pole wood and young timber can grow up and replace stands that became unsuitable for the Wood Warbler.

With regard to the second hypothesis referring to **increased nest predation** due to changes in the predator communities, Wesolowski et al. (2009) found that Wood Warbler population crashes in eastern Poland coincided with local rodent outbreaks. But the expected higher nest depredation caused by increased predator activity during the outbreaks of the rodents could only partially be confirmed. The authors concluded that the arriving Wood Warblers refused to settle in rodent outbreak areas what may result in the nomadic behavior of the species. Along the same lines, Gerber (2011) found that Wood Warbler territories had lower rodent densities than adjacent control areas without Wood Warblers. Why Wood Warblers avoid areas with high rodent density remains unclear. Grendelmeier (2011) has shown with trail cameras that rodents do not predate Wood Warbler nests in the study areas examined here. Furthermore, Flade & Schwarz (2004) argued that three ground-nesting forest species have significantly increased between 1989 and 2003. Holmes & Sherry (2001) analyzed abundances of forest birds in an unfragmented, undisturbed and relatively mature temperate deciduous forest in New Hampshire, USA, between 1969 and 1998. No indications were found for nest predation rates that would account for population declines.

Changes of the food supply as a consequence of climate change are considered to contribute to the decline of avian populations. According to the mismatch hypothesis, negative fitness consequences may result from different phenological responses to climate change of different trophic levels leading to a temporal mismatch between resource requirement and resource availability (e.g. Both et al., 2006). Different studies showed that broods missing the food supply peak produced less surviving offspring than broods not missing the food supply peak. Furthermore, an advancement of the laying date was observed for many bird species during the last few decades (Both, 2010). With regard to the

Wood Warbler, Maziarz & Wesolowski (2010) found that the timing of the Wood Warbler breeding in eastern Poland did not match the caterpillar peak, that is, the peak of the preferred food for nestlings. Instead, timing of breeding was constrained by the females' arrival time, which did not significantly change between 1976 and 2005 (Wesolowski & Maziarz, 2009). The mismatch between the breeding phenology of the Wood Warbler and the caterpillar peak had no effect on nestlings' development, perhaps because caterpillars were replaced by other prey items after the caterpillar peak (Maziarz & Wesolowski, 2010). Also, Reinhardt & Bauer (2009) concluded that food availability during the breeding time hardly explains the decline of Wood Warbler populations.

Concerning the **disturbance hypothesis**, no clear results are available. Schmid et al. (1998) observed a distinct decrease and local disappearance of Wood Warbler populations in forests near densely-settled areas. Kangas et al. (2010) found that open-cup nesters breeding on the ground, which is true for Wood Warblers, showed strongest negative responses to visitor pressure. Gerber (2011) could not find an effect of disturbance on territory choice. A possible explanation for the lacking effect may be that Gerber (2011) mainly examined study areas that were quite remote and thus not very frequented by humans.

Finally, the fifth hypothesis proposes that **habitat changes in migration stopover sites and/or in wintering sites** are the main causes for the population decline of Wood Warblers. According to Flade & Schwarz (2004), seven out of ten declining forest bird species in Germany are long-distance migrants, including the Wood Warbler Therefore, Flade & Schwarz (2004) concluded that environmental changes in the African wintering sites or at stopover sites along the way currently appear to be the biggest threat for German forest birds. Also, Reinhardt & Bauer (2009) suggest that the main causes of the extensive Wood Warbler population decline around Lake Constance during the last 20 years are environmental changes outside the breeding ground, because the breeding habitat did not considerably change.

5 Conclusions

Overall, this study suggests that RS variables derived from lidar data or other sources convey additional information for describing species-specific habitat needs to that provided by field variables. Lidar metrics mainly provide information on the vertical and horizontal stand structure. Therefore, lidar metrics and other RS variables are a valuable complement to variables gathered in the field. Furthermore, RS has additional advantages, such as data collection over large spatial extents for which collection in the field is impractical or impossible (Lefsky et al., 2002; Bradbury et al., 2005). Also, the use of lidar allows for direct vertical measurement of canopy and sub-canopy structure which provides critical information about other biophysical parameters, such as growing stock or productivity (Dubayah & Drake, 2000; Lefsky et al., 2002).

The analyses of the two spatial scales, nesting area and territory, suggest that Wood Warblers prefer rather uniform forest stands of intermediate age. Stands of these stages of stand development are characterized by a closed canopy, an open stem space and a sparse herb and shrub layer, features promoting the occurrence of the Wood Warbler. The analyses further showed that Wood Warbler occurrence is positively related to inclination and solar radiation during March.

With regard to forest management, it should be considered that every forest development phase has its own bird species composition. For example, Tree Pipit (*Anthus trivialis*), Dunnock (Prunella modularis) and Yellowhammer (*Emberiza citrinella*) ofen appear in regeneration, while other species, such as Eurasian Nuthatch (*Sitta europaea*), Eurasian Treecreeper (*Certhia familiaris*) and woodpeckers (*Picidae*), need stands with old trees. In beech-dominated stands, especially young and old stands exhibit high bird diversity (Winter et al., 2005; Mollet et al., 2006). According to Müller (2005), the following factors favor a high avian diversity: abundance of regeneration and shrubs, presence of mature broad-leaved trees, presence of coniferous tree species, proportion of oaks, broadleaves of high value (*Alnus*, *Fraxinus*) and pioneer deciduous trees (*Salix*, *Populus*), stand age, standing dead wood (snags, dead wood at living trees) and the availability of cavities. Furthermore, forest boundaries (i.e. habitat edges) are of high value for many bird species (e.g. Scherzinger, 1996). Even though many bird species prefer structurally rich stands, the Wood Warbler seems to favor a rather uniform environment. Forest management may locally contribute to the deterioration of suitable areas, for example when relatively closed forests are opened up due to harvesting. Therefore, the focus of forest management at a regional scale should be on sustainable regeneration so that sufficiently large suitable stands are always present and new suitable stands are steadily developing. In consideration of the Wood Warbler's habitat needs, femel harvesting system (*Femelschlag*), leading to a relatively homogeneous stand age structure, appears to be most appropriate to maintain structurally suitable stands for Wood Warblers. Selection forestry (*Plenterwald*/*Dauerwald*), leading to a heterogeneous age structure and many gaps on a small scale, is rather unsuitable.

Literature

Akaike, H., 1974. A New Look at the Statistical Model Identification. *IEEE Transactions of Automatic Control,* 19 (6), 716-723.

Allouche, O., Tsoar, A. & Kadmon, R., 2006. Assessing the accuracy of species distribution models: prevalence, kappa and the true skill statistic (TSS). *Journal of Applied Ecology,* 43, 1223-1232.

Baltsavias, E., 1999. Airborne laser scanning: basic relations and formulas. *ISPRS Journal of Photogrammetry & Remote Sensing,* 54, 199-214.

Batary, P. & Baldi, A., 2004. Evidence of an Edge Effect on Avian Nest Success. *Conservation Biology,* 18 (2), 389-400.

Bates, D., Maechler, M. & Bolker, B., 2012. Linear mixed-effects models using S4 classes. R package version 0.999999-0.

Bernasconi, A. & Schroff, U., 2003. *Verhalten, Erwartungen und Zahlungsbereitschaft von Waldbesuchern in der Region Bern,* Ed.: Arbeitsgemeinschaft für den Wald.

Bernasconi, A. & Schroff, U., 2008. Freizeit und Erholung im Wald. Grundlagen, Instrumente, Beispiele. *Umwelt-Wissen,* 0819, 1-69.

Bertiller, R. & Keel, A., 2006. 1000 ha Lichte Wälder für den Kanton Zürich. *Züricher Wald,* 5, 9-12.

Bibby, C. J., 1989. A survey of breeding Wood Warblers *Phylloscopus sibilatrix* in Britain, 1984-1985. *Bird Study,* 36 (1), 56-72.

Both, C., 2010. Food availability, mistiming, and climatic change. In: A. P. Moller, W. Fiedler & P. Berthold, Ed. *Effects of climate change on birds.* Oxford: Oxford University Press, 129-147.

Both, C., Bouwhuis, S., Lessells, C. & Visser, M. E., 2006. Climate change and population declines in a long-distance migratory bird. *Nature,* 441, 81-83.

Both, C., Van Turnhout, C., Bijlsma, R., Siepel, H., Van Strien, A. & Foppen, R., 2010. Avian population consequences of climate change are most severe for long-distance migrants in seasonal habitats. *Proceedings of the Royal Society B,* 277, 1259-1266.

Boyle, S. A. & Samson, F. B., 1985. Effects of Nonconsumptive Recreation on Wilflife: A Review. *Wildlife Society Bulletin,* 13 (2), 110-116.

Bradbury, R., Hill, R., Mason, D., Hinsley, S., Wilson, J., Balzter, H., Anderson, G., Whittingham, M., Davenport, I. & Bellamy, P., 2005. Modelling relationships between birds and vegetation strucutre using airborne LiDAR data: a review with case studies from agricultural and woodland environments. *Ibis,* Band 147, pp. 443-452.

Brändli, U.-B. (Ed.), 2010. *Schweizerisches Landesforstinventar. Ergebnisse der dritten Erhebung 2004-2006.* Birmensdorf, Bern: Eidgenössische Forschungsanstalt für Wald, Schnee und Landschaft WSL & Bundesamt für Umwelt BAFU.

Brassel, P. & Brändli, U.-B. (Ed.), 1999. *Schweizerisches Landesforstinventar: Ergebnisse der Zweitaufnahme 1993 - 1995.* Birmensdorf, Bern: Eidgenössische Forschungsanstalt für Wald, Schnee und Landschaft WSL & Bundesamt für Wald und Landschaft BUWAL.

Breckenridge, W., 1956. Measurements of the habitat niche of the least flycatcher. *The Wilson Bulletin,* 68 (1), 47-51.

Buchecker, M., 2008. Welche Ansprüche hat die Bevölkerung an ihre Wohnumgebung? Inhaltliche und prozedurale Voraussetzungen für eine bedürfnisgerechte Planung. *Forum für Wissen*, 43-54.

Bunnell, F. & Huggard, D., 1999. Biodiversity across spatial and temporal scales: problems and opportunities. *Forest Ecology and Management*, 115*,* 113-126.

Burfeld, I., van Bommel, F. & Gallo-Orsi, U., 2004. *Birds in Europe: population estimates, trends and conservation status.* Cambridge: BirdLife International.

Bürgi, M., 1999. A case study of forest change in the Swiss lowlands. *Landscape Ecology,* 14, 567-575.

Burnham, K. P. & Anderson, D. R., 2002. *Model Selection and Multimodel Inference - A Practical Information-Theoretic Approach.* Second edition, Ed. New York: Springer-Verlag New York, Inc..

Campell, N. & Reece, J., 2003. *Biologie.* 6. edition, Ed. Heidelberg, Berlin: Spektrum Akademischer Verlag GmbH.

Chen, J., Franklin, J. F. & Spies, T. A., 1992. Vegetation Responses to Edge Environments in Old-Growth Douglas-Fir Forests. *Ecological Applications*, 2 (4), 387-396.

Chetkiewicz, C.-L. B. & Boyce, M. S., 2009. Use of resource selection functions to identify conservation corridors. *Journal of Applied Ecology,* 46, 1036-1047.

Chust, G., Galparsoro, I., Borja, A., Franco, J., & Uriarte, A., 2008. Coastal and estuarine habitat mapping, using LIDAR height and intensity and multi-spectral imagery. *Estuarine Coastal and Shelf Science,* 78, 633-643.

Cohen, J., 1960. A coefficient of agreement for nominal scales. *Educational and phychological measurement,* XX (1), 37-46.

Dettmers, R. & Bart, J., 1999. A GIS Modeling Method Applied to Predicting Forest Songbird Habitat. *Ecological Applications,* 9 (1), 152-163.

Dubayah, R. O. & Drake, J. B., 2000. Lidar Remote Sensing for Forestry. *Journal of Forestry,* June 2000, 44-46.

Dunlavy, J. C., 1935. Studies on the phyto-vertical distribution of birds. *The Auk,* 52 (4), 425-431.

Ellenberg, H. & Klötzli, F., 1972. Waldgesellschaften und Waldstandorte der Schweiz. *Mitteilungen / Schweizerische Anstalt für das Forstliche Versuchswesen,* 8 (4), 589-930.

Everitt, B., 2002. *The Cambridge Dictionary of Statistics.* Second edition, Ed. Cambridge: Cambridge University Press.

Federal Statistical Office (FSO), 2001. *Waldmischungsgrad der Schweiz,* Neuchâtel.

Fielding, A. H. & Bell, J. F., 1997. A review of methods for the assessment of prediction errors in conservation presence/absence models. *Environmental Conservation,* 24 (1), 38-49.

Fischer, H. S., 1990. Simulation der räumlichen Verteilung von Pflanzengesellschaften auf der Basis von Standortskarten. Dargestellt am Beispiel des MaB-Testgebiets Davos, Zürich: *Veröffentlichungen des Geobotanischen Institues der ETH*, Stiftung Rübel.

Flade, M. & Schwarz, J., 2004. Ergebnisse des DDA-Monitoringprogramms, Teil II: Bestandesentwicklung von Waldvögeln in Deutschland 1989-2003. *Vogelwelt,* 125, 177-213.

Forman, R. & Godron, M., 1986. *Landscape ecology.* New York: John Wiley & Sons.

Freeman, E., 2012. Presence-Absence Model Evalutation. R package version 17.08.2012.

Fuller, R. J., 2012. Habitat quality and habitat occupancy by birds in variable environments. In: R. J. Fuller, Ed. *Birds and Habitat - Relationships in Changing Landscapes.* Cambridge: Cambridge University Press, 37-62.

Gatter, W., 2000. *Vogelzug und Vogelbestände in Mitteleuropa. 30 Jahre Beobachtung am Randecker Maar.* Wiebelsheim: AULA-Verlag.

Gerber, M., 2011. Territory choice of the Wood Warbler *Phylloscopus sibilatrix* in Switzerland in relation to habitat strucure and rodent density*,* MSc thesis, University of Zurich.

Gibson, L., Wilson, B., Cahill, D. & Hill, J., 2004. Spatial prediction of ruous bristlebird habitat in a coastal heathland: a GIS-based approach. *Journal of Applied Ecology,* 41, 213-223.

Glutz von Blotzheim, U. N. & Bauer, K. M., 1991. *Handbuch der Vögel Mitteleuropas.* Wiesbaden: AULA-Verlag.

Goetz, S., Steinberg, D., Dubayah, R. & Blair, B., 2007. Laser remote sensing of canopy habitat heterogeneity as a predictor of bird species richness in an eastern temperate forest, USA. *Remote Sensing of Environment,* 108, 254-263.

Gonseth, Y., Wolgemuth, T., Sansonnens, B. & Buttler, A., 2001. Die biogeographischen Regionen der Schweiz. Erläuterungen und Einteilungsstandard. *Umwelt Materialien*, 137, 1-48.

Grendelmeier, A., 2011. The enigmatic decline of the Wood Warbler *Phylloscopus sibilatrix*: nest predation and habitat characteristics, MSc thesis, University of Bern.

Grubbs, F. E., 1969. Procedures for Detecting Outlying Obersvations in Samples. *Technometrics*, February, 11 (1), 1-21.

Hastie, T., Tibshirani, R. & Friedman, J., 2009. 7.10 Cross-Validation. In: Second edition, Ed. *The Elements of Statistical Learning. Data Mining, Inference, and Prediction.* New York: Springer Science + Business Media, 241-248.

Hinsley, S., Hill, R., Gaveau, D. & Bellamy, P., 2002. Quantifying woodland structure and habitat quality for birds using airborne laser scanning. *Functional Ecology,* 16, 851-857.

Hinsley, S. A., Hill, R. A., Bellamy, P. E. & Balzter, H., 2006. The Application of Lidar in Woodland Bird Ecology: Climate, Canopy Structure, and Habitat Quality. *Photogrammetric Engineering & Remote Sensing,* 72 (12), 1399-1406.

Holmes, R. T. & Sherry, T. W., 2001. Thirty-year bird population trends in an unfragmented temperate deciduous forest: importance of habitat change. *The Auk,* 118(3), 589-609.

Hölzinger, J., 1999. *Die Vögel Baden-Württembergs. Band 3.1 Singvögel.* Stuttgart: Eugen Ulmer GmbH & Co..

Hunt, P. D., 1996. Habitat Seleciton by American Redstarts along a Successional Gradient in Northern Hardwoods Forest: Evaluation of Habitat Quality. *The Auk,* 113 (4), 875-888.

Hurvich, C. M. & Tsai, C.-L., 1989. Regression and Time Series Model Selection in Small Samples. *Biometrika,* 76 (2), 297-307.

Huth, F. & Wagner, S., 2013. Ökosystemleistungen von Dauerwäldern - eine aktuelle Analyse des Waldbaus. *Schweizerische Zeitschrift für Forstwesen,* 164 (2), pp. 27-36.

Hyde, P., Dubayah, R., Peterson, B., Blair, J.B., Hofton, M., Hunsaker, C., Knox, R. & Walker, W., 2005. Mapping forest structure for wildlife habitat analysis using waveform lidar: Validation of montane ecosystems. *Remote Sensing of Environment,* 96, 427-437.

Hyde, P., Dubayah, R., Walker, W., Blair, B., Hofton, M. & Hunsaker, C., 2006. Mapping forest structure for wildlife habitat analysis using multi sensor (LIDAR, SAR/InSAR, ETM+, Quickbird) synergy. *Remote Senisng of Environment,* 102, 63-73.

Irrgang, S., 1990. Dynamik der Artstruktur sowie der Biomasseproduktion und -akkumulation in den ersten Jahren nach Kahlschlag. *Archiv für Naturschutz und Landschaftsforschung,* 30, 231-252.

Isenburg, M., 2012. *LAStools: award winning software for rapid LIAR processing.* [Online] Available at: http://www.cs.unc.edu/~isenburg/lastools/ [Visit 24. 10. 2012].

Jedrzejewsk, B. & Jedrzejewski, W., 1998. Predation in vertebrate communities: the Bialowiezka primeval forest as a case study. *Ecological studies,* 135, 1-450.

Jennings, S., Brown, N. & Sheil, D., 1999. Assessing forest canopies and understorey illumination: canopy closure, canopy cover and other measures. *Forestry,* 72, 59-73.

Johnson, C. J., Seip, D. R. & Boyce, M. S., 2004. A quantitative approach to conservation planning: using resource selection functions to map the distribution of mountain caribou at multiple spatial scales. *Journal of Applied Ecology,* 41, 238-251.

Kangas, K., Luoto, M., Ihantola, A., Tomppo, E. & Siikamaki, P., 2010. Recreation-induced changes in boreal bird communities in protected areas. *Ecological Applications,* 20(6), 1775-1786.

Keller, V., Gerber, A., Schmid, H., Volet, B. & Zbinden, N., 2010a. Rote Liste Brutvögel. Gefährdete Arten der Schweiz, Stand 2010. *Umwelt-Vollzug,* 1019, 1-53.

Keller, V., Ayé, R., Müller, W., Spaar, R. & Zbinden, N., 2010b. Die prioritären Vogelarten der Schweiz: Revision 2010. *Der Ornithologische Beobachter,* Dezember, 107 (4), 265-285.

Knaus, P., Graf, R., Guélat, J., Keller, V., Schmid, H. & Zbinden, N., 2011. *Historischer Brutvogelatlas. Die Verbreitung der Schweizer Brutvögel seit 1950.* Sempach: Schweizerische Vogelwarte.

Knok, T., 2010. Dauerwald und Ökonomie. *Waldforschung aktuell,* 33, 31-32.

Korpel, S., 1995. *Die Urwälder der Westkarpaten.* Stuttgart, Jena, New York: Fischer.

Landis, R. J. & Koch, G. G., 1977. The Measurement of Observer Agreement for Categorical Data. *Biometrics,* 33 (1), 159-174.

Lefsky, M. A., Cohen, W. B., Parker, G. G. & Harding, D. J., 2002. Lidar Remote Sensing for Ecosystem Studies. *BioOne*, 52(1), 19-30.

Levins, R., 1966. The strategy of model building in population biology. *American Scientist,* 54 (4), 421-431.

Luoto, M., Kuusaari, M. & Toivonen, T., 2002. Modelling butterfly distribution based on remote sensing data. *Journal of Biogeography, 2*9, 1027-1037.

Mahrer, F., 1988. *Schweizerisches Landesforstinventar: Ergebnisse der Erstaufnahme 1982 - 1986.* Birmensdorf: Eidgenössische Anstalt für das Forstliche Versuchswesen; in Zusammenarbeit mit dem Bundesamt für Forstwesen und Landschaftsschutz.

Mallord, J. W., Charman, E. C., Cristinacce, A. & Orsman, C. J., 2012. Habitat associations of Wood Warblers Phylloscopus sibilatrix breeding in Welsh oakwoods. *Bird Study,* 59, 403-415.

Marchant, J. H., 1990. *Population trends in British breeding birds: based on work undertaken under contract to the Nature Conservancy Council.* Hertfordshire: British Trust for Ornithology.

Marchant, J. H., Hudson, R., Carter, S. P. & Whittington, P., 1990. *Population trends in british breeding birds.* Hertfordshire: British Trust for Ornithology.

Marti, J., 2007. Zur Habitatwahl des Waldlaubsängers *Phylloscopus sibilatrix* im Kanton Glarus. *Der Ornithologische Beobachter,* 104, 45-52.

Mazerolle, M. J., 2012. Model selection and multimodel inference based on (Q) AIC (c). R package version 1.26.

Maziarz, M. & Wesolowski, T., 2010. Timing of breeding and nestling diet of Wood Warbler Phylloscopus sibilatrix in relation to chanching food supply. *Bird Study,* 57, 540-552.

Merrill, T., Mattson, D. J., Wright, R. G. & Quigley, H. B., 1999. Defining landscapes suitable for restoration of grizzly bears Ursus arctos in Idaho. *Biological Conservation,* 87, 231-248.

Meyer, P., Tabaku, V. & v. Lüpke, B., 2003. Die Struktur albanischer Rotbuchen-Urwälder Ableitungen für eine naturnahe Buchenwirtschaft. Structural Characteristics of Albanian Beech (Fagus sylvatica L.) VirginForests - Deductions for Semi-Natural Forestry. *Forstwissenschaftliches Centrablatt.,* 122, 47-58.

Miller, J. R. & Hobbs, N. T., 2000. Recreational trails, human activity, and nest predation in lowland riparian areas. *Landscape and Urban Planning,* 50, 227-236.

Miller, S. G., Knight, R. L. & Miller, C. K., 1998. Influence of recreational trails on breeding bird communities. *Ecological Applications,* 8(1), 162-169.

Mollet, P., Birrer, S., Naef-Daenzer, B., Naef-Daenzer, L., Spaar, R. & Zbinden, N., 2006. *Situation der Vogelwelt im Schweizer Wald,* Sempach: Schweizerische Vogelwarte.

Morrison, M. L., Marcot, B. G. & Mannan, R., 1992. *Wildlife Habitat Relationships. Concepts and Applications.* Madison, Wisconsin: The University of Wisconsin Press.

Morsdorf, F., Meier, E., Kötz, B., Itten, K., Dobbertin, M. & Allgöwer, B., 2004. LIDAR-based geometric reconstruction of boreal type forest stands at single tree level for forest and wildland fire management. *Remote Sensing of Environment,* 92, 353-362.

Müller, J., 2005. *Waldstrutkuren als Steuergrösse für Artengemeinschaften in kollinen bis submontanen Buchenwäldern,* Weihenstephan: Dissertation, University of Munich.

Müller, J., Moning, C., Bässler, C., Heurich, M. & Brandl, R., 2009. Using airborne laser scanning to model potential abundance and assemblages of forest passerines. *Basic and Applied Ecologiy,* Band 10, pp. 671-681.

Nelson, R., Keller, C. & Ratnaswamy, M., 2005. Locating and estimating the extent of Delmarva fox squirrel habitat using an airborne LiDAR profiler. *Remote Sensing of Environment,* 96, 292-301.

Noble, G., 1939. The Role of Dominance in the Social Life of Birds. *Auk,* 56, 263-273.

Paton, P. W., 1994. The Effect of Edge on Avian Success: How Strong Is the Evidence?. *Conservation Biology,* 8 (1), 17-26.

Pavlovic, A., 2009. Raumnutzung von Waldstrukturen durch *Phylloscopus*-Arten anhand von Scannerdaten*,* Freising: Diplomarbeit, Fachhochschule Weihenstephan.

Pfister, C. & Messerli, P., 1990. Switzerland. In: B. Turner, Ed. *The earth as transformed by human action. Global and regional changes in biosphere over the past 300 years.* Cambridge: Cambridge University Press, 641-652.

Piper, W. H., 2011. Making habitat selection more "familiar": a review. *Behavioral Ecology and Sociobiology,* 65, 1329-1351.

Pontailler, J.-Y., Faille, A. & Lemée, G., 1997. Storms drive successional dynamics in natural forests: a case study in Fontainebleau forest (France). *Forest Ecology and Managment,* 98, 1-15.

Popescu, S. C. & Zhao, K., 2008. A voxel-based lidar method for estimating crown base height for deciduous and pine trees. *Remote Sensing of Envrionment,* 112, 767-781.

Quelle, M. & Tiedemann, G., 1972. Strukturanalyse von Waldlaubsängerrevieren im Raum Bielefeld. *Abhandlungen aus dem Landesmuseum für Naturkunde zu Münster in Westfalen,* 34(4), 95-102.

R Development Core Team, 2011. *R: A language and environment for statistical computing,* Vienna, Austria: R Foundation for Statistical Computing.

Reinhardt, A., 2003. Habitatwahl und Brutbiologie beim Waldlaubsänger (*Phylloscopus sibilatrix*) im Bodenseegebiet im Hinblick auf den derzeitigen Bestandesrückgang, Konstanz: Diplomarbeit, University of Constance.

Reinhardt, A. & Bauer, H.-G., 2009. Analyse des starken Bestandesrückgangs beim Waldlaubsänger *Phylloscopus sibilatrix* im Bodenseegebiet. *Vogelwarte,* 47, 23-39.

Reunanen, P., Nikula, A., Mönkkönen, M., Hurme, E. & Nivala, V., 2002. Predicting Occupancy for the Siberian Flying Squirrel in old-growth Forest Patches. *Ecological Applications,* 12(4), 1188-1198.

Ricklefs, R. E., 1990. *Ecology.* Third edition. Ed. New York: Freeman.

Rozenbergar, D., Mikac, S., Anic, I. & Diaci, J., 2007. Gap regeneration patterns in relationship to light heterogeneity in two old-growth beech-fir forest reserves in South East Europe. *Forestry,* 80 (4), 431-443.

Salek, M. & Lövy, M., 2012. Spatial ecology and habitat selection of Little Owl *Athene noctua* during the breeding season in Central European farmland. *Birds Conservation International,* 22, 328-338.

Scherzinger, W., 1996. *Naturschutz im Wald - Qualitätsziele einer dynamischen Waldentwicklung.* Stuttgart: Ulmer.

Schifferli, A., Géroudet, P., Winkler, R. & Jacquat, B., 1980. *Verbreitungsatlas der Brutvögel der Schweiz: kartographische Darstellung des Brutvorkommens aller einheimischen vogelarten in den Jahren 1972 bis 1976.* Sempach: Schweizerische Vogelwarte.

Schmid, H., Luder, R., Naef-Daenzer, B., Graf, R. & Zbinden, N., 1998. *Schweizer Brutvogelatlas - Verbreitung der Brutvögel in der Schweiz und im Fürstentum Liechtenstein 1993-1996*. Sempach: Schweizerische Vogelwarte.

Schulze, E.-D., Beck, E. & Müller-Hohenstein, K., 2005. *Plant Ecology.* Berlin: Springer.

Sellars, J. D. & Jolls, C. L., 2007. Habitat Modeling for *Amaranthus pumilus*: An Application of Light Detection and Ranging (LIDAR) Data. *Journal of Coastal Research,* 23 (5), 1193-1202.

Shaw, D. C., Freeman, E. A. & Flick, C., 2002. The Vertical Occurence of Small Birds in an Old-growth Douglas-fir-Wetern Hemlock Forest Stand. *Northwest Science*, 78 (4), 322-334.

Sherry, T. W., 1979. Competitive Interactions and Adaptive Strategies of American Redstarts and Least Flycatchers in a Northern Hardwoods Forest. *The Auk,* 96 (2), 265-283.

Spaar, R., Ayé, R., Zbinden, N. & Rehsteiner, U., 2012. *Elemente für Artenförderungs-programme Vögel Schweiz - Update 2011.* Ed. Sempach and Zürich: Schweizerische Vogelwarte und Schweizer Vogelschutz SVS/BirdLife Schweiz.

Sperduto, M. B. & Congalton, R. G., 1996. Predicting Rare Orchid (Small Whorled Pogonia) Habitat Using GIS. *Photogrammetric Engineering & Remote Sensing,* 62, 1269-1279.

Spurr, S. H. & Barnes, B. V., 1980. *Forest Ecology.* 3rd edition, Ed. New York, Chichester, Brisbane, Toronto, Singapore: John Wiley & Sons.

Swiss Ornithological Institute, 2013. *Settlement behaviour, predation and population fluctuations in the wood warbler.* [Online] Available at: http://www.vogelwarte.ch/territory-selection,-breeding-success-and-nest-predation-in-wood-warblers.html [Visit 10 1 2013].

Swisstopo, 2003. *Die Geodaten der Schweiz des Bundesamtes für Landestopografie für den professionellen Einsatz - 21 DTM-AV, DOM-AV, die hochpräzisen Terrain- und Oberflächenmodelle der Amtlichen Vermessung,* Wabern: Swisstopo Bundesamt für Landestopografie.

Swisstopo, 2005. *Die Geodaten der Schweiz des Bundesamtes für Landestopografie für den professionellen Einsatz - 17 DOM, das hochpräzise Oberflächenmodell,* Wabern: Swisstopo Bundesamt für Landestopografie.

Swisstopo, 2009. *Verfügbarkeit, Flugjahr, Flugperiode,* Wabern: Swisstopo.

Swisstopo, 2012. *Objektkatalog swissTLM3D 1.1,* Neuchâtel: Budesamt für Landes-topographie Swisstopo.

Taylor, R. & Knight, R. L., 2003. Wildlife Responses to Recreation and Associated Visitor Perceptions. *Ecological Applications,* 13 (4), 951-963.

Tian, Y., Davies-Colley, R., Gong, P. & Thorrold, B., 2001. Estimating solar radiation on slopes of arbitrary aspect. *Agricultural and Forest Meteorology,* Band 109, pp. 67-74.

Vierling, K., Vierling, L., Gould, W., Martinuzzi, S. & Clawges, R., 2008. Lidar: shedding new light on habitat characterization and modeling. *Frontiers in Ecology and the Environment,* 6(2), 90-98.

Wagner, W., Ullrich, A. & Briese, C., 2003. Der Laserstrahl und seine Interatkion mit der Erdoberfläche. *VGI - Österreichische Zeitschrift für Vermessung & Geoinformation,* 4, 1-16.

Wales, B. A., 1972. Vegetation analysis of north and south edges in a mature oak-hickory forest. *Ecological Monographs*, 42 (4), 451-471.

Weber, T. P., Houson, A. I. & Ens, B. J., 1999. Consequences of habitat loss at migratory stopover sites: a theoretical investigaton. *Journal of Avian Biology,* 30, 416-426.

Wesolowski, T. & Maziarz, M., 2009. Changes in Breeding Phenology and Performance of Wood Warblers Phylloscopus sibilatrix in a Primeval Forest: A Thirty-Year Perspective. *Acta Ornithologica,* 44(1), 69-80.

Wesolowski, T., Rowinski, P. & Maziarz, M., 2009. Wood Warbler Phylloscopus sibilatrix: a nomadic insectivore in search of safe breeding grounds?. *Bird Study,* 56, 26-33.

Whittingham, M., Swetnam, R., Wilson, J., Chamberlain, Dan. & Freckleton, R., 2005. Habitat selection by yellowhammers Emberiza citrinella on lowland farmland at two spatial scales: implications for conservation managment. *Journal of Applied Ecology,* 42, 270-280.

Wiens, J. A., Addicott, J. F., Case, T. J. & Diamond, J., 1986. Overview: The Importance of Spatial and Temporal Scale in Ecological Investigations. In: J. Diamond & T. J. Case, Ed. *Community Ecology.* Cambrige: Harper & Row, 145-153.

Willmanns, O., 1989. *Oekologische Pflanzensoziologie.* 4. Edition, Ed. Heidelberg: Quelle & Meyer.

Winter, S., Flade, M., Schumacher, H., Kerstan, E. & Möller, G., 2005. The importance of near-natural stand structures for the biocoenosis of lowland beech forests. *Forest Snow and Landscape Research,* Band 79, 1/2, pp. 127-144.

Zimmermann, N. & Kienast, F., 1999. Predictive mapping of alpine grasslands in Switzerland: Spies versus community approach. *Journal of Vegetation Science,* 10, 469-482.

Zweig, M. H. & Campell, G., 1993. Receiver-Operating Characteristic (ROC) Plots: A Fundamental Evaluation Tool in Clinical Medicine. *Cinical Chemistry,* 39 (4), 561-577.

Appendix

A1 Soil variables

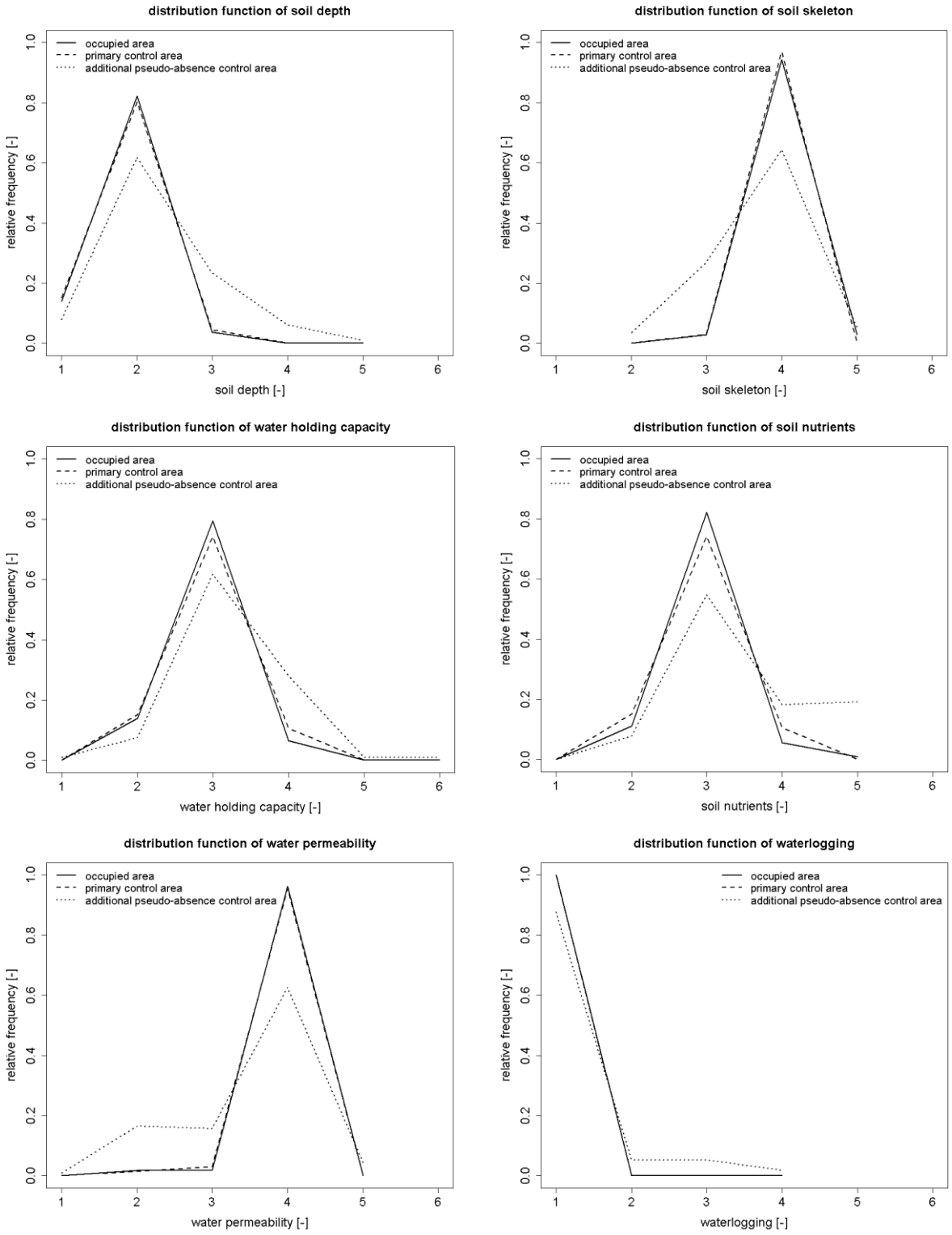

Fig. 16: Soil characteristics of the sample areas. 1 denotes extremely low, while 6 denotes extremely high characteristics. N=156.

A2 Processing of lidar metrics and non-lidar RS variables in ArcGIS

sample areas (.shp)

create shape file for every sample area

processing of lidar data (.las)

lasmerge: .las (several sample areas together)

las2shp: converts .las to points (not Multipoint!)

spatial join (join one to many): joins the ID of the sample area (shape file) to the points

add field (z, Double)

calculate geometry: writes the height of every point in the z field

calculation of nDSM

extract values to points: every point of the DSM receives the according value of the swissALTI3D

add field (h)

field calculator: h = z - value swissALTI3D → nDSM

export as .txt

meanCH

point to raster: maximum nDSM value per 2x2 cell

(cell size & snap raster: swissALTI3D)

raster to point: ID of sample area

spatial join(one to many, closest)

export as .txt

slope

buffer: 10 m around sample area

extract by mask: with swissALIT3D

slope

extract by mask: B46 (reduce buffered area to area of the according spatial scale)

zonal statistics: mean/sample area

int: outputs integer values

extract values to points (RASTERVALUE)

add field: slope

raster calculator: slope = RASTERVALUE

r_march

extract by mask: extract values of r_march for the sample areas

zonal statistics: mean/sample area

int: outputs integer values

extract values to points (RASTERVALUE)

add field: r_march

raster calculator: r_march=RASTERVALUE

export as .txt (slope and r_march together)

A3 Processing of lidar metrics and non-lidar RS variables in R

```
##############################################################################
                                Import the data into R
##############################################################################
## import the data (illustrated here using data from 2012, first part)
    B46_12_1_all <- read.table("B46_12_1_h.txt",sep=";",header=TRUE);
    summary(B46_12_1_all);
    df10_all <- data.frame(B46_12_1_all[,c("Territory","Type","h")]);
    B46_all_1 <- rbind(df10_all, …);                    # …: combination with other data
## number of signals per sample area
    count_B46_1 <- data.frame(table(B46_all_1["Territory"]));
    colnames(count_B46) <- c("Territory","#sig");
    summary(count_B46)
## number of signals < 1m per sample area
    B46_h1_all_1 <- B46_all_1[B46_all_1["h"]<1, ];
    count_B46_1m_1 <- data.frame(table(B46_h1_all_1["Territory"]));
    count_B46_1m <- rbind(count_B46_1m_1, …)            # …: combination with other data
    colnames(count_B46_1m) <- c("Territory","#sig_1m");
    summary(count_B46_1m)
## proportion of lidar signals < 1m
    r_1m <- matrix(count_B46_1m["#sig_1m"]/count_B46["#sig"]);
    colnames(r_1m) <- c("r_1m");
    summary(r_1m)
## negative values
    B46_neg_1 <- B46_all_1["h"]<0
    B46_n_1 <- B46_all_1[B46_neg_1,]
    B46_n <- rbind(B46_n_1[,c("Territory","h")], …)     # …: combination with other data
    plot(B46_n["Territory"],B46_n["h"])
    summary(B46_n)
    hist(B46_n["h"], nclass=100, main="negative values at territory scale", xlab="h < 0 [m]",
    ylab="count")
    nlevels(B46_n["Territory"])
## removal of negative values smaller than 3x sd
    sd(B46_n["h"])
    sdok_B46_12_1 <- B46_12_1_all["h"]>(sd(B46_n["h"])*-3)
    B46_12_1 <- B46_12_1_all[sdok_B46_12_1,]
    summary(B46_12_1)
    plot(B46_12_1["Territory"],B46_12_1["h"],main="B46_12_1", ylab="h [m]")
## combination of the data
    df10 <- data.frame(B46_12_1[,c("Territory","Type","h")]);
    B46 <- rbind(…,df10,…);                             # …: combination with other data

##############################################################################
                                calculation of the lidar metrics
##############################################################################
## meanVH, maxVH, VH95, sdVH
    aggB46_meanVH <- aggregate(B46$h, list(B46$Territory), mean);
    colnames(aggB46_meanVH) <- c("Territory","meanVH");
    aggB46_maxVH <- aggregate(B46$h, list(B46$Territory), max);
    colnames(aggB46_maxVH) <- c("Territory","maxVH");
    aggB46_VH95 <- aggregate(B46$h, list(B46$Territory), function(x) {quantile (x, probs = 0.95)});
    colnames(aggB46_VH95) <- c("Territory","VH95");
    aggB46_sdVH <- aggregate(B46$h, list(B46$Territory), sd);
    colnames(aggB46_sdVH) <- c("Territory","sdVH");
## pen50_2, pen10_2 and pen5_1
    B46_h2 <- B46[B46["h"]<2, ];
    B46_h50 <- B46[B46["h"]<50, ];
    B46_h10 <- B46[B46["h"]<10, ];
    B46_h1 <- B46[B46["h"]<1, ];
    B46_h5 <- B46[B46["h"]<5, ];
```

```
    pen50_2 <- matrix(table(B46_h2[,"Territory"])/table(B46_h50[,"Territory"]));
    colnames(pen50_2) <- c("pen50_2");
    pen10_2 <- matrix(table(B46_h2[,"Territory"])/table(B46_h10[,"Territory"]));
    colnames(pen10_2) <- c("pen10_2");
    pen5_1 <- matrix(table(B46_h1[,"Territory"])/table(B46_h5[,"Territory"]));
    colnames(pen5_1) <- c("pen5_1");
## meanVH<3m
    B46_h3_d <- B46[B46[,"h"]<3, ];
    aggB46_meanVH_3md <- aggregate(B46_h3_d$h, list(B46_h3_d$Territory), mean);
    colnames(aggB46_meanVH_3md) <- c("Territory","meanVH_3md");
## meanVH> 3m
    B46_h3 <- B46[B46[,"h"]>3, ];
    aggB46_meanVH_3m <- aggregate(B46_h3$h, list(B46_h3$Territory), mean);
    colnames(aggB46_meanVH_3m) <- c("Territory","meanVH_3m");
## meanCH
    setwd(" …")
    B46_12_1_CH <- read.table("B46_12_1_h_max.txt",sep=";",header=TRUE);
    df8_CH <- data.frame(B46_12_1_CH[,c("Territory","Type","GRID_CODE")]);
    B46_CH <- rbind(…, df8_CH, …);
    colnames(B46_CH) <- c("Territory","Type","CH");
    plot(B46_CH[,"Territory"],B46_CH[,"CH"],main="B46_CH",ylab="h [m]")
    aggB46_meanCH <- aggregate(B46_CH$CH, list(B46_CH$Territory), mean);
    colnames(aggB46_meanCH) <- c("Territory","meanCH");
## meanCH>3m
    B46_CH_3m <- B46_CH[B46_CH[,"CH"]>3, ];          # selection of values > 3m
    aggB46_meanCH_3m <- aggregate(B46_CH_3m$CH, list(B46_CH_3m$Territory), mean);
    colnames(aggB46_meanCH_3m) <- c("Territory","meanCH_3m");
## sdCH
    aggB46_sdCH <- aggregate(B46_CH$CH, list(B46_CH$Territory), sd);
    colnames(aggB46_sdCH) <- c("Territory","sdCH");
## sdCH>3m
    aggB46_sdCH_3m <- aggregate(B46_CH_3m$CH, list(B46_CH_3m$Territory), sd);
    colnames(aggB46_sdCH_3m) <- c("Territory","sdCH_3m");
## meanCC
    B46_meanCC <- matrix(table(B46_CH_3m[,"Territory"])/table(B46_CH[,"Territory"]));
    colnames(B46_meanCC) <- c("meanCC");
## meanCC_10m
    B46_CH_10m <- B46_CH[B46_CH[,"CH"]>10, ];
    B46_meanCC_10 <- matrix(table(B46_CH_10m[,"Territory"]) / table(B46_CH[,"Territory"]));
    colnames(B46_meanCC_10) <- c("meanCC_10");
## meanCC_15m
    B46_CH_15m <- B46_CH[B46_CH[,"CH"]>15, ];
    B46_meanCC_15 <- matrix(table(B46_CH_15m[,"Territory"]) / table(B46_CH[,"Territory"]));
    colnames(B46_meanCC_15) <- c("meanCC_15");
## meanCC_20m
    B46_CH_20m <- B46_CH[B46_CH[,"CH"]>20, ];
    B46_meanCC_20 <- matrix(table(B46_CH_20m[,"Territory"]) / table(B46_CH[,"Territory"]));
    colnames(B46_meanCC_20) <- c("meanCC_20");
## combine the metrics
    B46_results <- cbind(…);                    # …: list with all metrics
    colnames(B46_results) <- c(…);              # …: list with the names of the metrics

#############################################################################
                                    correlations
#############################################################################
cor(B46_results_all[,3:36],method="spearman",use="pairwise.complete.obs")
pairs(B46_results[,3:36],main="B46_results_all {cor spearman}")

#############################################################################
                                    GLMs (GLMMs)
#############################################################################
```

```
#open packages
    library(lme4)
    library(AICcmodavg)
    library(arm)
#dataset
    setwd("…")
    all <-read.table("WW10_12.txt",header=TRUE)
#standardize all values with a mean of 0 and a SD of 1
    all$x.meanVH <-as.numeric(scale(all$meanVH))
    all$x.meanVHlin <-as.numeric(scale(all$meanVH))    # linear term for quadratic model
    all$x.meanCH <-as.numeric(scale(all$meanCH))
    all$x.meanCHlin <-as.numeric(scale(all$meanCH))    # linear term for quadratic model
    all$x.meanVH_3md <-as.numeric(scale(all$meanVH_3md))
    all$x.meanVH_3m <-as.numeric(scale(all$meanVH_3m))
    all$x.meanVH_3mlin <-as.numeric(scale(all$meanVH_3m)) # for quadratic model
    all$x.meanCH_3m <-as.numeric(scale(all$meanCH_3m))
    all$x.meanCH_3mlin <-as.numeric(scale(all$meanCH_3m)) # for quadratic model
    all$x.maxVH <-as.numeric(scale(all$maxVH))
    all$x.maxVHlin <-as.numeric(scale(all$maxVH))       # linear term for quadratic model
    all$x.VH95 <-as.numeric(scale(all$VH95))
    all$x.VH95lin <-as.numeric(scale(all$VH95))         # linear term for quadratic model
    all$x.sdVH <-as.numeric(scale(all$sdVH))
    all$x.sdCH <-as.numeric(scale(all$sdVH))
    all$x.sdCH_3m <-as.numeric(scale(all$sdCH_3m))
    all$x.pen50_2 <-as.numeric(scale(all$pen50_2))
    all$x.pen50_2lin <-as.numeric(scale(all$pen50_2))   # linear term for quadratic model
    all$x.pen10_2 <-as.numeric(scale(all$pen10_2))
    all$x.pen5_1 <-as.numeric(scale(all$pen5_1))
    all$x.meanCC <-as.numeric(scale(all$meanCC))
    all$x.meanCClin <-as.numeric(scale(all$meanCC))   # linear term for quadratic model
    all$x.meanCC_10m <-as.numeric(scale(all$meanCC_10m))
    all$x.meanCC_10mlin <-as.numeric(scale(all$meanCC_10m)) # for quadratic model
    all$x.meanCC_15m <-as.numeric(scale(all$meanCC_15m))
    all$x.meanCC_15mlin <-as.numeric(scale(all$meanCC_15m)) # for quadratic model
    all$x.meanCC_20m <-as.numeric(scale(all$meanCC_20m))
    all$x.meanCC_20mlin <-as.numeric(scale(all$meanCC_20m)) # for quadratic model
    all$x.slope <-as.numeric(scale(all$slope))
    all$x.rmarch <-as.numeric(scale(all$rmarch))
    all$x.forest_type <-as.numeric(scale(all$WMG))
    all$x.dist_f <-as.numeric(scale(all$near_dist_f))
    #all$pooled<-as.character(all$area)            # ADAPTION FOR GLMMs
    #all$pooled<-factor(all$pooled)                # ADAPTION FOR GLMMs
    #all$nr.pair <- factor(all$nr.pair)            # ADAPTION FOR GLMMs
##############################################################################
## 1st step – within-group analysis
## height group
    Cand.models<-list()
    Cand.models[[1]] <- glm(PA ~ x.meanVH + x.meanVH_3md, family = binomial, data = all)
    #Cand.models[[1]] <- glmer(PA ~ x.meanVH + x.meanVH_3md + (1|pooled) + (1|nr.pair), #family =
    binomial, data = all)  # ADAPTION FOR GLMMs
    Cand.models[[2]] <- glm(PA ~ x.meanVH + x.meanVH_3md + x.maxVH, family = binomial, data =
    all)
    Cand.models[[3]] <- glm(PA ~ x.meanVH + x.maxVH, family = binomial, data = all)
    Cand.models[[4]] <- glm(PA ~ x.meanVH, family = binomial, data = all)
    Cand.models[[5]] <- glm(PA ~ x.meanCH + x.meanVH_3md, family = binomial, data = all)
    Cand.models[[6]] <- glm(PA ~ x.meanCH + x.meanVH_3md + x.maxVH, family = binomial, data =
    all)
    Cand.models[[7]] <- glm(PA ~ x.meanCH + x.maxVH, family = binomial, data = all)
    Cand.models[[8]] <- glm(PA ~ x.meanCH, family = binomial, data = all)
    Cand.models[[41]] <- glm(PA ~ x.meanVH_3md + x.meanVH_3m, family = binomial, data = all)
    Cand.models[[9]] <- glm(PA ~ x.meanVH_3md + x.meanCH_3m, family = binomial, data = all)
```

```
Cand.models[[10]] <- glm(PA ~ x.meanVH_3md + x.maxVH, family = binomial, data = all)
Cand.models[[11]] <- glm(PA ~ x.meanVH_3md + x.VH95, family = binomial, data = all)
Cand.models[[12]] <- glm(PA ~ x.meanVH_3md, family = binomial, data = all)
Cand.models[[13]] <- glm(PA ~ x.meanVH_3m, family = binomial, data = all)
Cand.models[[14]] <- glm(PA ~ x.meanCH_3m, family = binomial, data = all)
Cand.models[[15]] <- glm(PA ~ x.maxVH, family = binomial, data = all)
Cand.models[[16]] <- glm(PA ~ x.VH95, family = binomial, data = all)
Cand.models[[17]] <- glm(PA ~ x.meanVHlin + I(all$x.meanVHlin^2) + x.meanVH_3md, family =
binomial, data = all)
Cand.models[[18]] <- glm(PA ~ x.meanVHlin + I(all$x.meanVHlin^2) + x.meanVH_3md + x.maxVH,
family = binomial, data = all)
Cand.models[[19]] <- glm(PA ~ x.meanVHlin + I(all$x.meanVHlin^2) + x.meanVH_3md +
x.maxVHlin + I(all$x.maxVHlin^2), family = binomial, data = all)
Cand.models[[20]] <- glm(PA ~ x.meanVHlin + I(all$x.meanVHlin^2) + x.maxVH, family = binomial,
data = all)
Cand.models[[21]] <- glm(PA ~ x.meanVHlin + I(all$x.meanVHlin^2) + x.maxVHlin +
I(all$x.maxVHlin^2), family = binomial, data = all)
Cand.models[[22]] <- glm(PA ~ x.meanVHlin + I(all$x.meanVHlin^2), family = binomial, data = all)
Cand.models[[23]] <- glm(PA ~ x.meanCHlin + I(all$x.meanCHlin^2) + x.meanVH_3md, family =
binomial, data = all)
Cand.models[[24]] <- glm(PA ~ x.meanCHlin + I(all$x.meanCHlin^2) + x.meanVH_3md + x.maxVH,
family = binomial, data = all)
Cand.models[[25]] <- glm(PA ~ x.meanCHlin + I(all$x.meanCHlin^2) + x.meanVH_3md +
x.maxVHlin + I(all$x.maxVHlin^2), family = binomial, data = all)
Cand.models[[26]] <- glm(PA ~ x.meanCHlin + I(all$x.meanCHlin^2) + x.maxVH, family = binomial,
data = all)
Cand.models[[27]] <- glm(PA ~ x.meanCHlin + I(all$x.meanCHlin^2) + x.maxVHlin +
I(all$x.maxVHlin^2), family = binomial, data = all)
Cand.models[[28]] <- glm(PA ~ x.meanCHlin + I(all$x.meanCHlin^2), family = binomial, data = all)
Cand.models[[29]] <- glm(PA ~ x.meanVH_3md + x.meanVH_3mlin + I(all$x.meanVH_3mlin^2),
family = binomial, data = all)
Cand.models[[30]] <- glm(PA ~ x.meanVH_3md + x.maxVHlin + I(all$x.maxVHlin^2), family =
binomial, data = all)
Cand.models[[31]] <- glm(PA ~ x.meanVH_3md + x.maxVHlin + I(all$x.maxVHlin^2) + x.meanVH,
family = binomial, data = all)
Cand.models[[32]] <- glm(PA ~ x.maxVHlin + I(all$x.maxVHlin^2) + x.meanVH, family = binomial,
data = all)
Cand.models[[33]] <- glm(PA ~ x.meanVH_3md + x.meanCH_3mlin + I(all$x.meanCH_3mlin^2),
family = binomial, data = all)
Cand.models[[34]] <- glm(PA ~ x.meanVH_3md + x.maxVHlin + I(all$x.maxVHlin^2) + x.meanCH,
family = binomial, data = all)
Cand.models[[35]] <- glm(PA ~ x.maxVHlin + I(all$x.maxVHlin^2) + x.meanCH, family = binomial,
data = all)
Cand.models[[36]] <- glm(PA ~ x.meanVH_3md + x.VH95lin + I(all$x.VH95lin^2), family = binomial,
data = all)
Cand.models[[37]] <- glm(PA ~ x.meanVH_3mlin + I(all$x.meanVH_3mlin^2), family = binomial,
data = all)
Cand.models[[38]] <- glm(PA ~ x.meanCH_3mlin + I(all$x.meanCH_3mlin^2), family = binomial,
data = all)
Cand.models[[39]] <- glm(PA ~ x.maxVHlin + I(all$x.maxVHlin^2), family = binomial, data = all)
Cand.models[[40]] <- glm(PA ~ x.VH95lin + I(all$x.VH95lin^2), family = binomial, data = all)
Cand.models[[42]] <- glm(PA ~ 1, family = binomial, data = all)

# print AICc table
modnames.geo<-paste("mod", 1:length(Cand.models), sep=" ")
print(aictab(cand.set = Cand.models, modnames = modnames.geo, sort = TRUE), digits = 4, LL =
TRUE)

# print model-averaged estimates, standard errors and 95% CIs across all models per group
modavg(cand.set = Cand.models, parm = "x.meanVH", conf.level = 0.95, modnames =
modnames.geo, exclude=list("x.meanVHlin"))
```

```
    modavg(cand.set = Cand.models, parm = "x.meanCH", modnames = modnames.geo,
    exclude=list("x.meanCHlin"))
    modavg(cand.set = Cand.models, parm = "x.meanVH_3md", conf.level = 0.95, modnames =
    modnames.geo)
    modavg(cand.set = Cand.models, parm = "x.meanVH_3m", conf.level = 0.95, modnames =
    modnames.geo, exclude=list("x.meanVH_3mlin"))
    modavg(cand.set = Cand.models, parm = "x.meanCH_3m", conf.level = 0.95, modnames =
    modnames.geo, exclude=list("x.meanCH_3mlin"))
    modavg(cand.set = Cand.models, parm = "x.maxVH", conf.level = 0.95, modnames =
    modnames.geo, exclude=list("x.maxVHlin"))
    modavg(cand.set = Cand.models, parm = "x.VH95", conf.level = 0.95, modnames =
    modnames.geo, exclude=list("x.VH95lin"))
    modavg(cand.set = Cand.models, parm = "x.meanVHlin", conf.level = 0.95, modnames =
    modnames.geo, exclude=list("x.meanVHlin^2"))
    modavg(cand.set = Cand.models, parm = "I(all$x.meanVHlin^2)", conf.level = 0.95, modnames =
    modnames.geo)
    modavg(cand.set = Cand.models, parm = "x.meanCHlin", conf.level = 0.95, modnames =
    modnames.geo,exclude=list("x.meanCHlin^2"))
    modavg(cand.set = Cand.models, parm = "I(all$x.meanCHlin^2)", conf.level = 0.95, modnames =
    modnames.geo)
    modavg(cand.set = Cand.models, parm = "x.meanVH_3mlin", conf.level = 0.95, modnames =
    modnames.geo,exclude=list("x.meanVH_3mlin^2"))
    modavg(cand.set = Cand.models, parm = "I(all$x.meanVH_3mlin^2)", conf.level = 0.95, modnames
    = modnames.geo)
    modavg(cand.set = Cand.models, parm = "x.meanCH_3mlin", conf.level = 0.95, modnames =
    modnames.geo,exclude=list("x.meanCH_3mlin^2"))
    modavg(cand.set = Cand.models, parm = "I(all$x.meanCH_3mlin^2)", conf.level = 0.95,
    modnames = modnames.geo)
    modavg(cand.set = Cand.models, parm = "x.maxVHlin", conf.level = 0.95, modnames =
    modnames.geo,exclude=list("x.maxVHlin^2"))
    modavg(cand.set = Cand.models, parm = "I(all$x.maxVHlin^2)", conf.level = 0.95, modnames =
    modnames.geo)
    modavg(cand.set = Cand.models, parm = "x.VH95lin", conf.level = 0.95, modnames =
    modnames.geo,exclude=list("x.maxVHlin^2"))
    modavg(cand.set = Cand.models, parm = "I(all$x.VH95lin^2)", conf.level = 0.95, modnames =
    modnames.geo)
## vertical diversity group (same code as before)
    …
## penetration rate group
    …
## canopy cover group
    …
## geography group
    …
# 2nd step – across-group analysis
    (same code as before)

#############################################################################
                        Verification, Validation and 10-fold cross validation
#############################################################################
#open packages
    library(lme4)
    library(AICcmodavg)
    library(arm)
## dataset 1 (used for model building)
    setwd("…")
    all<-read.table("WW10_12.txt",header=TRUE)
#standardize all values with a mean of 0 and a SD of
    all$x.meanVH <-as.numeric(scale(all$meanVH))
    all$x.meanVHlin <-as.numeric(scale(all$meanVH))    # linear term for quadratic model
    …
```

```
## dataset 2 (for validation)
    all_2<-read.table("WW10_12_2.txt",header=TRUE)
#standardize all values with a mean of 0 and a SD of 1
    all_2$x.meanVH <-as.numeric(scale(all_2$meanVH))
    all_2$x.meanVHlin <-as.numeric(scale(all_2$meanVH))        # linear term for quadratic model
    …
# B_B46 (territory scale)
# predictive model 1: meanVHlin + meanVHlin^2, sdCH_3m, slope, r_march
    B46.binomial_1 <- glm(PA ~ x.meanVHlin + I(x.meanVHlin^2) + x.sdCH_3m + x.slope + x.rmarch,
    family = binomial, data = all)
    B46.binomial_1$coefficients <- c(-0.56,-0.39,-0.83,-1.17,0.81,0.48) # coefficients according to
    model-averaging
    B46.binomial_1$coefficients
    summary(B46.binomial_1)
# predictive model 2: maxVH, meanCC_10m^2, slope
    B46.binomial_2 <- glm(PA ~ x.maxVH + x.meanCC_10mlin + I(x.meanCC_10mlin^2) + x.slope,
    family = binomial, data = all)
    B46.binomial_2$coefficients <- c(-0.56,-1,0.95,-0.85,0.81) # coefficients according to model-
    averaging
    B46.binomial_2$coefficients
# predictive model 3: maxVH, meanCC_10m^2, slope, r_march
    B46.binomial_3 <- glm(PA ~ x.maxVH + x.meanCC_10mlin + I(x.meanCC_10mlin^2) + x.slope +
    x.rmarch, family = binomial, data = all)
    B46.binomial_3$coefficients <- c(-0.56,-1,0.95,-0.85,0.81,0.48) # coefficients according to model-
    averaging
    B46.binomial_3$coefficients
# predictive model 4: meanVHlin + meanVHlin^2, sdCH_3m, slope, r_march
    B46.binomial_4 <- glm(PA ~ x.meanVHlin + I(x.meanVHlin^2) + x.sdCH_3m + x.slope, family =
    binomial, data = all)
    B46.binomial_4$coefficients  <- c(-0.56,-0.39,-0.83,-1.17,0.81) # coefficients according to model-
    averaging
    B46.binomial_4$coefficients
# validation and verification for selected model
    B46.binomial <- B46.binomial_1
################################################################################
## verification for dataset 1
    pred <- data.frame(all$PA,predict.glm(B46.binomial,
    type="response",newdata=all),residuals(B46.binomial, type="response",newdata=all))
    pred_model_B46_1 <- cbind(all$terr.id, pred)
    colnames(pred_model_B46_1) <- c("Territory", "observed","predicted","residuals")
# TSS (This function calculates the threshold that maximizes the True Skill Statistic (TSS).)
    tss <- function(observed,prediction){
      levs <- seq(from=0.001,to=0.999,by=0.001)
      obsnum <- paste("obs_",1:length(observed),sep="")
      data1 <- data.frame(obsnum,observed,prediction)
      val <- numeric()
      sens <- numeric()
      spec <- numeric()
      thresh <- NA
      for (i in 1:length(levs)) {
        confmat <- cmx(data1,threshold=levs[i])
        sens <- c(sens,as.numeric(sensitivity(confmat)[[1]]))
        spec <- c(spec,as.numeric(specificity(confmat)[[1]]))
      }
      val <- sens + spec -rep(1,length(levs))
      to.average <- which(val==max(val))
      thresh <- mean(levs[to.average])
      return(thresh)
    }
    t_TSS_1 <- tss(pred_model_B46_1[,"observed"],pred_model_B46_1[,"predicted"])
    t_TSS_1
```

```
    cmx_pred_model_B46_1 <- data.frame(ID=1:length(pred_model_B46_1[ ,"observed"]),
    pred_model_B46_1[ ,"observed"], pred_model_B46_1[, "predicted"])
    Sen_B46_1 <- sensitivity(cmx(cmx_pred_model_B46_1,0.398),st.dev=TRUE)
    Spec_B46_1 <- specificity(cmx(cmx_pred_model_B46_1,0.398),st.dev=TRUE)
# fpos, fneg (with threshold from TSS: t_TSS_1)
    cmx_1 <- cmx(pred_model_B46_1[,c(1:3)],t_TSS_1)
    fpos_1 <- cmx_1[1,2]/(cmx_1[1,2]+cmx_1[2,2])
    fneg_1 <- cmx_1[2,1]/(cmx_1[1,1]+cmx_1[2,1])
    acc_1 <- cbind(fpos_1, fneg_1)
    acc_1
# AUC
    library(PresenceAbsence)
    auc(pred_model_B46_1, st.dev=TRUE, which.model = 1)
##############################################################################
## Validation for dataset 2
    pred <- data.frame(all_2$PA,predict.glm(B46.binomial, newdata=all_2, type="response"),
    residuals(B46.binomial, newdata=all_2, type="response"))
    pred_model_B46_2 <- cbind(all_2$terr.id, pred)
    colnames(pred_model_B46_2) <- c("Territory", "observed","predicted","residuals")
# TSS (with threshold from verification: t_TSS_1)
    cmx_pred_model_B46_2 <- data.frame(ID=1:length(pred_model_B46_2[,"observed"]),
    pred_model_B46_2[,"observed"], pred_model_B46_2[,"predicted"])
    Sen_B46_2 <- sensitivity(cmx(cmx_pred_model_B46_2,t_TSS_1),st.dev=TRUE)
    Spec_B46_2 <- specificity(cmx(cmx_pred_model_B46_2,t_TSS_1),st.dev=TRUE)
# fpos, fneg (with threshold from verification)
    cmx_2 <- cmx(pred_model_B46_2[,c(1:3)],t_TSS_1)
    fpos_2 <- cmx_2[1,2]/(cmx_2[1,2]+cmx_2[2,2])
    fneg_2 <- cmx_2[2,1]/(cmx_2[1,1]+cmx_2[2,1])
    acc_2 <- cbind(fpos_2,fneg_2)
    acc_2
# AUC
    auc(pred_model_B46_2, st.dev=TRUE, which.model = 1)
##############################################################################
# 10-fold cross validation
evalacc_10_binom<- function(glm.obj, filesppclim, dvar)
{
 xvs10=sample (rep(c(1:10), length=nrow(filesppclim))) #takes a sample from vector 1:10 for the
number of plots
 pred.xval10=rep (0, length=nrow(filesppclim)) #replicates the values vector (0) with the length of the
data frame
 fpos=rep(0, length=10)
 fneg=rep(0, length=10)
 auc=rep(0, length=10)
 sen=rep(0, length=10)
 spec=rep(0, length=10)

 for (i in 1:10)
 {
   tr10=filesppclim[xvs10!=i,]                          #takes the values with index 1-9
   te10=filesppclim[xvs10==i,]                          #takes the values wiht index 10
   fit = glm(glm.obj$formula, family=binomial, data=tr10)      #fits a model on values with index 1-9
   pred.xval10 [xvs10==i] = predict (fit, newdata=te10, type="response")
   #predicts model on values with index i

   pred10 = pred.xval10[xvs10==i]
   file10 = data.frame(ID=1:length(pred10),te10[,dvar],pred10)
   cmx_10 <- cmx(file10,0.327)
   fpos[i] <- cmx_10[1,2]/(cmx_10[1,2]+cmx_10[2,2])
   fneg[i] <- cmx_10[2,1]/(cmx_10[1,1]+cmx_10[2,1])
   auc[i] <- auc(file10, st.dev=FALSE, which.model = 1)
   sen[i] <- sensitivity(cmx(file10,0.327),st.dev=FALSE)
```

```
    spec[i] <- specificity(cmx(file10,0.327),st.dev=FALSE)
  }
  all.acc=cbind(fpos,fneg,auc,sen,spec)
  colnames(all.acc)=c("fpos","fneg","AUC","sensitivity","specificity")
  all.acc
}
evalacc_10_binom(B46.binomial,all, 'PA')

# calculation of 5% and 95% quantiles
    setwd("…")
    crossval<-read.table("cross_validation.txt",header=TRUE)
    rbind(quantile(crossval[,1],probs=c(0.05,0.95)),quantile(crossval[,2],probs=c(0.05,0.95)),quantile(cr
    ossval[,3],probs=c(0.05,0.95)),quantile(crossval[,4],probs=c(0.05,0.95)),quantile(crossval[,5],probs
    =c(0.05,0.95)),quantile(crossval[,6],probs=c(0.05,0.95)))

##############################################################################################
PREDICTION FOR CURRENT POTENTIAL RANGE
##############################################################################################
# data used for modelbuilding
    setwd("…")
    all<-read.table("WW10_12.txt",header=TRUE)
#standardize all values with a mean of 0 and a SD of 1
    all$x.meanVH <-as.numeric(scale(all$meanVH))
    all$x.sdCH_3m <-as.numeric(scale(all$sdCH_3m))
    all$x.slope <-as.numeric(scale(all$slope))
    all$x.rmarch <-as.numeric(scale(all$rmarch))
# new data (e.g. data from Jura)
    setwd("…")
    lidar_j <- read.table("Result_Jura.txt",sep=",");
    slope_j <- read.table("J_slope_rmarch.txt",sep=";",header=TRUE);
    var_j1 <- data.frame(lidar_j[,1],slope_j[,2:4],lidar_j[,3:4])
    colnames(var_j1) <- c("Region","POINTID","r_march","slope","meanVH","sdCH_3m");
    summary(var_j1)
    ok <- var_j1[,"slope"]>-9998
    var_j <- var_j1[ok,]
    summary(var_j)
    hist(var_j[,"r_march"],nclass=20)
    hist(var_j[,"slope"], nclass=20)
    hist(var_j[,"meanVH"], nclass=20)
    hist(var_j[,"sdCH_3m"],nclass=20)
# transformation according to data transformation for modelbuilding
    var_j$x.r_march <-scale(var_j$r_march,center=mean(all$rmarch),scale=sd(all$rmarch))
    var_j$x.slope <-scale(var_j$slope,center=mean(all$slope),scale=sd(all$slope))
    var_j$x.meanVH <-scale(var_j$meanVH,center=mean(all$meanVH),scale=sd(all$meanVH))
    var_j$x.sdCH_3m <-scale(var_j$sdCH_3m, center=mean(all$sdCH_3m), scale= sd(all$sdCH_3m))
    hist(var_j[,"x.r_march"],nclass=20)
    hist(var_j[,"x.slope"], nclass=20)
    hist(var_j[,"x.meanVH"], nclass=20)
    hist(var_j[,"x.sdCH_3m"],nclass=20)
# prediction
    pred <- -0.56 -0.39*var_j[,"x.meanVH"] -0.83*(var_j[,"x.meanVH"]^2) -1.17*var_j[,"x.sdCH_3m"] +
    0.81*var_j[,"x.slope"] + 0.48*var_j[,"x.r_march"]
    trans_pred  <- (2.71828182845904^pred)/(1+2.71828182845904^pred)
    pred_J <- cbind(var_j[,1:2],trans_pred)
    colnames(pred_J)=c("Region","POINTID","pred")
    write.table(pred_J, "…\pred_J.txt", sep=",", row.names=F)
```

A4 Python Code for processing of the lidar data for the prediction of the current potential range

```
import arcpy, string, time, subprocess, fileinput, os, time

# ---------------------------------------------
# Environment
arcpy.env.overwriteOutput = True
arcpy.env.extent = "MAXOF"
arcpy.CheckOutExtension('3D')

# ---------------------------------------------
# Input FeatureClass
pPath = r"Y:\Scratch"                          # output directory
inFC = r"…"+ "\\" + "j1_pol"                   # …: input directory; change name of area “xx_pol”
outFC = pPath + "\\" + "Temp.shp"
pDTM_AV          = r"\\speedy1\Data_1\_RASTER\swissalti3d"

OutputFile = r"Y:\Result.txt"
OutputFile_Result = open(OutputFile, 'w')

#---------------------------------------------
# Identify the geomety field

shapeName = arcpy.Describe(inFC).shapeFieldName

#---------------------------------------------
# Create search cursor
#
rows = arcpy.SearchCursor(inFC)

#---------------------------------------------
# Calculate the extent of all Polygons
#
Count = 0
for row in rows:
   Count += 1
   if Count < 1000000:                         # 'Count' is just for testing ...

      #---------------------------------------------
      # Create the geometry object
      #
      feat    = row.getValue(shapeName)
      extent  = str(feat.extent)
      a       = string.split(extent, " ")
      xmin    = round (float(a[0]),2)
      ymin    = round (float(a[1]),2)
      xmax    = round (float(a[2]),2)
      ymax    = round (float(a[3]),2)
      #---------------------------------------------
      # Name of the Field with unique Key
      #
      pName = str(int(row.GRIDCODE))
```

```
Zeit                = time.asctime()
print str(Zeit) + " ... Berechne " + str(pName)

pWhereClause = ' "GRIDCODE" = ' + pName
arcpy.Select_analysis(inFC,outFC,pWhereClause)

ToDo = r"H:\lastools\lastools\bin\lasclip.exe -i \\speedy1\Data_7\_LIDAR\LWN\DOM\LAZ\*.laz -o
" + pPath + "\\" + "j1_pol" + pName + "_DOM.laz -merged -poly " + pPath + "\\" + "Temp.shp"
process = subprocess.Popen(ToDo, shell=True)
process.wait()

pOutDTM = pPath + "\\" + "DTM_CLIP.tif"
pOutDTM_Ascii = pPath + "\\" + "DTM_CLIP.asc"
arcpy.Clip_management(pDTM_AV, extent, pOutDTM, "", "", "NONE")
arcpy.RasterToASCII_conversion(pOutDTM, pOutDTM_Ascii)

pOutHeight = pPath + "\\" + "j1_pol" + pName + "_nDOM.las"
ToDo = r"H:\lastools\lastools\bin\lasheight.exe -i " + pPath + "\\" + "j1_pol" + pName + "_DOM.laz
-replace_z -drop_below -1 -ground_points " + pOutDTM_Ascii + " -o " + pOutHeight
process = subprocess.Popen(ToDo, shell=True)
process.wait()

# average ndom (meanVH)
pOutVH = pPath + "\\" + "j1_pol" + pName + "_meanVH.xyz"
ToDo =  r"H:\lastools\lastools\bin\lasgrid.exe -i " + pPath + "\\" + "j1_pol" + pName + "_nDOM.las
-step 500 -ll " + str(xmin) + " " + str(ymin) + " -elevation -average -oxyz"  + " -o " + pOutVH
process = subprocess.Popen(ToDo, shell=True)
process.wait()

# CHM (highest value per 2x2 m)
pOutCH = pPath + "\\" + "j1_pol" + pName + "_CH.tif"
ToDo =  r"H:\lastools\lastools\bin\lasgrid.exe -i " + pPath + "\\" + "j1_pol" + pName + "_nDOM.las
-step 2 -elevation -highest"  + " -o " + pOutCH
process = subprocess.Popen(ToDo, shell=True)
process.wait()

pOutCH_P = pPath + "\\" + "j1_pol" + pName + "_CH.shp"
field = "VALUE"
arcpy.RasterToPoint_conversion(pOutCH, pOutCH_P, field)
OutFC = pPath + "\\" + "j1_pol" + pName + "_CH_3D.shp"
Height_Field = 'GRID_CODE'
arcpy.FeatureTo3DByAttribute_3d(pOutCH_P, OutFC, Height_Field)

# CHM to las
pOutCH_las = pPath + "\\" + "j1_pol" + pName + "_CH_3D.las"
ToDo = r"H:\lastools\lastools\bin\shp2las.exe -i " + pPath + "\\" + "j1_pol" + pName +
"_CH_3D.shp " + " -o " + pOutCH_las
process = subprocess.Popen(ToDo, shell=True)
process.wait()

# sd CH_3m
pOutsdCH = pPath + "\\" + "j1_pol" + pName + "_sdCH_3m.xyz"
```

```
    ToDo =  r"H:\lastools\lastools\bin\lasgrid.exe -i " + pPath + "\\" + "j1_pol" + pName + "_CH_3D.las
    -step 500 -clip_z_above 3 -oxyz -elevation -stddev"  + " -o " + pOutsdCH
    process = subprocess.Popen(ToDo, shell=True)
    process.wait()

    for line in fileinput.input(pOutVH):
       pLine = string.split(line,",")
       VH  = pLine[2]
    for line in fileinput.input(pOutsdCH):
       pLine = string.split(line,",")
       sdCH  = pLine[2]

    OutputFile_Result.write("j1_pol," + str(pName)+"," + str(VH)[:-1]+","+str(sdCH)[:-1]+"\n")

    if os.path.isfile(pOutHeight):
       os.remove(pOutHeight)

    if os.path.isfile(pOutVH):
       os.remove(pOutVH)

    if os.path.isfile(pOutCH):
       os.remove(pOutCH)

    if os.path.isfile(pOutCH_P):
       os.remove(pOutCH_P)

    if os.path.isfile(pOutCH_las):
       os.remove(pOutCH_las)

    if os.path.isfile(pOutsdCH):
       os.remove(pOutsdCH)

OutputFile_Result.close()
```